

ASSESSING IMPACTS OF CLIMATE CHANGE AND LAND- USE INTERVENTIONS ON FLOODING IN NYABUGOGO CATCHMENT (KIGALI -RWANDA)

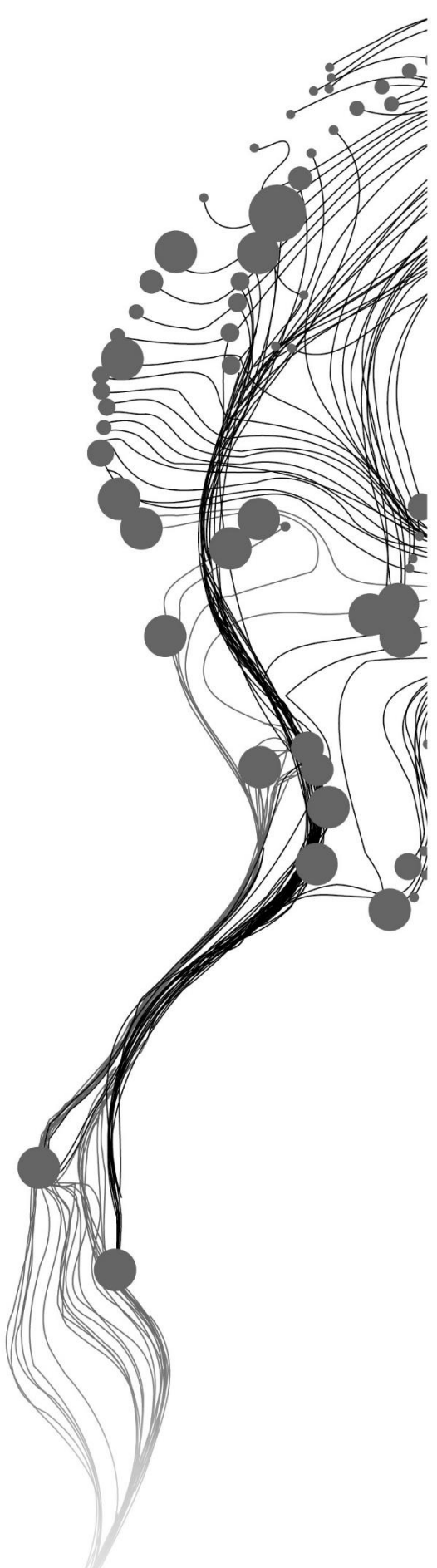
MAMELINE UMUTESI

August, 2021

SUPERVISORS:

Dr. Ing.T.H.M.Rientjes

Dr.ir.M.J.Booij



ASSESSING IMPACTS OF CLIMATE CHANGE AND LAND- USE INTERVENTIONS ON FLOODING IN NYABUGOGO CATCHMENT (KIGALI -RWANDA)

MAMELINE UMUTESI

Enschede, The Netherlands, August, 2021

Thesis submitted to the Faculty of Geo-Information Science and Earth Observation of the University of Twente in partial fulfilment of the requirements for the degree of Master of Science in Geo-information Science and Earth Observation.

Specialization: Water Resources and Environmental Management

SUPERVISORS:

Dr. Ing. T.H.M. Rientjes (Tom)

Dr. ir. M.J. Booij

THESIS ASSESSMENT BOARD:

Dr. ir. C.M.M. Mannaerts (Chair)

Dr. Alemseged Haile (External Examiner, Arba Minch University Ethiopia]

DISCLAIMER

This document describes work undertaken as part of a programme of study at the Faculty of Geo-Information Science and Earth Observation of the University of Twente. All views and opinions expressed therein remain the sole responsibility of the author, and do not necessarily represent those of the Faculty.

ABSTRACT

Flooding is a very common disaster in Rwanda. It is recognized that a sound understanding of the effect of climate change and land use change on extreme hydrological events in catchments is required since such changes heavily affect the hydrological responses of the catchments. This study has assessed the hydrological and flooding behaviors of the Nyabugogo catchment (Kigali-Rwanda) due to land use changes under extreme rainfall due to climate change. The change in climate was analyzed between the period (1981-2005) and (2021-2050) for RCP4.5 and RCP8.5 emission scenarios. With outputs of regional climate models through empirical quantile mapping, corrected future rainfall projections were obtained while the observed rainfall was used for the baseline period. The results for RCP8.5 have shown an increase in monthly rainfall for both the short and long rainy seasons with November being the wettest month of the year. RCP4.5 showed both increase and decrease of rainfall for some months. Annual rainfall was also calculated, and relative to the baseline period, a slight increase was obtained for RCP4.5 while RCP8.5 has shown a considerable increase in the future annual rainfall. The analysis showed that the extreme rainfall events based on the 99th percentile and return periods of 10, 50, and 100-years, these events will become more frequent and increase in magnitude due to climate change under RCP8.5. The results showed that daily extreme rainfall will increase in magnitude under RCP8.5, with 24% while RCP4.5 showed opposite behavior. The increase and decrease of rainfall is associated with ENSO phenomena which usually influences the extreme events in the region and is expected to influence future climate of the region.

The HEC-HMS rainfall-runoff model was used to examine the effect of land use change and climate change on the streamflow hydrograph and peak flows. The results from rainfall-runoff modeling showed that the peak flows will increase with future land use by 29.0%, 37.9% and 45.9% for return periods of 10, 50, 100-years respectively. The increase in peak flows was attributed to the increase of urban runoff response caused by an increase in impervious areas for the future period. Streamflow and peak flows have also increased as a result of climate change for RCP8.5 22.4%, 26.9%, and 29.6% for return periods of 10, 50, 100-years. The RCP4.5 scenario showed a reduction in peak flows with (-25.25, -33.7, and -36.34%) for return periods of 10, 50 and 100years respectively. The combined effects of land use change with extreme rainfall for RCP8.5 scenario showed a larger increases in peak flows for Nyabugogo catchment by 61%, 63.3%, 69.6 % for return periods of 10, 50, and 100-years respectively. From the results, was concluded that land-use change has more impacts on streamflow than climate change in the Nyabugogo catchment. The streamflow hydrograph for different scenarios served as inflow boundaries for the flood model.

The 1D2D SOBEK hydrodynamic model for the Nyabugogo commercial hub was forced by the boundary inflows from the hydrological model for different scenarios and different return periods. The increase and decrease behaviors observed in extreme rainfall and streamflow and peak flows for land use change, and climate change, respectively were reflected in flooding behavior. For three flood characteristics assessed (flood water depth, velocity, and flood extent), land use change showed an increase in flooding compared to the present time. The study has concluded that land use change contribute the most to producing more flooding in the Nyabugogo catchment in the future,, while the climate change due to high emission scenario RCP8.5 will take second place. The combined effects of land use and climate change under high emission scenario RCP8.5 exacerbate flooding with a large flood extent. The medium emission scenario RCP4.5 reduced the flooding compared to the current case. This study was the first to assess flooding using the extreme rainfall information from regional climate models for the study area. It was concluded that the RCMs can serve for future flood assessment under a changing climate. Studying the effects of climate change and land-use changes on flooding is useful for water managers for better planning and awareness.

Keywords: RCMs, RCP4.5, RCP8.5, extreme rainfall, land-use changes, climate change, flooding

ACKNOWLEDGEMENTS

My sincere gratitude and praises are for my forever friend Jesus Christ for his favour, mercy, power on me, and he revealed himself to me through this journey. I will be forever grateful

I would like to thank the kingdom of the Netherlands for providing me the OKP scholarship; through it, I have been able to pursue and complete my studies without any problem. For this scientific and interesting journey of writing my thesis, I would like to give special thanks to my first supervisor Dr. Ing.T.H.M.Rientjes, and second supervisor, Dr.ir.M.J.Booij, for your guidance, constructive criticisms and insightful comments during this learning curve; they helped me to complete my thesis. It was good to have you two as my supervisors, and we always had great discussions. In the same way, I would like to thank the ITC faculty and water resources department for the shared knowledge in this two-year journey.

I would like to extend my thanks to the Enschede Seventh-Day Adventist church, especially the English group. The shared social life, the moral support, and your prayers helped me to pass through all. Thank you, Esther, for being my sister; I enjoyed and loved being called “Bucura.”

I thank the Rwandan community in ITC and Enschede. Thank you for being supportive and helping me to have fun during this journey. I thank all my friends I meet here in Enschede, special thanks to Jina for being therefore always for me. Special thanks to my mentor prof John; I am grateful for your ideas and support. Thanks to Welela and Moses for being there for me, I am grateful for our friendship.

I thank everyone who contributed to my studies by sharing ideas and knowledge with my classmates, and special thanks to Ransford, Emma, and Kingsley. Thank you, Patience for your laptop helped me to complete my model simulations. Thanks to Eng. Davis Bugingo from Rwanda Water Board for providing me the requested information and supporting me to grow in my career.

Last but not least, I would like to thank my family. Thank you, my mom, for being on my side always, understanding, and praying for me. I am blessed to be your daughter. To my two sisters and one brother, my lovely aunt, my cousin-sister Saoula. God heard your prayers all. To Laetitia, my prayer partner Renata and our bible study group, to Ake, thank you all for any support in any way.

Be blessed all !!!! Mwarakozeeee cyaneeee !!!!!

TABLE OF CONTENTS

1.	INTRODUCTION.....	9
1.1.	Background and justification.....	9
1.2.	Research problem.....	10
1.3.	Research Objectives.....	11
1.4.	Research Hypothesis.....	11
1.5.	Thesis outline.....	11
2.	LITERATURE REVIEW.....	12
2.1.	Regional climate models.....	12
2.2.	Representative Concentration Pathways (RCPs).....	12
2.3.	Bias correction of climate model data.....	13
2.4.	Extreme rainfall.....	13
2.5.	Land use /cover changes in hydrological studies.....	14
2.6.	Rainfall-runoff modeling / inflow boundaries.....	14
2.7.	Flood modeling in urban areas.....	15
3.	STUDY AREA AND DATA AVAILABILITY.....	16
3.1.	Study area description.....	16
3.2.	Data collection and pre-processing.....	19
3.3.	RCMs simulations and projections.....	27
4.	RESEARCH DESIGN AND METHODS.....	28
4.1.	Conceptual framework.....	28
4.2.	Objective One: To acquire climate change data (precipitation) from RCMs, compare and analyze the projections among the set of RCMs.....	29
4.3.	Objective Two: Extreme rainfall events.....	31
4.4.	Objective two : To design extreme rainfall for floods modeling.....	32
4.5.	Objective three: To develop a rainfall-runoff model for simulating impacts of climate and land-use changes on streamflow in the Nyabugogo catchment.....	33
4.6.	Objective Four: To simulate Flooding for Nyabugogo commercial hub under changing climate and land use.....	43
5.	RESULTS.....	46
5.1.	Objective One: To acquire climate change data (precipitation) from RCMs, compare and analyze the projections among the set of RCMs.....	46
5.2.	Objective Two: To derive extreme rainfall and analyze their change between baseline and future periods.....	52
5.3.	Objective three: To develop a rainfall-runoff model for simulating impacts of climate and land-use changes on streamflow in the Nyabugogo catchment.....	56
5.4.	Impacts of climate change and land-use changes on streamflow.....	63
5.5.	Objective Four: To simulate Flooding for Nyabugogo commercial hub under changing climate and land use.....	66
6.	DISCUSSION.....	71
6.1.	Acquiring climate change data (precipitation) from RCMs, compare and analyze the projections among the set of RCMs.....	71
6.2.	Deriving extreme rainfall and analyze their change between baseline and future periods.....	72
6.3.	Developing rainfall-runoff model for simulating impacts of climate and land-use changes on streamflow in Nyabugogo catchment.....	73
6.4.	Simulating flooding for Nyabugogo commercial hub under changing climate and land-use.....	74
7.	CONCLUSION AND RECOMMENDATION.....	75

7.1.	Conclusion	75
7.2.	Limitations of this study.....	76
7.3.	Recommendations.....	77

LIST OF FIGURES

Figure 1-1: Flood event of February 23rd 2013. Source : (Munyaneza et al., 2013).....	10
Figure 2-1: Study area conceptualization (top) and location of flood model domain(down) by (Manyifika, 2015) respectively. Table 2-1: Four Representative Concentration Pathways Source: (Vuuren et al., 2011)	13
Figure 3-1: Location of Nyabugogo catchment (left) in Rwandan boundary(right).....	16
Figure 3-2: Study area conceptualization (top) and location of flood model domain(down) by (Manyifika, 2015) respectively.	17
Figure 3-3: Nyabugogo catchment topography.....	18
Figure 3-4: Nyabugogo catchment soil map.....	19
Figure 3-5: Current(existing) and projected land-use for Nyabugogo (right and left), respectively.....	20
Figure 3-6: Areal representation of rainfall variables using Thiessen polygons in Nyabugogo catchment	21
Figure 3-7: Monthly rainfall for all nine stations (1981-2005).....	22
Figure 3-8: Double mass curves of rainfall showing data consistency for different stations.....	23
Figure 3-9: Historical annual rainfall from 1981 to 2017	23
Figure 3-10: Discharge hydrograph for Nyabugogo catchment for the period (1981-2017).....	25
Figure 3-11: Corrected discharge for Yanze river sub catchment (2011-2014).....	26
Figure 3-12: Rusumo discharge hydrograph for period (2011-2013).....	26
Figure 3-13: Muhazi discharge hydrography for the period (2011-2013).....	27
Figure 4-1: Flowchart of the methodology.....	28
Figure 4-2: Summary of the process and the used methods in the HEC-HMS Model.	34
Figure 4-3: Schematic representation of calibration process	42
Figure 4-4: 1D2D SOBEK schematization of Nyabugogo commercial hub flood model by (Manyifika, 2015; Ali, 2016)	45
Figure 5-1: Observed and simulated RCMs monthly rainfall for the historical period(1981-2005)	47
Figure 5-2: The daily mean monthly rainfall standard deviation at Kigali station	48
Figure 5-3: CDFs of uncorrected RCM simulations in the baseline(top) and future projections under RCP4.5 and 8.5 scenarios (bottom) compared to CDF of observed rainfall at Kigali station.	49
Figure 5-4: CDFs of the results from empirical quantile mapping of RCMs for RCP4.5 and 8.5 with comparison to the observed rainfall respectively	50
Figure 5-5: Relative changes in average monthly rainfall between baseline(1981-2005) and future periods (2021-2050) for RCP4.5 and 8.5 at Kigali and Kawangire station.....	52
Figure 5-6: Frequency distribution of extreme rainfall (99th percentile).....	53
Figure 5-7: CDF of Gumbel distribution of daily extreme rainfall for different return periods at Kigali and Kawangire stations, respectively.	54
Figure 5-8: Comparison of hourly rainfall distribution of Gitega_Kigali to synthetic storm types in the region (Fiddes 1974”, Schmidt and Schulze 1987) Table 5-1: derive daily extreme rainfall for 10,50 and 100- year return periods for different stations.....	56
Figure 5-9: Hydrological Soil Groups in Nyabugogo Catchment	56
Figure 5-10: Curve number for current (up) and future period (down) respectively	57
Figure 5-11: Comparison of simulated and observed hydrograph for Yanze subcatchment (2011-2012) ..	60
Figure 5-12: Comparison of simulated and observed discharge for calibration (top graph) and validation (bottom graph) for Muhazi lake basin.....	61
Figure 5-13: Comparison of simulated and observed streamflow hydrographs for Nyabugogo for two events in 2013.....	63

Figure 5-14: Streamflow hydrograph for 100-year return period extreme rainfall of the current case, RCP4.5 and RCP8.5 scenarios respectively.....64

Figure 5-15: Streamflow hydrography for 100year return period extreme rainfall due to land use change only (top) and land use combined with RCP4.5 and RCP8.5 scenarios respectively.....65

Figure 5-16: Mean maximum depth(left), mean maximum velocity(right) and area of inundation(bottom) of different for scenarios.....66

Figure 5-17: Maximum flood depth for different scenarios for the 100-year return period.....67

Figure 5-18: Maximum velocity for different scenarios for 100-year return period.....68

LIST OF TABLES

Table 2-1: Four Representative Concentration Pathways Source: (Vuuren et al., 2011).....	13
Figure 2-1: Study area conceptualization (top) and location of flood model domain(down) by (Manyifika, 2015) respectively.	
Table 2-2: Four Representative Concentration Pathways Source: (Vuuren et al., 2011)	13
Table 3-1: Summary of the data used in the research.....	18
Table 3-2: The current and planned land use distribution in the Nyabugogo catchment	20
Table 3-3: Meteorological variables inside and around Nyabugogo catchment.....	20
Table 4-1: Selected Regional Climate Models (RCMs) and Driving Global Circulation Models (GCMs) ..	29
Table 4-2: Hydrological soil groups for the current study based on soil textures (Report(TR-55), 1986)...	36
Table 4-3: CN lookup table adapted in determining the CN grid with the existing land-use.....	36
Table 4-4: CN lookup table adapted in determining the CN grid with the future planned land-use	36
Table 4-5: Manning's Roughness Coefficient adopted from (Ali, 2016)	44
Table 5-1: : Deriving daily extreme rainfall for 10,50 and 100- year return periods for different stations.	54
Table 5-2: Short duration peak intensities for the storm in mm recorded at Gitega-(Kigali)station.....	55
Table 5-3: The main physical characteristics of basins	58
Table 5-4: Selected events, calibrated and validated parameters for Yanze basin.....	59
Table 5-5: : Muhazi lake basin selected events , calibrated and validated parameters	62
Table 5-6: Summary of the results for peak flows for current and expected land use and climate change scenarios with expected changes as percentage in brackets for Nyabugogo catchment.....	63
Table 5-7: Maximum flood depth statistics derived from different scenarios.....	69

1. INTRODUCTION

1.1. Background and justification

The increase of population leading to deforestation and expansion of agriculture and urban areas and , the possible increase in rainfall due to climate change triggered by the greenhouse effect lead to an increase in floods risk in many cities (Jothityangkoon et al., 2013). Flooding events have been reported in many countries and regions, and in many cases, the frequency and magnitude of the recently observed floods have been found to be more severe than in the observed long recorded floods (Syvitski & Robert Brakenridge, 2013). The impacts that come with these severe flooding events are devastating (Stevens et al., 2016).

Changes in climate that lead to extreme events have been observed since the 1950s. Studies show that the number of heavy precipitation events increased in many regions compared to where they have decreased. This increase in heavy precipitation with extreme discharges increased the risk of severe flooding in many catchments worldwide (Pachauri., 2014). Climate models predicted that extreme events are expected to increase in the future due to climate change. For instance, Jarraud & Steiner.(2012) argued that heavy precipitation will become more frequent and intense in many regions.

Changes in land use come with a very strong effect on flooding because human beings have heavily modified the natural landscapes. Some large areas have been drained or deforested, leading to an increase or decrease of antecedent moisture and causing floodings. It is ever more recognized that land management and water are intimately linked (Rogger et al., 2016). It is probable that hydrological changes will continue in the coming decades due to the loss of forests and natural lands (Wheater & Evans, 2009). These changes in land use, together with urbanization, reduce the infiltration capacity of an area and increase overland runoff from rainfall and snowmelt. Therefore, peak discharges and frequent floods become more severe (Saberifar & Noor, 2017; Konrad, 2003). Hence, posing a threats to the water sector and bringing challenges to sustainable development.

East Africa was reported to experience a high risk of flooding. The interannual variability of rainfall has increased, and extreme floods have also plagued the region (Nicholson, 2017). Shongwe et al. (2011) reported an increase in hydro-meteorological disasters in the region, such as floods and droughts. Generally, climate studies for Africa do not show any uniformity about the future climate across the continent. Zhou et al. (2019) used GCMs and RCMs from CMIP5 for future projections under low emission scenarios (RCP2.6) and high emission scenarios (RCP8.5) and reported that the precipitation levels will increases in some regions while southern Africa will experience droughts.

Like the African continent, the future climate of Rwanda is also uncertain based on the findings from some studies conducted so far Nahayo et al. (2018) used MIROC_4h under RCP 4.5 for future projections of precipitation in 4-climatological regions of Rwanda for the 2015-2035 window. The future projections indicated that there will be an increase in rainfall for the majority of the months. This increase in rainfall was also noticed by (Rukundo & Doğan, 2016) after using SRES emission scenarios for rainfall projection in the period 2011-2040. Uhorakeye & Möller (2017) studied the potential impacts of climate change on the future of Rwandan hydropower generation with HadGem2-ES and MIROC-ESM-CHEM for RCP4.5 and RCP8.5 scenarios. Both models showed considerable reductions in annual precipitations for the period 2030 to 2060. They also found that the inter-annual variations in annual rainfall are expected to dominate the future climate, where changes are expected to reach 50%.

Rwanda is highly susceptible to climate change because of its dependence on agriculture, which accounts for 33% of the GDP in 2013 (Warner, 2018). Rain-fed agricultural activities are more common in Rwanda, which makes the country highly vulnerable to variation in rainfall patterns. The vulnerability of Rwanda to disasters is further increased by the high population density with 460 persons per square kilometre and is expected to increase due to the annual population growth of 2.7% (K. Warner, 2018). Rwanda is one of the fastly developing countries, where there is an increase in urban areas, which exacerbate floodings during extreme events. Though the country is very vulnerable to climate change and floodings, very little attention has been paid in flood prediction for the coming future.

Nyabugogo catchment is located in the city of the Kigali and its surrounding; its hydrological processes has been significantly changed with the extreme rainfall due to climate change together with an intensification of anthropogenic activities such as urbanization. Downstream of this catchment is Nyabugogo commercial hub in Kigali downtown which plays important role for the lives of Kigali citizens due to its different businesses, and it connects the city with the rest of the country due to large bus parking. However, this place has been experiencing devastating floods events, which lead to loss of lives and properties. Therefore, it's of much importance to carry the studies on hydrological extremes in this catchment.



Figure 1-1: Flood event of February 23rd 2013. Source : (Munyaneza et al., 2013)

1.2. Research problem

The occurrence of severe floods was observed in Kigali, and the Nyabugogo catchment and their magnitudes and frequencies significantly increased over time, specifically in recent years. For Nyabugogo catchment, the urban expansion, extreme rainfall as a result of climate change, the topography (steep slopes up to 50%) of the area, uncontrolled agriculture, and inadequate drainage systems are the main factors that exacerbate flooding in this catchment. Flood events in Nyabugogo led to the loss of people's lives, injuries, economic loss, and a burden to the government (REMA, 2019; Rukundo & Doğan, 2016).

The recent analysis of rainfall trends in Rwanda indicated the increase of occurrence in extreme rainfall around the country (Ministry of Foreign Affairs of the Netherlands, 2018). The temporal rainfall distribution has shown changes with rainfall increase in the short rainy season, while the long rainy season rainfall has shown declining trends. The studies on future climate also indicate the increase in extreme rainfall with intra-seasonal and intra-annual variability (Byamukama, 2009; Uhorakeye & Möller, 2017; Rukundo & Doğan, 2016)

Climate change and flooding in Rwanda have drawn the researcher's attention (Munyaneza et al., 2013; Rukundo & Doğan, 2016; Uhorakeye & Möller, 2017, Icyimpaye et al., 2021). However, studies that are incorporating both the impacts of extreme rainfall due to climate change and impacts of land-use changes on flooding have not yet been done. Therefore, this study aims to use projected RCM extreme rainfall under RCP4.5 and 8.5 emission scenarios, incorporating land use planning of 2050 to assess future flooding (water depth, velocity, and areas of inundation) in the Nyabugogo catchment. It serves to inform the city planners regarding flooding risk in the future to be prepared for sustainable adaptations and land use management.

1.3. Research Objectives

1.3.1. Main Objective

To assess the impacts of climate change and land-use interventions on flooding in Nyabugogo catchment (Kigali-Rwanda) under two RCPs scenarios for 2050.

1.3.2. Specific objectives and Questions

1. To acquire climate change data (precipitation) from RCMs and then compare and analyse the projections among the set of RCMs
 - which are RCMs available to represent the past and future projected climate and extreme climate conditions in the Nyabugogo catchment?
 - Is bias adjusting for RCM simulations and projections required?
2. To retrieve extreme rainfall and statistically analyse their change over time
 - To which extent are will extreme rainfall change due to climate change compared to the current situation
3. To develop a rainfall-runoff model to simulate daily streamflow for the Nyabugogo catchment
 - How do land-use changes, as well as climate change, affects streamflow in the Nyabugogo catchment?
 - How do both combined extreme rainfall and land-use changes affect runoff behavior and peak flows?
4. To simulate Flooding for Nyabugogo commercial hub
 - How do flood characteristics (i.e. depth, velocity and extent) change under projected changes in rainfall extremes and land use interventions for the Nyabugogo flood model domain?

1.4. Research Hypothesis

The increases in frequency and magnitude of extreme rainfall by climate change have more impacts on the severeness of future flood events than impacts by land-use interventions and changes.

1.5. Thesis outline

The current study is presented in six chapters. After this one covering the introduction, chapter two provides a literature review of the main concepts covered in the current study. Chapter three describes the study area, data availability, and pre-processing. Chapter four provides the methods used to answer the research questions and to achieve the objectives. Chapter five presents study findings. Chapter six discusses and explains the study findings. The last chapter, seven, provides the conclusion about the study and recommendations for future work.

2. LITERATURE REVIEW

This Chapter briefly explains the key concepts related to climate change, rainfall extremes, and land-use changes leading to floodings. It elaborates the state of the art that this current study is related to. It highlights the attention of researchers regarding climate and land-use changes impacts on hydrological processes.

2.1. Regional climate models

Climate models are primary tools that help us to estimate and understand the processes that govern the climate system, including climate change. Global circulation models (GCMs) cover the entire planet. Regional climate models (RCMs) cover a specific region. GCMs are with a coarse resolution between 100 to 200km. Due to their coarse resolution, outputs of GCMs cannot be used in decision-making for a specific city or local region, especially where the topography is complex. To overcome the issue of coarse resolution for GCMs, the downscaling of their outputs is essential. RCMs have been developed for dynamic downscaling of GCMs data. RCMs are available for fine resolution between 25-50 km, and the resolution might be finer than this. RCMs are driven by GCMs data as boundary. RCMs outputs are openly available in Coordinated Regional Downscaling Experiment (CORDEX) project based on the region. Various studies have adopted the use of RCMs for hydrological impacts studies. RCMs are used for a future climates projections such as rainfall and flood prediction based on the RCMs simulations in the baseline periods. Teutschbein & Seibert. (2010) argued that the progress made in regional climate modeling recently made the use of RCMs data more attractive in hydrological studies.

In Africa, various studies used RCMs from CORDEX Africa to assess their performance in representing the hydrological processes. For instance, Nikulin et al.(2012) used ten RCMs driven by ERA-Interim reanalysis to simulate rainfall over the African continent. They found that the ensemble mean improves precipitation simulation compared to a single RCM. They concluded that an ensemble of RCMs could deliver useful information on projected precipitation over Africa. Mascaro et al.(2015) assessed the performance of CORDEX Africa regional climate for simulating the hydrological cycle in the Niger River Basin; from their results, they stated that a set of RCMs from CORDEX Africa can be used for water-related projects planning in Niger River Basin. Besides, Haile et al.(2017) simulated impacts of climate change on water availability in Ethiopia and found that it is essential to use the RCMs ensemble when dealing with hydrological simulations because the ensemble gives better results than a single RCM. During this study, three RCM outputs with 44 km from CORDEX-Africa were used to obtain rainfall projection for the future horizons. The information about CORDEX-Africa can be found here <http://www.csag.uct.ac.za/cordex-africa/>

2.2. Representative Concentration Pathways (RCPs)

Representative Concentration Pathway (RCP) is the greenhouse gas concentration trajectory that was adopted by IPCC. The four pathways were used for the IPCC fifth Assessment Report (AR5) in 2014. These pathways illustrate different future climates depending on the volume of greenhouse gases emitted in the coming years. These RCPs were designed by considering forcing agents such as land use & land cover data, socio-economic change, climate data. They also consider the effect of carbon dioxide concentration in the atmosphere and other greenhouse gases and aerosols. Each RCP covers the period between 1850-2100 (Jubb et al., 2013). These pathways are characterized by radiative forcing by the end of the 21st century. The four RCPs span the year 2100. They consist of one mitigation scenario, which leads to a very low forcing level (RCP2.6), two medium stabilization emission scenarios (RCP4.5 and RCP 6), and a very high emission scenario (RCP8.5). The latter rises due to little effort to reduce emissions by 2100 (Vuuren et al., 2011).

The current study assessed the possible extreme rainfall and flooding in the future window(2021-2050) based on both RCP4.5 (medium) and RCP8.5 (high). Table 2-1 shows four RCPs with a corresponding short descriptions.

Table 2-1: Four Representative Concentration Pathways Source: (Vuuren et al., 2011)

	Description
RCP 8.5	Rising radiative forcing pathway leading to 8.5 W/m ² (~1370 ppm CO ₂ eq) by 2100.
RCP 6	Stabilization without overshoot pathway to 6 W/m ² (~850 ppm CO ₂ eq) at stabilization after 2100
RCP 4.5	Stabilization without overshoot pathway to 4.5 W/m ² (~650 ppm CO ₂ eq) at stabilization after 2100
RCP 2.6	Peak in radiative forcing at ~3 W/m ² (~490 ppm CO ₂ eq) before 2100 and then decline (the selected pathway declines to 2.6 W/m ² by 2100).

2.3. Bias correction of climate model data

Both Global and Regional Climate models are known to be associated with systematic biases in their outputs compared to observed data. These errors are mainly due to the used of large grid boxes, simplified physics, or incomplete knowledge of the earth's climate system. Therefore, this leads to the failure in representing climate, especially on the small spatial and temporal scales (Piani et al., 2010). Hence, the direct use of uncorrected climate model outputs in climate impact assessment can give unrealistic results.

In order to reduce the biases and errors in climate models outputs, there are various methods developed for that purpose. However, the quality of the observed datasets determines the quality of the bias-adjusted outputs. Therefore, to have reliable bias-adjusted outputs, the observed datasets with good quality must be available (Räty et al., 2014). Methods such as the delta change approach, linear and multiple scaling, and quantile mapping are often used in bias correction. delta change method assumes that the climate scenarios will stay unchanged, it does not take into account the changes in climate variability, such as increase of long dry spells or extreme rainfall. (Räty et al., 2014). Multiple and linear regression are also often used for bias correction. By using the historical observations and the model output of the same period, regression analysis can be made. Hence, using the obtained regression parameters, the bias-adjusted future time series can be created. Nowadays, quantile mapping is often used for bias adjusting in future projections.

Quantile mapping includes calculating changes in cumulative distribution functions (CDFs) of daily RCM output between baseline and future periods quantile by quantile. Furthermore, they are rescaled based on the observed CDFs, and they are added quantile by quantile to the observed datasets to obtain the calibrated future CDFs (Amengual et al., 2012). Several studies used quantile mapping to correct biases in regional climate model projections. (Jakob Themeßl et al., 2011) used quantile mapping to correct bias in daily precipitation projections. This method indicated improvements in mean, variance, frequency, intensity, and extreme daily rainfall and in quantiles (Cannon et al., 2015). As this study was dealing with extreme rainfall projections for future floods simulation, quantile mapping was used to find the future rainfall time series.

2.4. Extreme rainfall

Extreme rainfall events are one of the most serious challenges that society may face in a changing climate. Different researchers showed that change in climate has a significant relationship with the occurrence of extreme weather events (Huber, &Gulledge, 2011; Kuswanto.; 2015). One of the obvious extreme events is

heavy rainfall leading to flooding disasters. Heavy rainfall frequently occurs in tropical climate. These extremes come with huge losses such as human lives, resources, environmental degradation; therefore, the work of predicting these events is very necessary (Kuswanto et al., 2015).

In case of urban floods, the estimation of extreme rainfall is required for designing the hydraulic structures such as dam spillways, bridges, culverts, and other urban stormwater drainage systems for flood risk management and for the quantification of the risk of failure of the existing hydraulic structures. By referring to Nathan & Weinmann, (2013), the extreme rainfall associated with return periods of 50 to 2000 years is considered to be very large and rare. Therefore, the rare extreme rainfall is important for designing capable hydraulic structures. Though there is no single method for extreme rainfall estimation, however, many countries have developed their own standard techniques and guidelines that mostly involve the probabilistic approach and statistical analysis of long observed annual maximum rainfall data (Smithers & Schulze, 2004). The current study made use of annual maximum rainfall based on observed rainfall series for 25 years (1981-2005), and the projected rainfall (2021-2050) from regional climate models outputs to estimate design rainfall for return periods of 10, 50, and 100 year using distribution function.

2.5. Land use /cover changes in hydrological studies

Land use /land cover changes such as the change from forest to agriculture, pasture to arable land, from agriculture or grassland to urbanized areas act as drivers for changes. Though a number of the studies that combine impacts of climate change and land-use change indicate that climate change has more significant effects on flooding than land-use changes; but, to study the hydrological responses to land use changes is necessary (Akter et al., 2018). The land use/cover information is used as inputs in hydrological models to simulate hydrological response behavior due to the land use/cover changes over time.

Several studies assessed the impacts of urbanization and land use changes on hydrological processes. Akter et al. (2018) used a hydrological model to simulate hydrological behavior due to the increase in urban areas in Belgium. They found that urban peak flow and total peak flow significantly increased as urbanization increased. Emam et al. (2016) studied the impacts of projected land-use changes and climate change on flood behavior using a rainfall-runoff model in Indonesia. The results revealed that the increase due to projected land use alone by 2030 was 20%. Gumindoga et al., (2014) assessed the impacts of urbanization of two catchments in Harare, Zimbabwe. The results showed that urban areas have significantly increased while woodlands decreased between 1986 and 2008. That increase in urban areas led to a streamflow increase of 84.8% and 73 % for those two catchments, respectively, between 1980 and 2010.

Nyabugogo catchment has both rural and urban areas of the city of Kigali. Urban expansion is taking place in all vicinity of the city, thus increasing the impervious areas. Recently, the city of Kigali has released a new land use planning that extends to 2050. The land use plan clearly indicates that the urban areas will increase during this period, thus increase the impervious areas in the catchment. Hence, studying the impacts that are associated with this expected increase in impervious areas is important for flood forecasting as these impervious areas reduce the time of concentration of runoff, thus, speeding up the runoff and flooding process.

2.6. Rainfall-runoff modeling / inflow boundaries

Hydrological models use mathematical formulas to compute the runoff, leaving the catchment after the rainfall has fallen in the watershed. Therefore, they provide useful information in water resources management and planning, such as flood protection and mitigation. Climate change is considered to modify hydrological behavior. For the proper assessment of runoff, the information on meteorology, geology, topography, soil, and land use/cover pattern is required for proper planning and mitigation of natural

hazards such as flooding. Several methods are available in the literature for the determination of runoff with regards to the above-mentioned factors (Darji et al., 2019). These days, the Geographic Information System (GIS), in combination with hydrological models, is often used for estimation of runoff (Crookston & Tullis, 2012). A range of hydrological models are available and have been successfully applied for runoff estimation. These models include SWAT (Soil and Water Assessment Tool), HEC-HMS (Hydrologic Engineering Center-Hydrologic Modeling System), WEPP (Water Erosion and Prediction Project), TOPMODEL (Crookston & Tullis, 2012; Birhanu et al., 2019; Darji, Prakash, Mehmood, & Pham, 2019).

For the current study, GIS was used in conjunction with HEC-HMS for rainfall-runoff modeling to estimate the streamflow and boundary inflows for the flood model. HEC-HMS has been successfully applied in several studies for the simulation of climate and land-use change impacts on runoff. Ali et al. (2011) successfully applied a calibrated HEC-HMS model on future land use scenarios to assess the possible land use effects on the storm-runoff generation in Pakistan. HEC-HMS was applied to simulate rainfall-runoff in the Koraiyar basin watershed due to land use change (Natarajan & Radhakrishnan, 2021). Emam et al. (2016) used HEC-HMS to simulate the peak river discharge for the current and future conditions due to climate and land use changes in the upper Ciliwung River basin in Jakarta, Indonesia. The findings of that study revealed that the land use in conjunction with the climate scenario increased peak flow by 130% in 2030 caused by the rainfall of 50-year return period.

2.7. Flood modeling in urban areas

Hydrodynamic models are robust tools in urban storm management. One-dimensional flow (1D) is the most common tool used to simulate water in the river channels and urban drainage systems. Models such as MIKE11, HEC-RAS, INFOWORK CS, and SWMM can be used to simulate the performance of hydraulic drainage systems (DHI, 2007; Fan et al., 2017). These models apply a 1D Saint Venant flow equations with the assumption that the flow velocity is perpendicular to the cross-section. i.e., only in one direction. However, 1D Flow models can only predict the excessive volume from river channels and drainage systems.

2D models such as FESWMS and MIKE21 are used to simulate urban flooding (Mignot et al., 2006; Dottori & Todini, 2013). These models give a better description of the flood characteristics such as flood depth, extent, velocity, and duration. 2D models apply 2D (X and Y directions) shallow water equations. However, the 2D calculation can be time-consuming, and large variations in cell sizes may arise due to the complex urban underlying surface, that leads to lower efficiency as the time step is limited by the numerical stability and is mostly determined by the small cells in mesh (Fan et al., 2017). Therefore, to accurately simulate the detailed urban flood inundation and propagation, coupling a 1D and 2D hydrodynamic model is essential in order to consider the flow interactions between the river drainage system and surface inundation, respectively (Fan et al., 2017).

1D2D hydrodynamic models are suitable tools to simulate urban inundation. 1D for the river network and 2D for rectangular grids, which symbolize floodplain topography, consist of the spatial model domains that allow the complex urban flood events simulation such as from drainage flow, overland flow, street flow (Suman & Akther, 2014). The real system characteristics are realized in flood models by means of parameterization. The significant inputs to the flood model are channel and floodplain topography, boundary conditions (inflows), surface roughness, and channel cross-section. In a 1D2D models, such as SOBEK, the continuity and momentum equations are present, and they ensure the conservation of mass and momentum, respectively.

3. STUDY AREA AND DATA AVAILABILITY

3.1. Study area description

Nyabugogo catchment is located in the central part of Rwanda, and it extends into three provinces: the city of Kigali and parts of the North and East provinces. It is located between 1°94'S and 30°04'E with a total drainage area of 1647km². The primary land use is agriculture, which occupies 58% of the total catchment area. The Nyabugogo commercial hub, which is affected by frequent flash floods, is located in the downstream part of the Nyabugogo catchment and northwest of Kigali. It is dominated by commercial activities and an extensive bus park (Munyaneza et al., 2011; Nhapi, 2011). Fig.[3-1] shows the location of the Nyabugogo catchment in the Rwandan boundary.

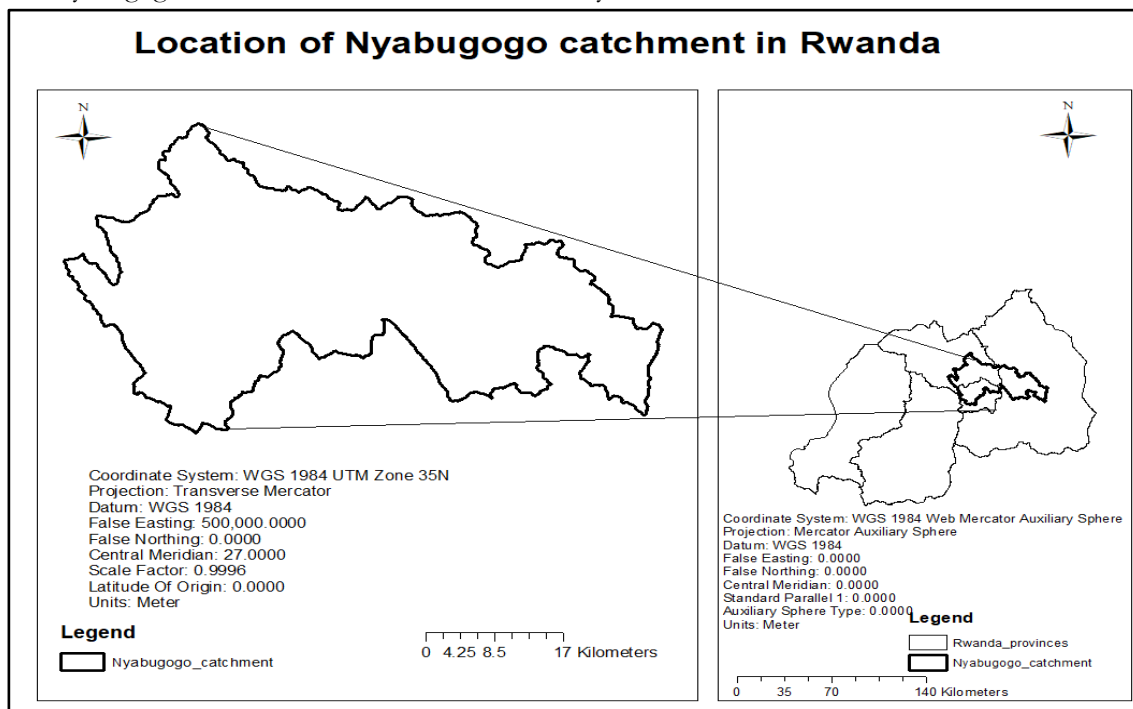


Figure 3-1: Location of Nyabugogo catchment (left) in Rwandan boundary(right)

3.1.1. Study area conceptualization

In this research, rainfall-runoff and hydraulic models were required to achieve the main objective of this study. The rainfall-runoff model is needed to estimate upstream and lateral boundary conditions for the flood model. Therefore, the entire Nyabugogo catchment was divided into fourteen sub-catchments. This was done in order to determine the upstream boundary inflows to the flood model domain. The flood model domain schematized by Manyifika (2015) and adopted by Ali (2016) was used for the current study. Figure 3-2 indicates Nyabugogo catchment conceptualization. It shows the locations of gauging stations for three gauged sub-catchments (Rusumo, Muhazi, and Yanze) and one gauging station (at Nemba) for the entire catchment located downstream of the catchment and at the end of the flood plain. Figure 3-3 shows the flood model domain as delineated by (Manyifika, 2015) and it is located downstream of the Nyabugogo catchment.

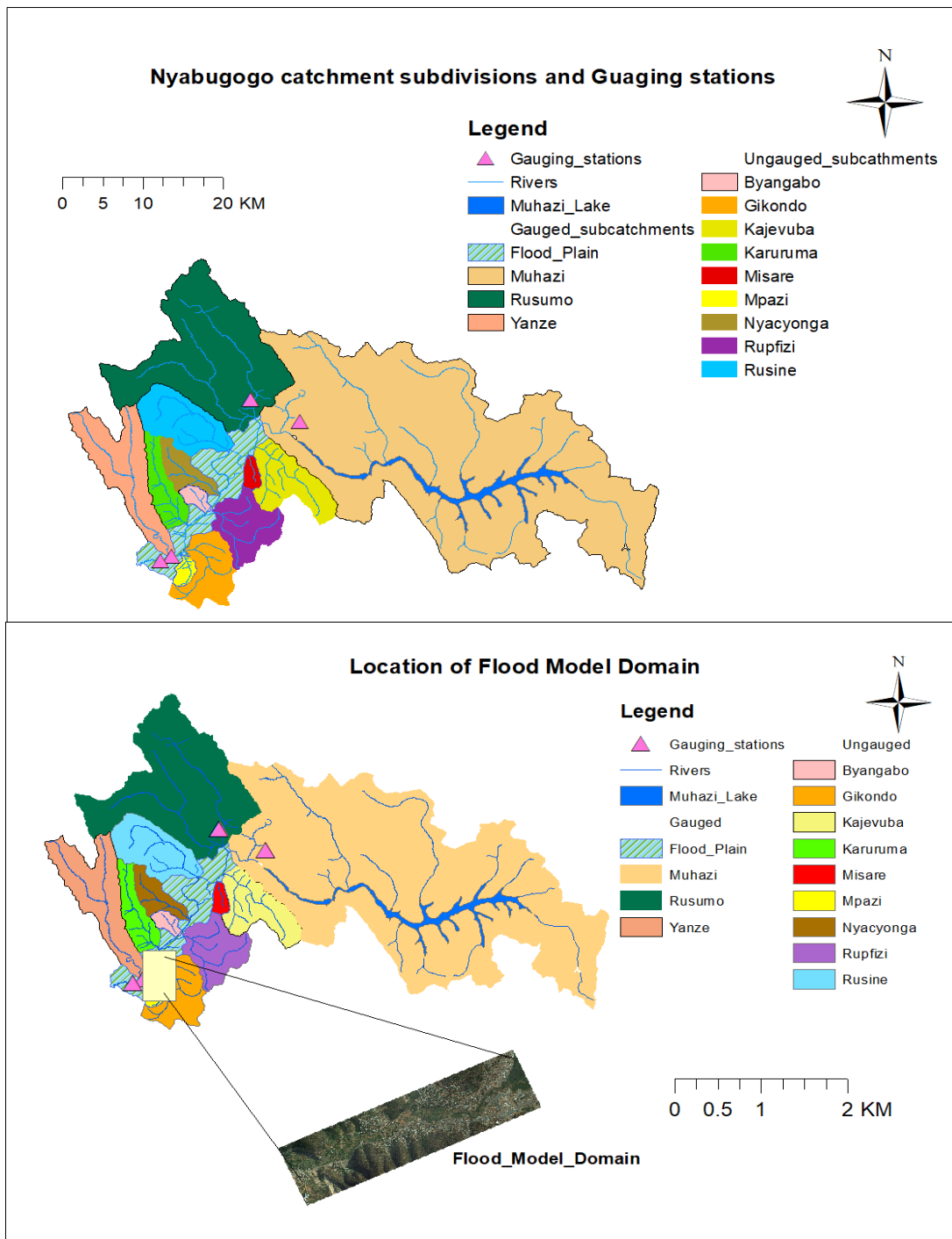


Figure 3-2: Study area conceptualization (top) and location of flood model domain(down) by (Manyifika, 2015) respectively.

Table 3-1: Summary of the data used in the research

Data type	Data	Year	Format	Data source
Climate data	Rainfall	1981-2005	NetCDF	CORDEX-AFRICA
Climate data (RCP4.5 and RCP8.5)	Rainfall	2021-2050	NetCDF	CORDEX-AFRICA
Meteorological data	Rainfall	1981-2017	Excel	Rwanda Meteorological Agency
STRM-DEM	Elevation	2014	Raster	Rwanda Water Board
Soil data	spatial	2014	Raster	Rwanda Water Board
Land use present time	Spatial	2012	tiff file	City of Kigali
Land use projected	Spatial	2050	shapefile	City of Kigali
Hydrological data (for Yanze, Muhazi, Rusumo and Nyabugogo) subbasins	Water stages	2011-2013	Excel	Rwanda Water Portal: https://waterportal.rwb.rw/data/surface_water

3.1.2. Topography and climate of the study area

The topography of the Nyabugogo catchment lies between 1354 and 2278 m a.s.l. The eastern part is dominated by the Muhazi sub-catchment with Lake Muhazi. This sub-catchment and the flood plain (southwest) make the flat area of the catchment. The northern and western parts contain some mountains and high elevation. The climate of the catchment is similar to the country's climate, which is temperate and of equatorial type. The annual rainfall in Rwanda is between 800 and 1600 m, according to the region and altitude. The average temperature is between 16°C and 23°C based on the altitude. Rwandan climate is characterized by four seasons. The long dry season from June to September, short dry season from January to February. The long rain season extends from March to May, and the short rain season extends from October to December (Abimbola et al., 2017).

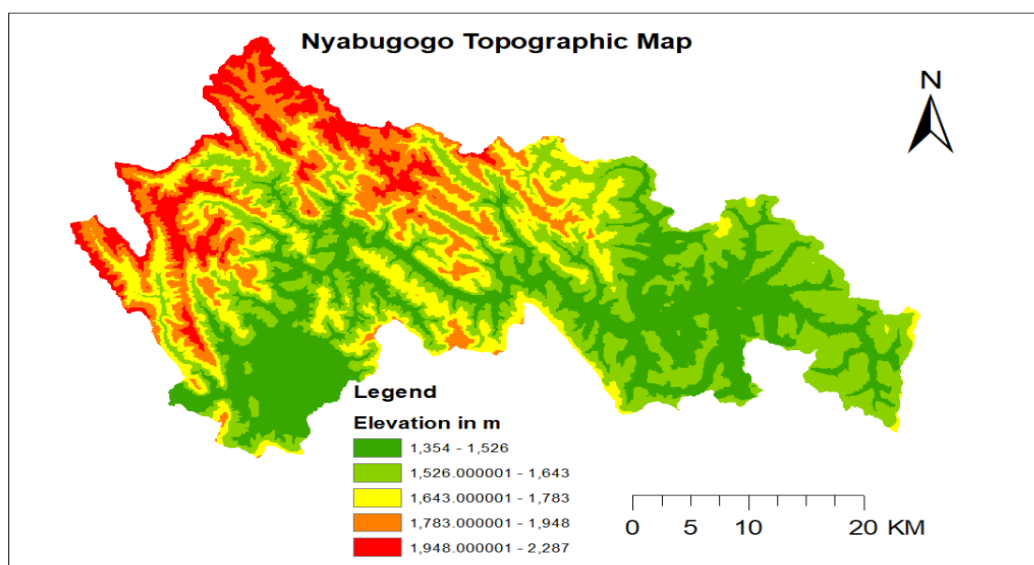


Figure 3-3: Nyabugogo catchment topography

3.1.3. Soil Map

The shale soil type is predominant in the west of the catchment. The central and east are dominated by schist and quartzite with pegmatite and granite. The dominant soil classes are ferrallisols, acritol, luvisols, and lixisol. The central and flood plain of the catchment are characterized by clay soils which lead to low infiltration (Manyifika, 2015).

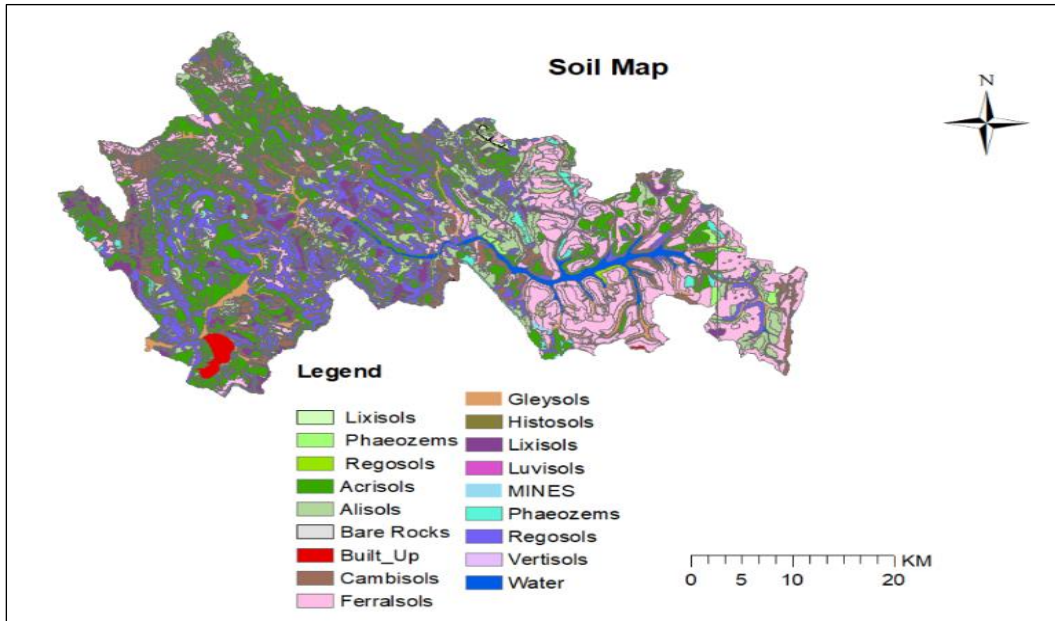


Figure 3-4: Nyabugogo catchment soil map

3.2. Data collection and pre-processing

3.2.1. Existing and future land-use data

The current study attempted to use current and planned land use to assess the impacts on flooding due to land-use changes. The existing land use (2012) was available for the whole country. However, the projected land use (2050) was available only in Kigali city. Therefore, for future land use, the part of the catchment that lies within Kigali was considered to change in the future, while the rest of the catchment was assumed to remain the same in the future. This assumption was also based on the fact that the remaining part of the catchment is located in rural areas, with rainfed agriculture and natural areas being dominant. Therefore, no many changes can be expected as in the city of Kigali.

Figure[3-4] shows for the existing and future land use of the Nyabugogo catchment, it is clearly shown that the catchment is dominated by agriculture. The natural areas and open spaces that include wetlands, protected areas, recreational areas and grassland also occupied a large part of the catchment. For this study, the land-use types for the Nyabugogo catchment were reclassified into five classes. The built-up areas in the southwest are also clearly indicated as the Nyabugogo catchment contains a large part of the city of Kigali. In addition, the relative shows that the built-up areas will increase from 2.62% (2012) to 8% (2050) in the Nyabugogo catchment. The current study takes into consideration the master plan of Kigali, which is being implemented up to 2050, for assessing the land-use change impact on flooding in the Nyabugogo commercial hub. The Master plan gives a long-term prediction of the city.

Table 3-2: The current and planned land use distribution in the Nyabugogo catchment

LULC_Class	Existing (2012)		Planned land use (2050)		Change in percentage
	Area(km ²)	Area(%)	Area(Km ²)	Area(%)	
Built-up	44	2.62	136	8.2	8.51
Forest	144	8.654	150	9.2	0.524
Sparse forest	11	0.66	53	3.2	2.52
Water-body	38	2.3	38	2.3	0
Wetlands	3	0.18	25	1.5	1.32
Parks and open spaces	373	22.416	288	17.3	-5.14
Agriculture seasonal	846	50.84	810	48.6	-2.25
Agriculture Perennial	205	12.319	164	9.84	-2.48

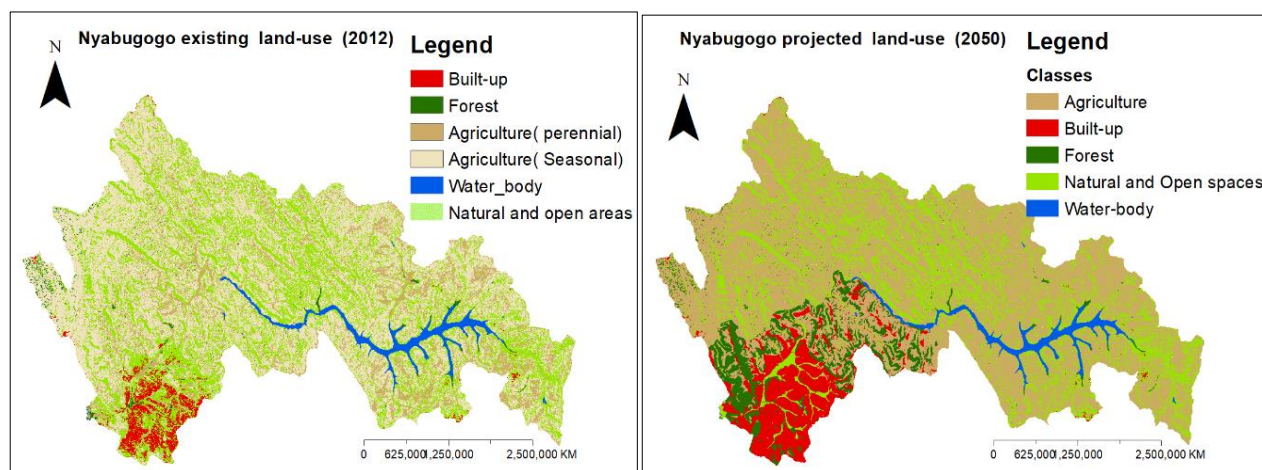


Figure 3-5: Current(existing) and projected land-use for Nyabugogo (right and left), respectively

3.2.2. Meteorological data -Rainfall

Rwanda Meteorological Agency (RMA) is in charge of measuring, storing, and managing all meteorological variables in Rwanda. Time series of rainfall (1981-2005) were provided by Rwanda Meteorological Agency (RMA). Table3-2 shows the location of meteorological stations inside or closer to the Nyabugogo catchment that measures rainfall.

Table 3-3: Meteorological variables inside and around Nyabugogo catchment

Station Name	Location		Elevation(m)
	latitude	Longitude	
Gitega	-1.95	30.06	1518
Kigali_ Aero	-1.95	30.11	1495
Cyinzuzi	-1.76	30	1951
Kawangire	-1.81	30.43	1498
Byumba_meteo	-1.61	30.05	2185
Zaza	-2.11	30.4	1367
Kabarore	-1.62	30.38	1481
Kibungo_Kazo	-2.15	30.5	1474

kiziguro	-1.63	30.28	1448
Gatsibo	-1.55	30.4	1509

3.2.2.1. Rainfall data preprocessing

The historical datasets of rainfall for all stations covering the period 1981 to 2017 were provided by RMA. The preliminary visual inspection showed no missing values in rainfall data. These historical datasets have no missing values because of the quality checking and merging of stations data with satellite estimates which is done by the RMA staff. The TAMSAT satellite is used (Siebert et al., 2019). The satellite datasets comprise high resolution 0.0375 degrees (4 by 4 km) satellite-derived daily rainfall estimates for all Africa from January 1983 to December 2016. Therefore, nine rainfall stations in and closer to the study area were provided, and all stations were considered for this study because of their area of influence on the Nyabugogo catchment and the quality of the data.

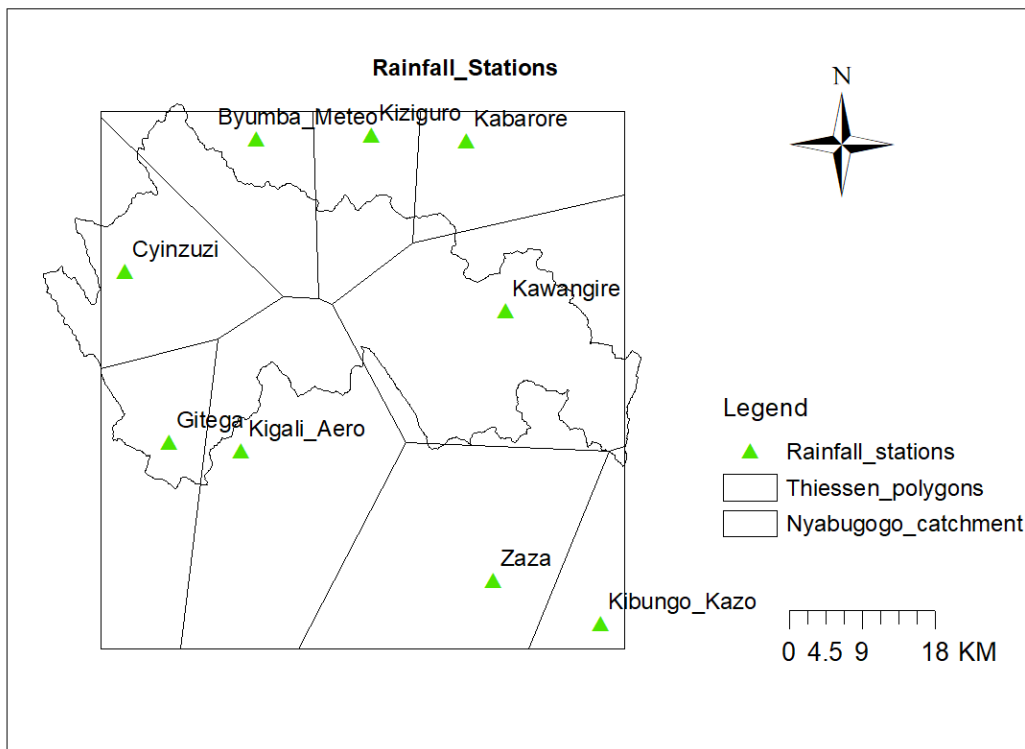


Figure 3-6: Areal representation of rainfall variables using Thiessen polygons in Nyabugogo catchment

The quality checking revealed no missing values in the rainfall data. Therefore there was no necessity of filling in or correction methods. However, consistency analysis was carried out to assess the similarity among different rainfall stations before further application. The aerial estimate of rainfall for Nyabugogo catchment was done by using the Thiessen polygon method as one of the widely used methods and described by many researchers (Brassel & Reif, 1979; Han & Bray, 2006; Olawoyin, 2017). The area of influence of each polygon was dividing with the total area of the catchment to estimate the weight of a given rainfall station to the catchment. Equation[3-1] expresses how to estimate the weight of each station mathematically.

$$P = \frac{1}{A} \sum_{S=1}^{S=n} (A_s P_s) \tag{3-1}$$

Where P and Ps are the average rainfall station rainfall, respectively. A is the catchment area while As is the rainfall station area of influence on the catchment, and n is the number of rainfall stations that influence the targeted catchment.

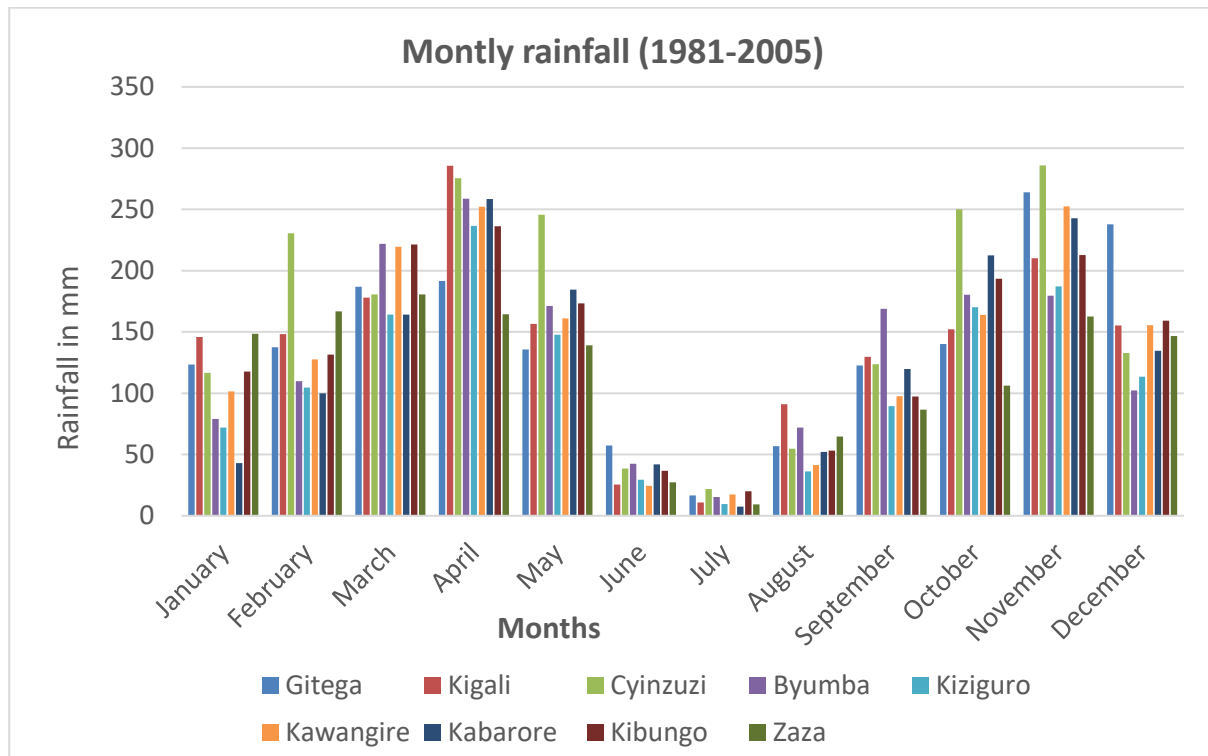


Figure 3-7: Monthly rainfall for all nine stations (1981-2005)

A consistency analysis of rainfall data was done. The double mass curve analysis was done based on annual cumulative rainfall for each station against the annual average cumulative rainfall of surrounding stations (Survsy, 1960). The double mass curves for all stations were virtually unbroken straight lines which indicate the consistency in rainfall records, although at some moments, the points were scattered slightly on both sides of the line. However, all stations proved to have very high regression coefficients ($R^2 > 0.99$). Therefore, the irregularities in stations were not of importance, and the data were considered of adequate quality for the current study. Fig. [3-7] shows examples of the double mass curves for four stations (Kiziguro, Cyinzuzi, Gitega, and Kibungo).

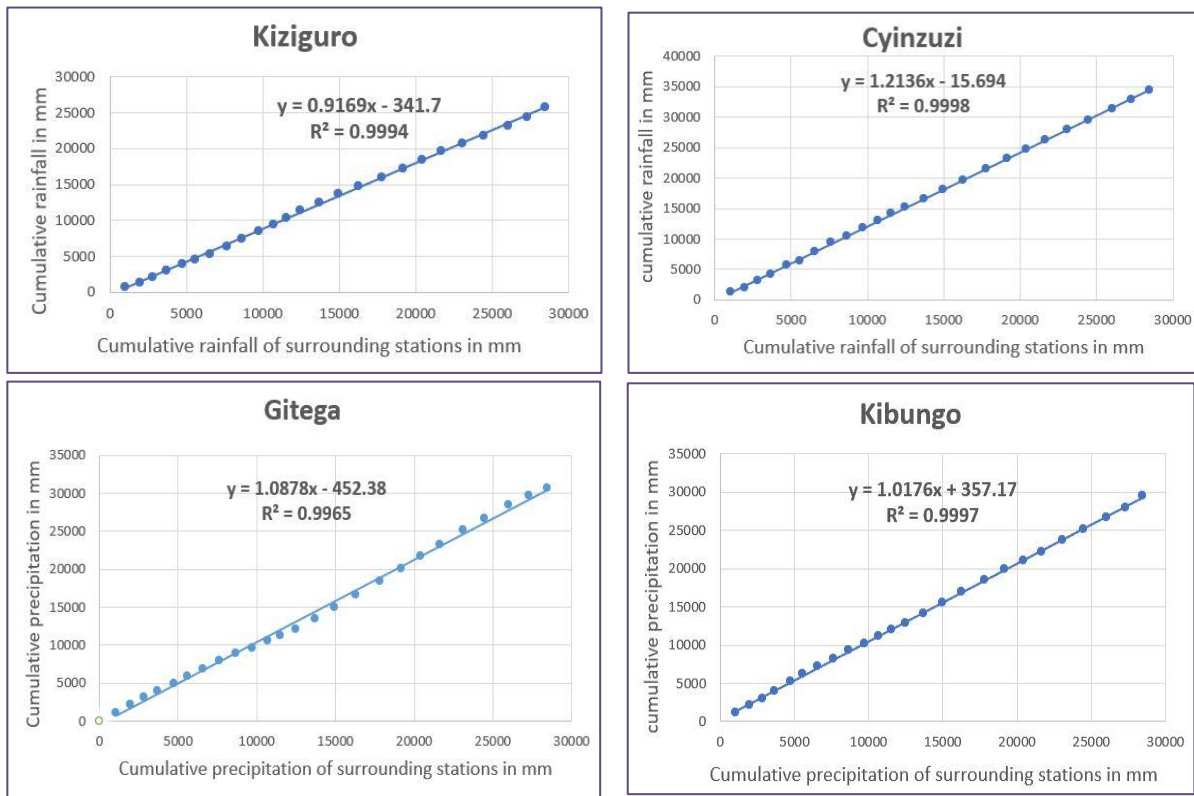


Figure 3-8: Double mass curves of rainfall showing data consistency for different stations

The long-term annual rainfall from aerial representation for the entire catchment is 1017 mm/year. In general, the rainfall dataset covers almost four decades (1981-2017). The annual rainfall increased significantly from 1995, with 2003 having the highest annual rainfall (1429 mm/year) and started to reduce again from 2008. The last period (2013-2017) shows a significant reduction in annual rainfall, with 2017 having the lowest value (484mm/year). Figure [3-8] clearly shows the temporal changes in annual rainfall.

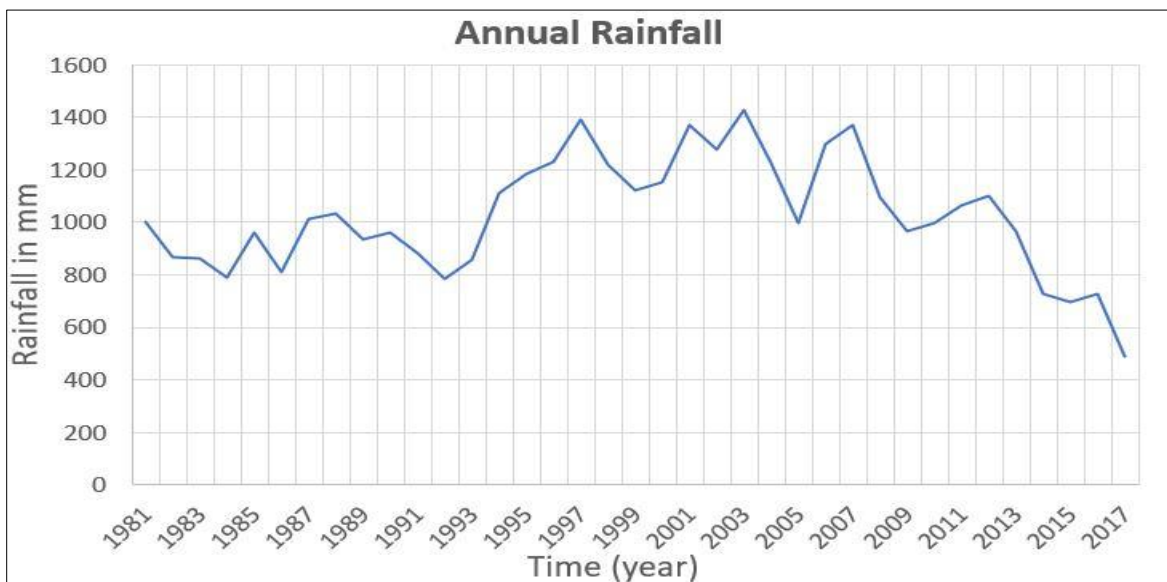


Figure 3-9: Historical annual rainfall from 1981 to 2017

3.2.3. Hydrological data

It is important to have catchment runoff time series in hydrological modeling. The time series help to understand the hydrological response of a given catchment. The river water stages time series were available for the overlapping period 2011-2013 for three subbasins(Yanze, Rusumo, and Muhazi) and for the entire Nyabugogo catchment. These water stages time series were downloaded from the Rwanda water portal. Rating curves were available for only two stations (Nemba for the entire catchment and Yanze sub-catchment). Therefore, this study adopted the rating curves developed by (Manyifika, 2015) after conducting few fields measurements for two other gauged upstream sub-catchments (Rusumo and Muhazi). Therefore, three sub catchments and the entire Nyabugogo catchment are considered gauged while the remaining catchments were considered ungauged. The water levels also were not temporally overlapping for all four gauging stations and were having a lot of missing values. The overlapping period for all four basins 2011-2013 was considered. These available hydrological stations data were qualitatively assessed and corrected and were used for calibration and validation of the rainfall-runoff model.

3.2.3.1. Hydrological data processing

The visual inspection and plots could not clearly show the missing dates for some periods. Therefore, a python code was used to reveal the missing dates in the available water levels. The comparison of produced hydrographs with rainfall was made to asses discharge data consistency and the reflection of extreme rainfall events in the runoff.

Nyabugogo River catchment

Nyabugogo river is the main river in the Nyabugogo catchment. It begins from the outlet of Lake Muhazi and crosses the entire catchment, where it receives many tributaries (Manyifika, 2015). Moreover, the Nemba gauging station located downstream of the Nyabugogo catchment records water stages for the Nyabugogo river. The datasets contained missing values for many years. Therefore, it was difficult and not feasible to fill in missing values for the period of five to ten years gaps. Since the observed discharge data were needed for the validation of the rainfall-runoff model of the entire Nyabugogo catchment for the selected rainfall-runoff events, the dataset was considered to be useful for this purpose despite the missing values, and as mentioned above period 2011-2013 was considered.

The outliers were corrected to fit a newly constructed stage-discharge relationship. The missing values for the short term, such as few days were filled in by applying simple linear interpolation between the value before and after each gap. The rating curve for Nyabugogo is presented in eq.[3-2]

$$Q=5(H-0.1)^2 \quad 3-2$$

Where Q= is discharged in m³/s, H is water stages in m.

Finally, rainfall was plotted with discharge to visually check the reflection of rainfall change in river stream flow, from fig.[3-10], the produced hydrograph is mostly consistent with rainfall in the same periods.

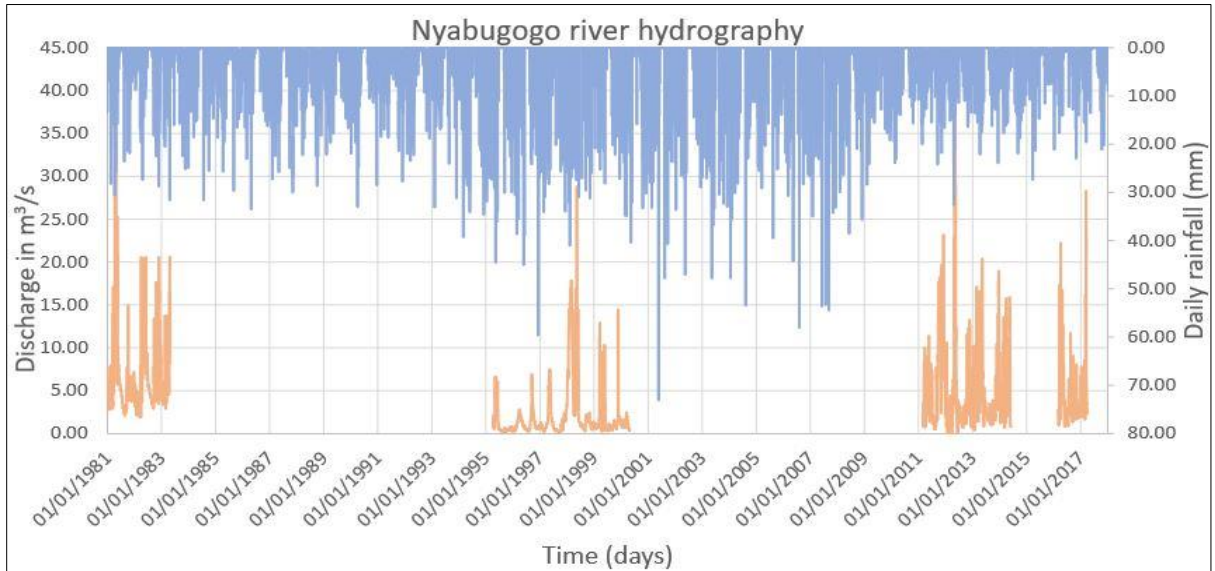


Figure 3-10: Discharge hydrograph for Nyabugogo catchment for the period (1981-2017)

Yanze River sub-catchment

Yanze river is the last downstream tributary to the Nyabugogo river. Its outlet is located closer to the flood model domain. Therefore, it contributes to boundary conditions of the flooding domain. Short-term water stages (2011-2014) records were available with some missing values in between. As mentioned above, a rating curve for Yanze was available. Therefore, it was used to convert the available water stages records into discharges.

The same procedure mentioned for Nyabugogo was followed to process Yanze hydrological data. There were some missing values and outliers. The latter was removed and corrected. Missing values for a short time were filled in by using simple interpolation. The erroneous data were corrected, and missing values were filled in. The rating curve for Yanze is expressed in eq.[3-3] and it was used to convert available water into discharges. The corrected and filled discharges were produced, as it is shown in fig.[3-11]. The peak discharge is shown in 2012, which was the year recorded to have a lot of floods.

$$Q=5(H+0.15)^{2.5} \quad [3-3]$$

Where Q = is discharged in m^3/s , H is water stages in m .

The obtained corrected hydrography was plotted against rainfall to check the discharge consistency and the reflection of rainfall in the runoff. The results showed the consistency and relationship between rainfall and produced runoff, especially for baseflow, but also the correlation is visible on peak flows, see fig.[3-11]

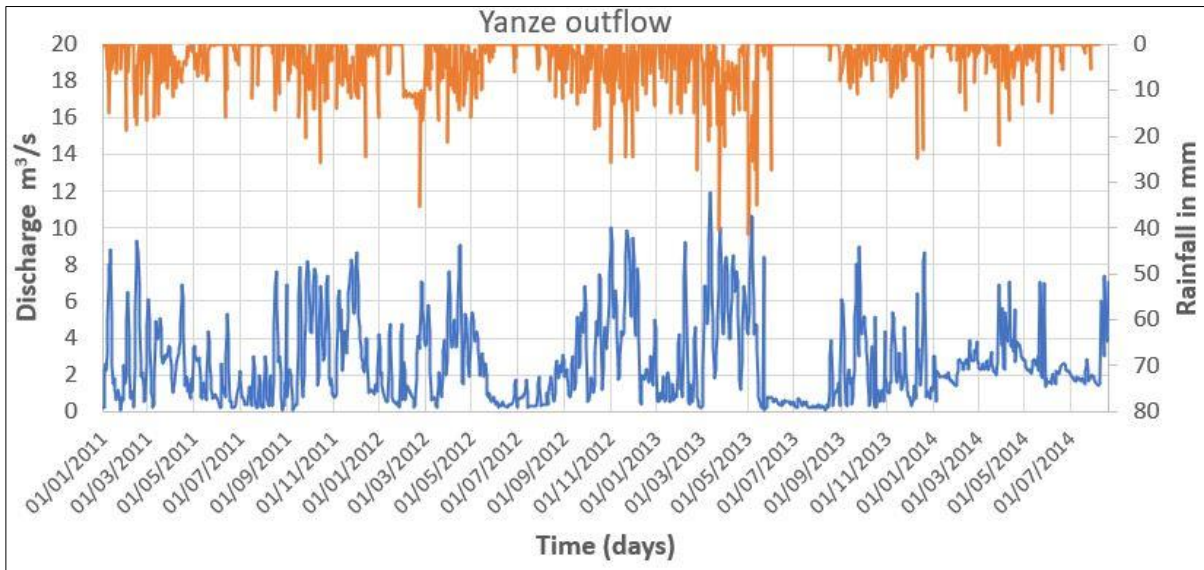


Figure 3-111: Corrected discharge for Yanze river sub catchment (2011-2014)

Rusumo river sub catchment

Rusumo sub catchment is the most upstream sub catchment located in the north part of the Nyabugogo catchment. Water stages of Rusumo were available, and they contain missing values as was observed for the above subbasins. Therefore the correction method is applied, and outliers are removed and corrected. Fig.[3-12] shows the corrected stream discharges for the Rusumo subbasin for the period 2011-2014.

The stage-discharge for Rusumo produced by (Manyifika ,2015) is expressed as

$$Q=1.283448*(H-0.10)^{2.01592} \tag{3-4}$$

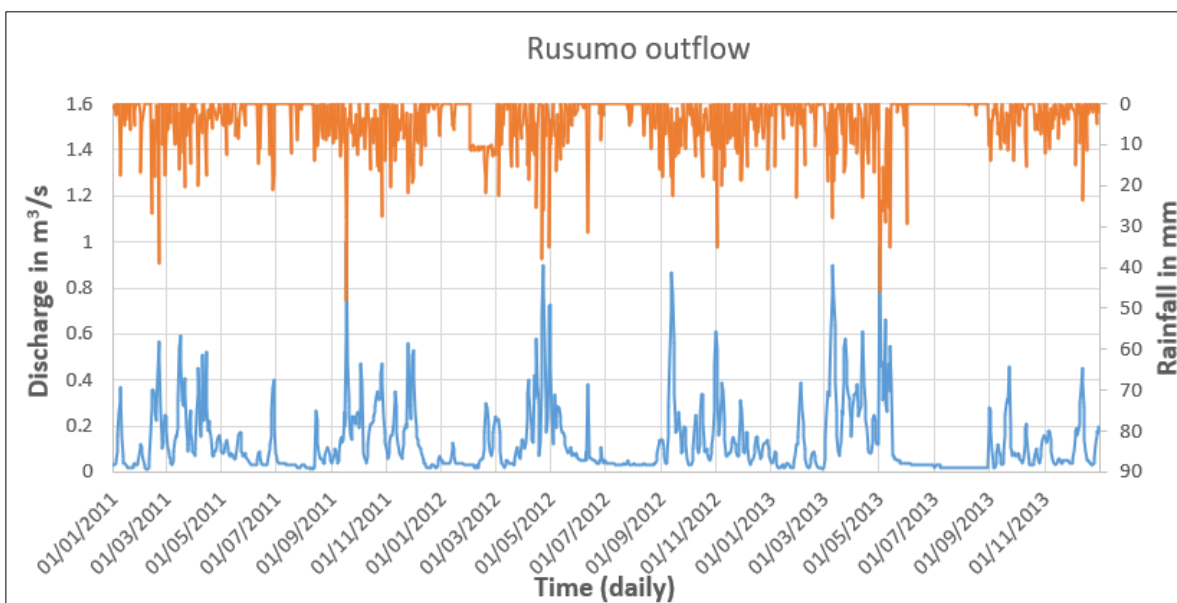


Figure 3-12: Rusumo discharge hydrograph for period (2011-2013)

Lake Muhazi sub catchment

The Muhazi lake sub catchment is the biggest sub catchment in the Nyabugogo catchment as it occupies more than half of the total catchment. The lake has dyke at the outlet, which controls the lake outflow (Manyifika, 2015). At the outlet of this lake is where the Nyabugogo river starts. The water levels for these sub catchments were also downloaded from Rwanda water portal. The missing values for short periods were filled in. the water levels available for this basin were for 2011-2013. Fig.[3-13] shows the discharge hydrograph for this sub catchment.

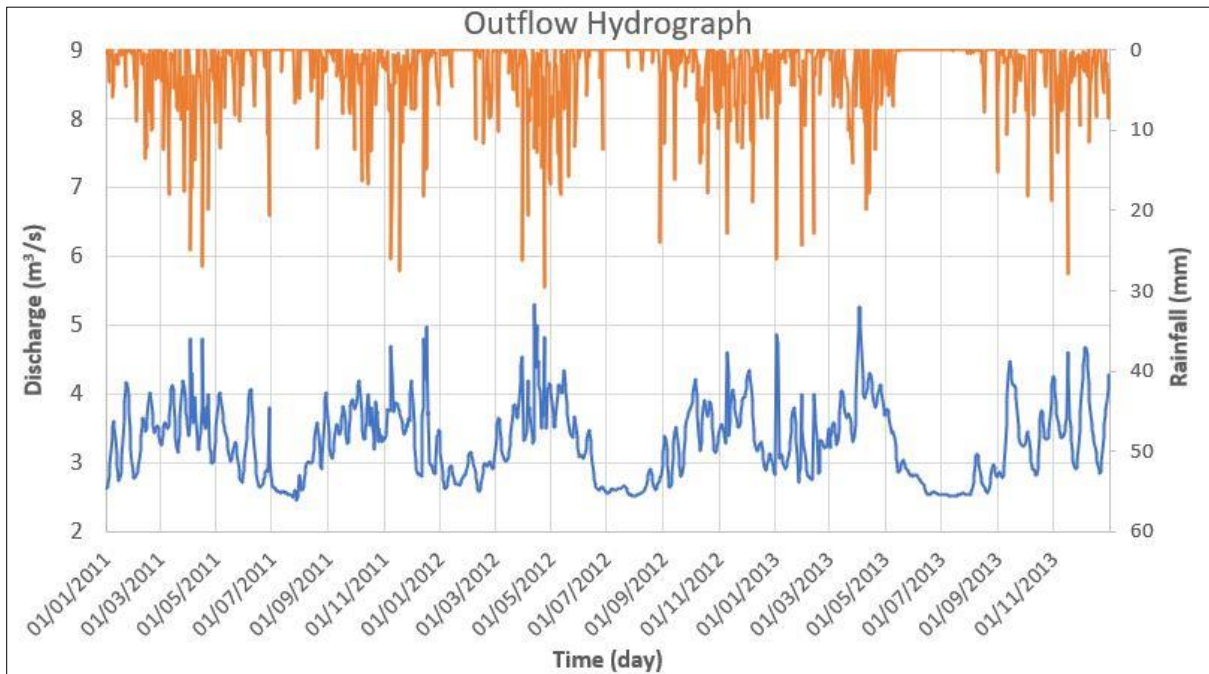


Figure 3-13: Muhazi discharge hydrography for the period (2011-2013)

3.3. RCMs simulations and projections

The climate data (rainfall) were downloaded from CORDEX-Africa for the baseline period (1981-2005) and (2021-2050) for a future periods. The downloaded variables were in NetCDF format. Spider (Python 3.8) was used to manipulate and convert data stored in NetCDF based on RCMs outputs to other formats. Each NetCDF contained a unique variable data for five years temporal scale. Python was used to convert NetCDF to GEO-TIFF, MPR, and finally to Excel format. The RCM output was polarly rotated. Therefore, the spider did mirror rotate of the images and made a subset of data to study domain. The mirror rotated image was masked with the Nyabugogo Catchment shapefile and the selected meteorological stations. This was done in ArcGIS. Nyabugogo catchment and all surrounding meteorological stations fall within four RCM grid boxes. Therefore, four points closer to the center with four meteorological stations were selected in order to make a subset of RCM output to study the domain.

4. RESEARCH DESIGN AND METHODS

4.1. Conceptual framework

The main aim of this study was to assess the impacts of climate and land-use changes on flooding in the Nyabugogo catchment (Rwanda). To achieve this objective, rainfall-runoff modeling and 1D2D flood modeling were employed. This section explains briefly how the formulated objectives and questions are addressed and how the data on land use and climate are used for modeling. Regional climate models were used to obtain projections of extreme daily rainfall for the time period 2050. The HEC-HMS rainfall-runoff model was used to estimate streamflow runoff from extreme rainfall under changing land use conditions. The 1D2D SOBEK flood model was, by means of model, inflow boundary flows forced by respective streamflow discharges. The flood characteristics (i.e., water depth, velocity, and areas of inundation) for the current time period and the future period were established by the 1D2D SOBEK model. Figure [4-1] provides a flow chart on the methodology adopted in the research.

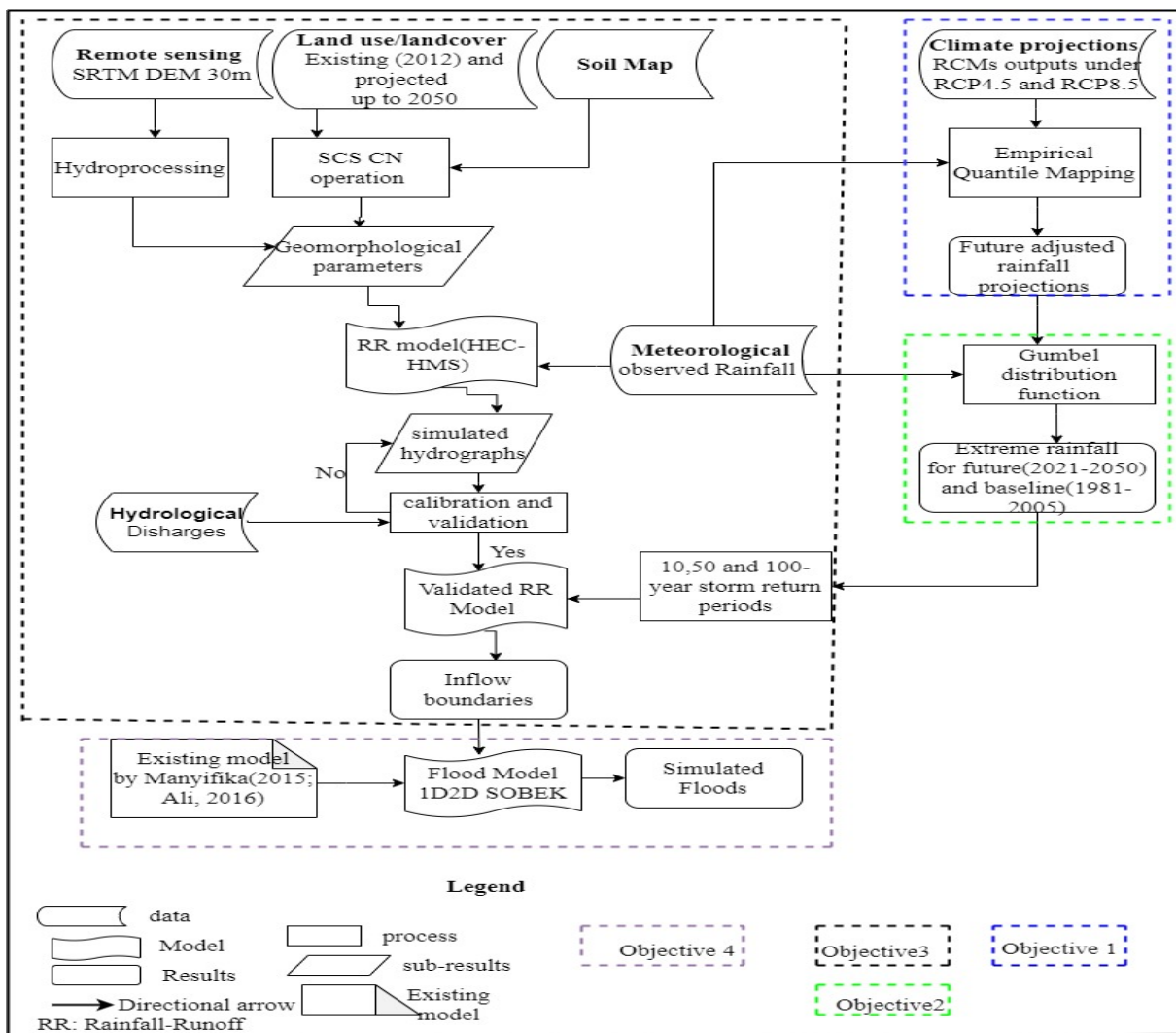


Figure 4-1: Flowchart of the methodology

4.2. Objective One: To acquire climate change data (precipitation) from RCMs, compare and analyze the projections among the set of RCMs

4.2.1. CORDEX AFRICA and its experiments

Coordinated Regional Climate Downscaling Experiment (CORDEX) is a Coupled Model Inter-comparison Project such as (CMIP,3,5, 6) investigative Model Intercomparison Project (MIP) and requesting specific CMIP outputs for regional climate downscaling. The CORDEX vision is to advance and coordinate the science and application of regional climate downscaling through global partnerships. CORDEX Africa comprises five different experiments: historical, radiative forcing of 2.6 W m⁻² (rcp2.6), radiative forcing of 4.5 W m⁻² (rcp4.5), and radiative forcing of 8.5 W m⁻² (rcp8.5). For this study, RCM information and RCM climatic output time series were obtained from the CORDEX-AFRICA website: (<https://climate4impact.eu/impactportal/data/esgfsearch.jsp#project=CORDEX&domain=AFR-44&>).

The meteorological variables with daily frequency such as precipitation (pr), minimum temperature (Tmin), maximum temperature (Tmax) are available at AFR_44 domain, 0.39° horizontal resolution (44km spatial resolution).

4.2.2. Regional Climate Models (RCMs) selection

For this study, Regional Climate Models (RCMs) were used to obtain rainfall estimates for future period (i.e. rainfall projections). Under CORDEX-AFRICA, data on climate projections for a number of RCMs is available for use in research. Nevertheless, detailed climate change impacts studies cannot incorporate all the models projections (Lutz et al., 2016). Therefore, the general approach is to select one or a few climate models based on multiple criteria as the selection itself is not straightforward. For the selection of RCMs, four criteria were used. Firstly, RCMs were selected based on the fact RCM have been used in various studies. Outcomes were proven to give acceptable simulations compared to the observed climate data in East Africa and in Africa in general, where the study area is located (Endris et al., 2013, Dosio et al., 2015, Bucchignani et al., 2018, Ayugi et., 2020, Wu et al., 2020). Secondly, selected RCMs to have climate simulations performed for the selected baseline period (1981-2005) as well the as future projections for both emission scenarios RCP4.5 and RCP8.5 for the future time window (2021-2050).Thirdly, the RCM outputs must be available on a daily time step. Fourthly, the RCM outputs must not have missing values. Three regional climate models with a single driving General Circulation Model for each, as shown in Table 4-1, were selected and used for the current study. This study attempted to use the ensemble mean of the regional climate models because (Ayugi et., 2020, Endris et al. (2013) show that ensemble estimates have a better agreement with the observed data than the estimates from individual models.

The historical period (1981-2005) selected was based on the availability of observed datasets in the study area .The future window (2021-2050) with two emission scenarios RCP4.5and RCP8.5, was selected to match the available time period with land-use planning of 2050 used in this study.

Table 4-1: Selected Regional Climate Models (RCMs) and Driving Global Circulation Models (GCMs)

RCM Name	Driving GCM	Contributing institute	Reference
REMO2009 (MPI)	MPI-M-MPI-ESM-LR	MPI-CSC, Max Planck Institute for Meteorology, Climate Service Centre, Germany	(Endris et al., 2013) (Ogega et al., 2020)
RCA4 (SMHI)	MIROC-MIROC5	Swedish Meteorological and Hydrological Institute, Sweden	(Wu et al., 2020), (Ayugi et., 2020) (Ogega et al., 2020)

CanCM4(CCCma)	CCCma_CanESM2	Canadian Centre for Climate Modelling and Analysis, Canada	(Mascaro et al., 2015) (Osima et al., 2018)
----------------	---------------	--	--

4.2.3. Assessing the RCM simulations compared to observed data

Once the RCM outputs were downloaded and preprocessed, comparison approaches were used to assess the simulations and predictive ability of each RCM relative to the observed rainfall in the baseline period. This comparison was also made to evaluate if bias adjustment was required in future projections. The comparison was made on monthly rainfall and mean monthly standard deviation. The monthly comparison was used because the fine time, such as daily, was not showing the realistic comparison. Basically, the deviation of simulated RCM outputs from observed rainfall indicates that model simulation alone is unlikely to give reliable estimates of either the mean value or daily variability of precipitation in a future climate. In that case, there is a need for bias adjustment in order to have confidence in their future rainfall projections. In addition, the precipitation estimates from RCMs were considered rainfall estimates because the study area lies in a tropical climate (Abimbola et al., 2017); therefore, no snow or freezing will occur.

4.2.4. Empirical Quantile Mapping

The numerical model simulations often show typical systematic deviations from the observed climate data, limiting their usability for further application. The biases in RCM outputs may arise from the driving circulation model, physics behind RCM (Noguer et al., 1998), such as spatial resolution, local topographic features (Themeßl, 2012), etc. Therefore, it is of much importance to adjust the bias in climate model outputs in order to have a better agreement with observed actual data (Maraun, 2013). The bias correction methods range from simple scaling approaches to more sophisticated techniques that use probability mapping.

Among the various available methods for bias correction, the delta change approach and quantile mapping are widely applied. However, the delta approach does not adjust RCM simulations but uses RCM to change mean signals and observations (Teutschbein & Seibert, 2012). This method includes adding the difference between climatological means between RCM baseline and future period to observed data. It uses an assumption that the variability in climate scenarios remains unchanged (Amengual et al., 2012). The current study adopted Empirical Quantile Mapping (EQM) presented in (Amengual et al., 2012a). (Themeßl et al., 2011) after a comprehensive inter-comparison of seven Downscaling Error correction methods (DECMs) for daily precipitation found that this method outperforms the other investigated DECMs. This method return means, variability and shape errors of the simulated RCM cumulative distribution functions (CDFs) of climate variables and is able to reproduce the extreme variables (Themeßl et al., 2012). This technique implements statistical transformation for the post-processing of RCM outputs. It involves the transformation of distribution functions of simulated variables into observed ones by using a mathematical function (Enayati et al., 2020; Themeßl et al., 2011). Eq.[4- 1] shows the expression of the formula

$$X^0 = f(x^m) \quad [4-1]$$

Where X^0 = observed variable; x^m = simulated variable; f = transformation function

Quantile mapping uses quantile-quantile relations to converge the modeled variables distribution functions to observed counter parts; therefore, with CDFs of both modeled and observed variables time series, their quantile relation can be determined by the following expression

$$X^0 = F^{-1}_o [F_m(x^m)]$$

In which $F_m(x^m)$ = CDF of x^m ; and $F^{-1}_o[]$ = inverse form of the CDF of x^o that is referred to as the quantile function

Unlike other quantile mapping methods, Empirical Quantile Mapping is a non-parametric QM method that uses a non-parametric function. “It estimates values of the empirical CDFs of modeled and observed time series for regularly spaced quantiles. It uses interpolations to adjust a datum with unavailable quantiles” (Enayati et al., 2020).

The technique involves calculating changes, quantile by quantile, in CDFs of daily RCM outputs between the baseline period and future time period. The obtained changes are rescaled based on the observed CDF for the same control period and later added quantile by quantile to these observations to find new calibrated future CDFs that transmit the climate change signal (Amengual et al., 2012a)

The change (Δ_i) between RCM uncorrected simulated variables for baseline period values indicated as (S_{ci}) and uncorrected future period values indicated as (S_{fi}) of climate variability such as precipitation for i^{th} quantile shown by eq.[4-2]. Hence, changes (Δ_i) in quantile by quantile in CDFs are obtained. The uncorrected data represents the RCM modeled values without bias adjustment. Likewise, the mean value of RCM simulated variables for the baseline period ($S_{c\text{mean}}$) and simulated counterparts for the future period values ($S_{f\text{mean}}$) are also calculated in order to obtain mean changes (Δ_{mean}) in the simulated values eq.[4-3]. Furthermore, the (Δ'_i) is calculated as a difference between Δ_i and Δ_{mean} by eq.[4-4] in order to obtain changes in quantile by quantile of CDFs and then added to observed values (o_i) quantile by quantile to get bias-adjusted future values (p_i) with eq.[4-5].

$$\Delta_i = S_{fi} - S_{ci} \tag{4-2}$$

$$\Delta_{\text{mean}} = S_{f\text{mean}} - S_{c\text{mean}} \tag{4-3}$$

$$\Delta'_i = \Delta_i - \Delta_{\text{mean}} \tag{4-4}$$

$$P_i = O_i + \Delta'_i \tag{4-5}$$

Where:

Δ_i = daily change between future raw simulated and uncorrected baseline variables, S_{fi} = future simulated uncorrected variables, S_{ci} = baseline simulated raw variables, Δ_{mean} = change in the mean of future simulated uncorrected variables and baseline simulated raw variables, $S_{f\text{mean}}$ = mean in future simulated raw variables, $S_{c\text{mean}}$ = mean in baseline simulated uncorrected variables, Δ'_i = difference between Δ_i - Δ_{mean} , O_i = Observed variables in the baseline period and P_i = future adjusted variables (precipitation for this study).

4.3. Objective Two: Extreme rainfall events.

The flooding events are most likely to be caused by extreme rainfall events instead of low intensity of rainfall. Therefore, this study identified the extreme rainfall events from the RCMs outputs and observed rainfall in the baseline periods. The definition of the extreme events in this study followed the definition given by National Centers for Environmental Information (NCEI): <https://www.ncdc.noaa.gov/climate-information/extreme-events>. By definition, the extreme events are in the outmost ten percent of the RCM simulation sample set. Therefore, the 10th and 90th percentiles values of the sample set are considered as low and high extreme rainfall events, respectively. The 10th percentile denotes the dry climate corner, while the 90th percentile represents the wet climate corner. However, since this study was interested in flood modeling, only high extreme rainfall events were identified. The 99th percentile was calculated for both RCPs and the

obtained values we compared with observed rainfall for each station to assess the changes in the future extreme rainfall events. The 99th percentile was selected to identify the most severe flood events.

4.4. Objective two : To design extreme rainfall for floods modeling

For estimating the peak flood discharges and floods at the desired location, it is important to determine the design storms for that purpose. For arriving at such a design rain event, the statistical analysis by fitting the probability distribution to the rainfall is carried out. Among different probability distributions, the family of the Extreme Value Distributions including Extreme Value Type-1(Gumbel), Generalized Extreme Value, Extreme Value Type-2(Frechet), and Extreme Value Type-3 (Weibull), is widely applied for Extreme Value Analysis of rainfall (Casas et al., 2011; Vivekanandan, 2017). Among the distribution functions, Gumbel distribution has the advantage of having the only positive values as the rainfall time series are always positive (i.e. rainfall has values large or equal to zero). Therefore, the Gumbel is employed in this study in the present research to analyse the extreme values. The parameters of the Gumbel distribution were determined by using the Maximum Likelihood Method (MLM), and these parameters are used to determine daily extreme rainfall for different return periods.

For the current study, the Gumbel distribution function was fitted by annual maximum rainfall extracted from daily rainfall data observed at rain gauges during the baseline period (1981-2005). the same procedure was repeated for annual maximum rainfall of daily rainfall for future projections (2021-2050) under both emission scenarios (RCP4.5&8.5) and then were used to estimate daily extreme rainfall values. The descriptive statistics such as standard deviation, average, coefficient of variation were determined for both observed rainfall and future projections. The CDF of the Gumbel Distribution Function was also developed and is given by the equation below

$$\text{CDF: } F(R) = e^{-e^{-(R-\alpha)/\beta}} \quad \beta > 0, \text{ where } (R_1, R_2, R_3, \dots, R_N) \quad [4-6]$$

Where β and α are scale and location parameters of the distribution respectively. These parameters are calculated by Maximum Likelihood Method (MLM) and are used to estimate the rainfall (R_T) for different return periods from $R_T = \alpha + Y_T$, where $Y_T = -\ln(-\ln(1-(1/T)))$ is called reduced variate for a given return period T (year) (Vivekanandan, 2017).

4.4.1. Daily extreme rainfall distribution

Daily rainfall (10, 50, and 100-year return period) was distributed throughout the day. This was done in order to design the hyetograph that is required in the HEC-HMS rainfall-runoff model. The synthetic rainfall distribution found in (SCS 1986) was used for this purpose.

The (National Resources Conservation Service) NRCS Curve Number (CN) Method uses synthetic rainfall distributions to distribute the daily rainfall throughout the day. Basically, these synthetic rainfall distributions were developed for some areas, such as the continental United States. However, the regions where they are not available such as the current study area, will need to be developed. The method is based on the concept of rearranging the storm pattern so that the greatest rainfall depth value occurs at the middle of the total duration. More description can be found in TP-149 (SCS, 1973).

The Gitega- station in Kigali provided 10-minute precipitation data from March 2019 to November 2020. These data were used to distribute daily extreme rainfall throughout the day. The developed distribution was based on the short time rainfall record. Hourly rainfall distributions from Gitega station were compared with theoretical storm distributions from other studies in the region to assess their satisfactoriness. These

studies include (Fiddes 1974 “The prediction of storm rainfall in East Africa”, Schmidt and Schulze 1987 “Design stormflow and peak discharge rates for small catchments in South Africa”) with reference to the similar study by (FONERWA 2019) in a volcanic region of Rwanda.

The provided 10-minute precipitation in the period (March 2019–March 2020), only 11 days had more than 10 mm rainfall. The selection criteria were based on the rainfall-producing runoff. This means the storms with a total depth equal or greater than 10 mm rainfall depth that could produce runoff were considered to avoid incorporating minor drizzle throughout a day. The disaggregation of the daily precipitation values using a synthetic storm distribution allows determining the intensity of different duration storms for the different return periods.

4.5. Objective three: To develop a rainfall-runoff model for simulating impacts of climate and land-use changes on streamflow in the Nyabugogo catchment

4.5.1. Rainfall-Runoff Modelling

In the current study, the HEC-HMS rainfall-runoff model was selected among other hydrologic models. It was selected based on the fact that it is a semi-distributed hydrological model which allows simulating spatial geographic variations in the subbasins explicitly. This model enables the division of the watershed into small subbasins and then allows to simulate runoff behavior from different geographic locations. It explicitly allows assessing the impacts of land-use changes on streamflow through the use of intermediate curve numbers in the software. This model requires less data, making it a good option in data-scarce areas such as the current study area. The main inputs to the model are rainfall, soil and land use/cover types, and discharge for calibration of the model. The model can be used for continuous or event-based simulation based on the purpose of the study. In this research, the model was needed to simulate boundary inflows for the 1D2D SOBEK flood model from extreme rainfall events for flood modeling.

4.5.2. HEC-HMS Model

The HEC-HMS program with different sub-models that are included in the program is described in HEC-HMS technical reference (Report (TR-55), 1986) and (Feldman, 2000). It is a conceptual model that simulates the hydrologic behavior of the catchments. ArcGIS with ArcHydro together with HEC-GeoHMS were used to delineate the sub-basins in order to generate the characteristics of the basin (area, basin centroid, reach length, slopes). STRM DEM (30m) was used to delineate stream networks and subbasins and were imported in HEC-HMS as basin files.

HEC-HMS is arranged in four main modules: first, the basin model that consists of hydrological elements such as subbasin, reach, junction, source, diversions, and sink (outlet). Second, the meteorological model is provided with the rainfall data, which is connected to all sub-basins. Thirdly, the control specifications model includes the start and end time, date, and duration time stamps for the simulation. And finally, the input data is in the form of time series where rainfall and stream flow gauges are connected to the basins.

HEC-HMS includes several methods that are arranged, from losses methods that estimate initial losses from the rainfall before the runoff starts to the methods that regulate the baseflow. For the current study, the choice of each method (sub-model) in HEC-HMS was mainly based on the ability of the method to estimate the required parameters with regard to the available data. Figure [4-2] shows a summary of the process and the methods used to simulate runoff in the HEC-HMS model

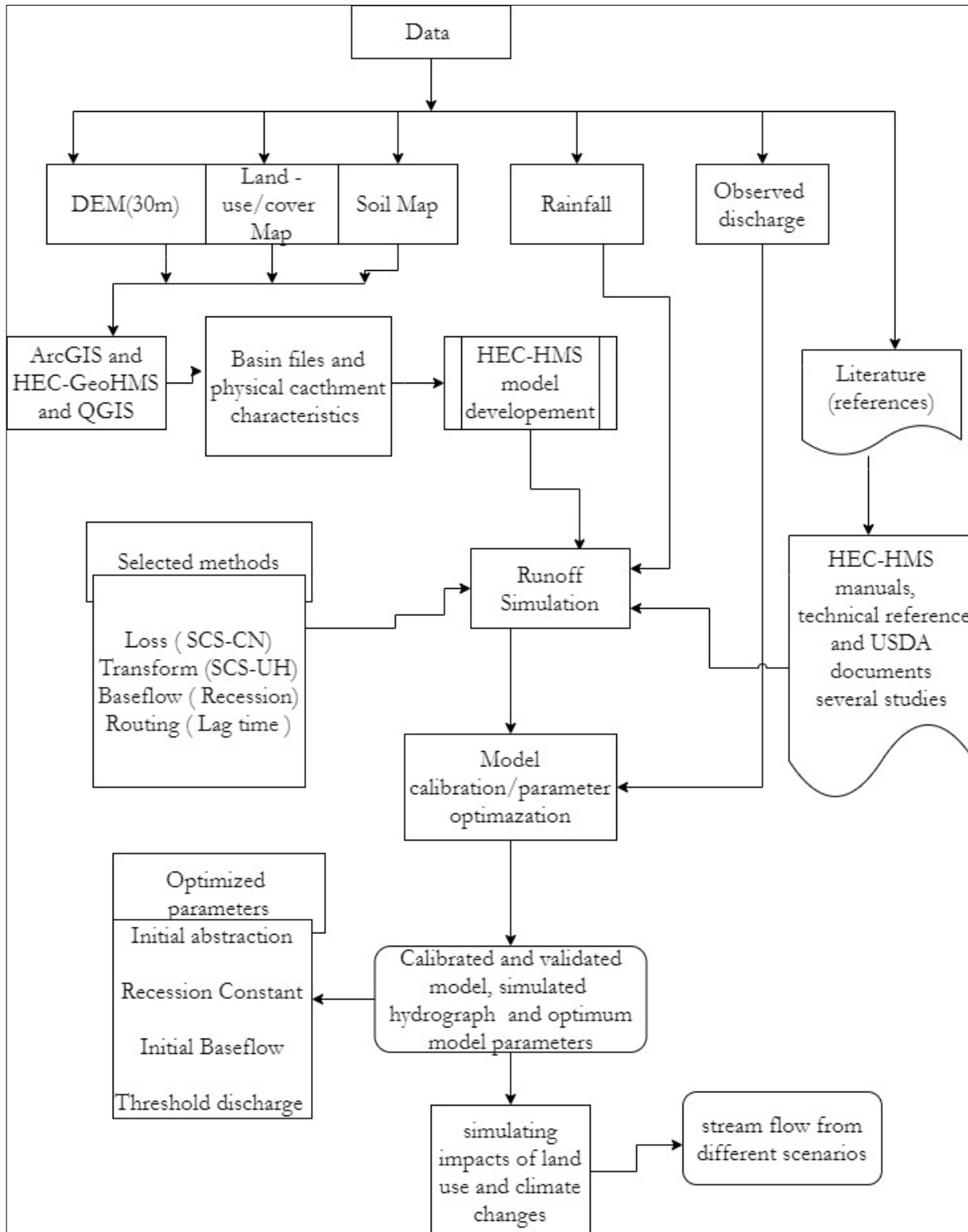


Figure 4-2: Summary of the process and the used methods in the HEC-HMS Model.

4.5.2.1. Runoff estimation

In HEC-HMS, twelve different methods are available to compute the runoff volume, and they are known as loss methods. Some methods were designed for continuous simulation, while others are for events only. Loss methods consider the initial losses from the rainfall before the runoff begins; therefore, runoff volume

is calculated from cumulative excess rainfall. Although some of these methods consider the percentage of the impervious areas in the watershed and the initial losses before calculating runoff volume, they do not explicitly address the impacts of land-use changes for runoff volume except SCS Curve Number method (Report(TR-55), 1986)

This method allows the computation of runoff as a function of cumulative precipitation, land-use/cover, soil types, and antecedent soil moisture. Thus, it explicitly incorporates the effect of land-use changes for runoff through the use of an intermediate parameter called curve number (CN) that is used as input in the HEC-HMS software. With this method, the changes in land-use/cover are first observed in changed curve number values between studied periods. Subsequently, these changes propagate in the computed runoff volumes. In addition, the SCS CN loss method is an event-based loss method. This study was interested in simulating the runoff from selected extreme rainfall events to find inflow boundaries for flood modeling. Therefore, the SCS-CN method was the suitable option for the current study compared to other available loss methods in the HEC-HMS software

4.5.2.2. SCS-Curve Number (CN) loss method

The SCS CN loss method is one of the most popular methods used to compute the depth of surface runoff from a certain event for a small catchment. It is simple, easy to understand, and useful for ungauged watersheds. Its efficient performance is partly based on using a reduced number of parameters (Tramblay et al., 2010). It is widely accepted because it accounts for the most runoff-producing watershed characteristics such as land use, soil type, land treatment, and antecedent moisture condition (Mishra et al., (2004). The SCN-CN method was developed by the Soil Conservation Service of the United States in the Department of Agriculture (USDA-SCS, 2004).

The SCS CN loss method is based on one parameter called the curve number. This method computes runoff volumes by determining the volume of water that is intercepted, evaporated, infiltrated, transpired, and stored in surface depression, and it subtracts it from the precipitation. That amount of rainfall that is subtracted is called initial abstraction (Ia).

The SCS-CN loss method calculates directed runoff (Q) by using the following mathematical equation

$$Q = \frac{(P-Ia)^2}{(P-Ia)+s} \quad P > Ia \quad [4-7]$$

Where:

P= total precipitation (mm), P should be greater or equal to Ia. Otherwise, Pe will be zero (0). Ia= initial abstraction (mm), Q= direct runoff in (m³/s) or excess rainfall in (mm), S= potential maximum retention (mm) . S parameter is interpreted as the maximal water retention capacity, and it acts as the initial condition of the model reliant on the antecedent moisture conditions (Tramblay et al., 2010).

The main factors that are used to calculate the curve numbers (CN) are hydrological soil groups (HSG), the land cover type, land treatment, hydrological condition, and antecedent moisture condition. Curve numbers are in the range of 100 for water bodies and 30 for permeable soils having a high infiltration rate. Moreover, this method considers whether the impervious areas are directly connected to a drainage system or whether they are connected to pervious areas before entering the drainage systems. The directly connected impervious surfaces are the portion in the basin for which all precipitation goes to runoff without any loss; this means no evaporation, no infiltration, no interception, while the rainfall falling on the pervious areas will be subjected to losses. In the current study, curve numbers were calculated based on the hydrological soil groups (HSG) and land-use and hydrological conditions (Report(TR-55), 1986). The procedures and

the CN look-up tables followed to calculated curve numbers are described in detail in (Report(TR-55), 1986). The soil and land-use land/cover classification for the current study were explained in chapter3

Hydrologic soil groups (HSG)

The infiltration rate of the soil varies based on surface intake and subsurface permeability. The Hydrological soil groups fall into four categories, namely A, B, C, and D (United States Department of Agriculture, 1986). with the minimum infiltration capacity is found for bare soil. The hydrological soil groups of the Nyabugogo catchment were established with the help of the SPAW model and ArcGIS software. The SPAW model allows determining the hydrological soil group based on soil textures and saturated hydrological conductivity (Saxton & Willey, 2009).

Table 4-2: Hydrological soil groups for the current study based on soil textures (Report(TR-55), 1986)

HSG	Soil textures
A	Sand, loamy sand, or sandy loam
B	Silt loam or loam
C	Sandy clay loam
D	Clay loam, silt clay loam, sandy clay, silty clay, or clay

Curve Number calculation procedure for the current study

The obtained hydrological soil groups were combined with land-use/ land-cover classes through the union Tool of ArcGIS, and DEM was required in HEC-Hydro. Generally, ArcGIS and HEC-Hydro, and QGIS software were used to complete the procedure of estimating the weighted curve numbers values for current and future periods. The look-up tables are used to relate curve numbers with certain soil hydrological groups and land-use/cover types. For the current study, two look-up tables were developed based on the current and future land-use/cover by considering that the hydrological soil groups will remain unchanged in the future. The land-use/cover classes were not equal for the current and future periods as for the future as-built-p class was detailed for the future. Therefore, based on the percentage area cover of each built-up sub-class in the future, the weighted curve number for built-up areas in each hydrological soil group was estimated for the future period. This was done to avoid the curve numbers underestimation for built-p areas in the future period as the percentage of the built-up area increases for the future period. Tables 4-3 and 4-4 show the CN lookup tables used to calculate CN for the study area for both current and future periods following CN lookup tables in (Report(TR-55), 1986).

Table 4-3: CN lookup table adapted in determining the CN grid with the existing land-use

Land-use	HSG A	HSG B	HSG C	HSG D
Wetlands	98	98	98	98
Water-body	100	100	100	100
Sparse forest	36	60	73	79
Forest	30	55	70	77
Glass land and open spaces	44	65	77	82
Built-up	61	75	83	87
Agriculture (seasonal)	72	81	88	91
Agriculture (Perennial)	67	78	85	89

Table 4-4: CN lookup table adapted in determining the CN grid with the future planned land-use

Land-use	HSG A	HSG B	HSG C	HSG D
Water-body	100	100	100	100
wetland lands	98	98	98	98

Sparse forest	36	60	73	79
Forest	30	55	70	77
Grasslands and open spaces	44	65	77	82
Residential low density	54	74	80	85
Residential medium density	61	75	83	87
Residential high density	77	85	90	92
Commercial	89	92	94	95
Industrial	81	88	91	93
Transportation	98	98	98	98

For the watershed that comprises different soil types and land use, a weighted CN is calculated with the following equation

$$CN_{weighted} = \frac{\sum AiCN_i}{\sum Ai} \tag{4-8}$$

Where $CN_{weighted}$ is the weighted or composite CN used for runoff computation, i is an index of watershed subdivisions of uniform soil and land-use types, CN_i is the curve number of watershed subdivision i , and A_i is the drainage area for watershed subdivision i . for the current study, the average CN for each subbasin was calculated using the zonal statistical tool in QGIS.

Once the curve number is calculated, the potential maximum retention S (mm) can be calculated using eq 4-8. Practically, the curve number (CN) is used to compute potential maximum retention

[4-9]

$$S = \left[\begin{array}{l} \frac{1000-10CN}{CN} \text{ foot - pound system} \\ \frac{25400-254CN}{CN} \quad [SI] \end{array} \right]$$

Once the S potential maximum retention is obtained, the initial abstraction is calculated by using the following relation

$$I_a = \lambda S \tag{4-10}$$

Where: λ = Initial abstraction ratio

In most cases, the initial abstraction ratio largely depends on the climatic conditions. Originally, it is considered as a constant value 0.2 based on the original SCS-CN method (Report(TR-55), 1986).

Therefore, the unique runoff amount is determined by substituting I_a with S , and the eq.[4-7] becomes a function of P and S .

$$Q = \frac{(P-0.2s)^2}{(P-0.8s)} \tag{4-11}$$

The Initial abstraction I_a (mm): the initial abstraction is the portion of the rainfall that is deducted from the total depth rainfall at the begging of the rainfall-runoff event. It represents the presence of vegetation, which prevents permanent or temporary precipitation from reaching the soil surface; thus, rainfall is initially intercepted by vegetation. It also represents water in surface depression and infiltration, evaporation that

takes place before runoff begins. The initial value of I_a (mm) can be estimated in two alternatives. The first is to let the model define an initial value by using the eq.[4-12] based on the conclusion of studying several experimental basins in the united states (Ahbari, Stour, Agoumi, & Serhir, 2018).

$$I_a = 0.2 \frac{25400 - 254CN}{CN} \quad [4-12]$$

I_a = initial abstraction in mm; CN= curve number

Once the CN is entered into the software, the model uses the above equation to calculate initial abstraction. The value 0.2 is set as default in the model, and then this value is multiplied to potential surface retention obtained from curve number see eq.4-9.

The another option is to calculate I_a (mm) based on observed rainfall-runoff events. I_a varies from watershed to watershed and from event to event; this second option may help to estimate the nearly true value of the initial abstraction based on accurate observations. Under the current study, the author opted for the first alternative because the temporal resolution (daily) of the available rainfall-runoff data restricted the use of the second option. The optimum initial abstraction value for each event was obtained through model calibration.

SCS CN loss method limitations

The use of the SCS CN loss method has some limitations. The studies proved that the initial abstraction is not the same for all watersheds and mostly depends on the initial conditions prior to the rainfall (Mishra et al., 2004, Mishra & Singh, V. P., 2013). It was shown that a single watershed could have a set of curve numbers as well. This is due to the heterogeneity of the watershed characteristics such as temporal and spatial variability in rainfall, quality of observed rainfall-runoff data, and variability of the antecedent rainfall with the associated soil moisture amount (Ponce & Hawkins, 1996, Baltas et al., 2007). Therefore, the studies conducted on the applicability of the SCS-CN method suggested the need for further improvement or repairing of the method (Mishra & Singh, V. P., 2013)

4.5.2.3. 4.3.2.3. Direct Runoff estimation

Two types of models are available in the HEC-HMS program to compute the direct runoff from excess rainfall. These models transform excess rainfall into point runoff (Feldman, 2000). The first category is made of empirical models. These are the traditional unit Hydrograph UH models that attempt to establish the relationship between excess rainfall and runoff without considering the detailed internal processes. The parameters and equations used for these models lack fully physical meaning; however, they are selected, and they can be optimized for some goodness of fit-criterion. The second category is made of conceptual models. These models represent to the possible extent all physical mechanisms that govern the movement of excess rainfall over the watershed land surface and in small collector channels of the watershed. These conceptual models are referred to as kinematic wave models. For conceptual models to compute runoff from rainfall, they required a set of elements that describe the watershed's physical characteristics. Ponce (1991) argued that the kinematic wave model is suitable for small watersheds less than 2.5 km² where the physical details of the watershed can be determined without compromising the nature of the model; thus, the use of UH models for large-area is recommended (Feldman, 2000). Therefore, for the current study, kinematic wave models could not be used since the area of the watershed under study is greater than 2.5km², and not all the required watershed characteristics for this method were available for the current study. Then, an empirical model which is based on unit hydrography was selected.

The empirical models based on UH uses excess rainfall to compute runoff.

For the current study, SCS UH model was chosen. SCS UH Model is based on the dimensionless single-peaked UH. This dimensionless UH expresses the UH discharge, U_t , as a ratio to the UH peak discharge, U_p for anytime t , a fraction of T_p , which is a time to UH peak. SCS suggested that UH peak and time of UH peak are related by the equation:

$$U_p = C \frac{A}{T_p} \quad [4-13]$$

Where:

U_p is UH peak discharge, C is a conversion factor (2.08 in SI and 484 in foot-pound system), A is the watershed area, T_p is the time to UH peak discharge. The T_p is related to the duration of excess precipitation through the following formula.

$$T_p = \frac{\Delta t}{2} + t_{lag} \quad [4-14]$$

Where Δt is excess precipitation duration, t_{lag} is the watershed lag time which is defined as the time difference between the center of mass of excess precipitation and the peak of UH. The SCS UH hydrograph peak and time to peak are estimated as a function of the time of concentration.

$$t_{lag} = 0.6 T_c \quad [4-15]$$

where T_c is the time of concentration for a given watershed.

SCS UH model is simple and is easy to understand. It is based on a single parameter lag time. The lag time is derived for gauged watersheds. However, the method is applicable for ungauged watershed since SCS suggested that UH lag time may be related to the time of concentration T_c as expressed in eq4-15. The T_c can be determined for ungauged watersheds based on physical basin characteristics where the observed data are not available. The lag time enables the estimation of model parameters for the future based on the characteristics of the catchment. This marks the choice of this model under the current study over the other transform methods in the program.

Due to the lack of observed stream flow time series, in this study, time of concentration was estimated as the function of geometrical characteristics of the catchment by using the Williams formula (Williams, 1922). This method was selected to determine the time of concentration based on the fact that that it was described for the mountainous and steep slope areas such as the current study area (Nyabugogo catchment).

$$T_c = 21.3L \frac{1}{A^{0.1} S^{0.2}} \quad [4-16]$$

Where T_c is the time of concentration in minutes, T_c is the time that takes the most distant runoff to travel to the interesting point in the watershed. T_c is a summation of all travel time for consecutive components of the drainage delivery system. The travel time is the time it takes the water to travel from one point to another in the watershed. L is the length of the main channel, S is the slope of the watershed, A is the basin area. Once T_c is computed, then lag time is calculated using eq.[4-15].

Once the lag time is obtained, the program solves equation 4-14 and 4-13 to obtain time to UH peak discharge and UH peak discharge. Therefore, with U_p and T_p known, the UH can be found from the dimensionless form which is built into the program with the multiplication (Feldman, 2000).

4.5.2.4. Modeling Baseflow

The baseflow method estimates the responses of the sustained runoff prior to the precipitation that was temporarily stored in the watershed and combined with the delayed subsurface flow from the storm event

being simulated. In most stream channels, baseflow is composed mainly of groundwater that infiltrates the river and is known as base runoff.

In this study, the exponential recession method was used to simulate the baseflow. The recession method uses a single exponential equation eq.[4-17] that relates initial baseflow and the baseflow at time t . this helps to determine the baseflow for each timestamp during the simulation.

$$Q_t = Q_0 k^t \quad [4-17]$$

where:

Q_t (m^3/s) is the baseflow at any time t , Q_0 (m^3/s) is the initial baseflow at time zero, K is the exponential decay constant or recession coefficient. K is defined as the ratio of baseflow at time t to the baseflow of one step earlier. The starting baseflow value Q_0 is the initial condition in the model. Q_0 is a specified flow rate (m^3/s), or it can be specified as flow per unit area ($m^3/s / km^2$).

The recession coefficient for this study time was one day, thus, K (per Δt). It is calculated by plotting the recession limb in a semi-logarithmic plot, which appears as a straight-line plot with a constant slope independent of the initial Q_0 value. Therefore, the recession constant k is calculated as the negative slope of a least-squares fit the pairs $((t-t_0), \ln Q(t))$.

The recession constant parameter impacts the slope of the baseflow hydrograph. K varies between 0 and 1. K equal to 1 gives a constant/flat baseflow response, while lower values indicate the watershed with quick recession. The recession coefficient depends on the simulation time step and the area of the subbasin. The short time step increases the value of K , and the large area subbasins have a large value of K compared to small basins (Jakada et al., 2019).

Once baseflow is computed, the total runoff is calculated as a summation of baseflow and direct runoff in the HEC-HMS software.

This graph shows the recession changes subject to ground water storage in the basin. As time progresses, the infiltration of groundwater to the channel reduces and results in higher values for K that result in a more gradual recession and baseflow discharges that will converge to a more constant value. The recession curve 1 shows the quick recession and this yield in low values of K while the recession curve two shows slow recession and this yield in high recession coefficient compared to the first one.

4.5.2.5. Modeling flow in the channel/ routing method

Once the model parameters converting the rainfall into runoff have been estimated, the estimated runoff hydrographs have to be routed downstream to generated the streamflow at the outlet of the basin. It is achieved through the use of routing methods. These methods compute the downstream hydrograph based on the upstream hydrograph and the characteristics of the stream network system (i.e. Stream network density and respective cross-sectional flow areas) that convey the amount of water. These models govern the water movement in the channels before they leave the basin. Some of these methods in HEC-HMS simulate the flow of water in the channels by solving both continuity and momentum equations, also known as St. Venant or the dynamic wave equations.

In the HEC-HMS program, there are six routing models. A simple form of routing method was chosen for the current study. This is because the sub-catchments under the current study are relatively small. The travel time of water in the channels to the outlet is small time such as a few hours. However, the observed data to estimate model parameters for some models were not available. Therefore, a simple lag routing model was

selected. With this model, the time of concentration T_c can be estimated from available watershed physical characteristics, and then lag time can be determined as a portion of T_c as indicated in equation.[4-18]

For the current, the observed hydrographs were not available; therefore, the lag time was estimated as time of concentration in the following formula:

$$T_{lag}=0.6T_c \quad [4-18]$$

The lag routing method is based on time of concentration (T_c) and travel time of water (T_t). The travel time is the time it takes water to travel from the beginning of the channel to the end of the channel. Travel time is a component of T_c . T_c is the time for runoff to travel from the most distant point of the watershed to the outlet of the catchment. Time of concentration T_c is the summation of all travel time for consecutive components of the drainage conveyance.

Technical Release 55 (TR-55) (SCS, 1986) gives details about time of concentration and travel time and their calculations. Therefore, the travel time between the beginning and the end of each channel was calculated by using the following equation

The travel time T_t is the ratio of flow length to flow velocity.

$$T_t=L/3600v \quad [4-19]$$

Where

T_t = travel time in min, L = flow length in ft, V = average velocity in ft/s (feet later converted to meters)
3600 = conversion factor from seconds to hours

Once the travel time is obtained, the time of concentration is obtained as the summation of travel time

$$T_c=T_{t1}+T_{t2}+T_{tn} \quad [4-20]$$

T_c =time of concentration (T_c)

N =number of segments

For the current study, the entire flow length (channel) for all streams with respective sub catchment was considered as one flow segment. Therefore, travel time was calculated only on that segment, and time of concentration was equal to the travel time for each channel.

$$T_c=T_t$$

The length of each channel was known from stream delineation. However, the average velocity was not known. Average velocities for estimating travel time are given in (SCS, 1986). Therefore, the average velocity was calculated based on the slope of each stream channel. (SCS, 1986) gives the relationship of average velocity and slope for paved and unpaved areas.

Based on the knowledge of the author for the study area, all stream channels are unpaved except for one channel in the Mpazi sub-catchment. Thus, the average velocity for each stream channel was determined by using the average velocity table from (SCS 1986). The average velocity is the function of the watercourse slope and channel type. With flow length L and average velocity V known, the travel time was calculated by

using equation 4-20. After Obtaining the travel time, which is equal to T_c of concentration in this study, Lag time was calculated following relation given by (Feldman 2000) and equation [4-21]

$$T_{lag} = 0.6 * T_c \quad [4-21]$$

Finally, with lag time into the model, the program routs the upstream hydrograph to the end of the stream channel without changing the ordinates but only lagged in time.

4.5.2.6. Model Calibration

The model calibration involves tuning the model parameters with the objective to achieve the model estimates that are in the range of observed real data. This shows how well the model can represent the observed values.

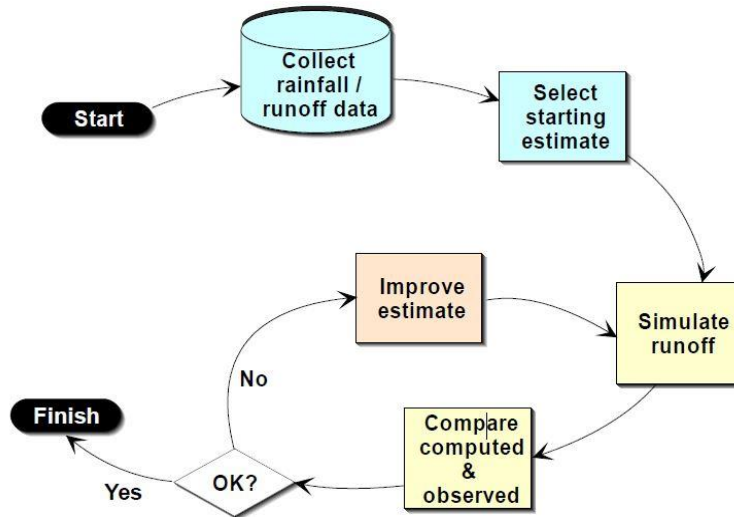


Figure 4-3: Schematic representation of calibration process

The performance of the model has to be determined. There are different objectives functions that can be used to assess the model performance. For this study, two goodness of fit functions were used to evaluate model performance: Nash-Sutcliffe (NSE) model efficiency and relative volume error (RVE). NSE =1 means a perfect match, 0.8 to 0.9 means excellent performance, while 0.6 and 0.7 means adequate model performance. For RVE, 0 is a perfect match; the values between -5% and +5% indicate a well-performed model. RVE between +5% to +10% or -5% to -10% indicates a fairly performing model.

$$NSE = 1 - \frac{\sum_{i=1}^n (Q_{sim(i)} - Q_{obs(i)})^2}{\sum_{i=1}^n (Q_{obs(i)} - \bar{Q}_{obs})^2} \quad [4-22]$$

Where Q_{obs} = the observed flow, Q_{sim} = simulated flow \bar{Q}_{obs} = the mean of observed flow, and n is the number of days

$$RVE = \left(\frac{\sum_{i=1}^n Q_{sim(i)} - \sum_{i=1}^n Q_{obs(i)}}{\sum_{i=1}^n Q_{obs(i)}} \right) 100\% \quad [4-23]$$

Where Q_{sim} = simulated flow, Q_{obs} = the observed flow, and n = number of days

4.5.2.7. Simulating streamflow considering climate and land-use changes

Once the HEC-HMS model was calibrated, it was used to simulate the rainfall-runoff relation by using projected extreme rainfall under climate change conditions and projected land-use changes by 2050. The simulated streamflow hydrographs served to simulate streamflow inflow boundaries of the 1D2D SOBEK flood model.

Four cases were considered to study impacts of climate and land use on streamflow which was later used in flood modeling. These cases are the following:

1. Current case or baseline period: where present land-use and extreme rainfall estimated based on the observed rainfall for the baseline period were used (1case)-(1case)
2. Considering the impacts of land use change only: this means by updating the curve number and impervious areas for the future periods. The rainfall inputs to the model remained unchanged as this is the same as used in case1. (1case)
3. Considering impacts of extreme rainfall due to climate change under RCP4.5 and 8.5 scenarios but land-use remained unchanged to represent land-use of the current period (i.e.as in case1) (2cases).
4. Considering the combined effects of projected extreme rainfall under RCP4.5 and 8.5 climate change scenarios and with land-use change projections for the period 2050 (2cases).

For each case return period of 10, 50 and 100-years was used, and this makes the total number of the cases simulated to be equal to 18.

4.6. Objective Four: To simulate Flooding for Nyabugogo commercial hub under changing climate and land use.

4.6.1. 1D2D SOBEK flood model

The current study has adopted an one dimensional (1D) hydraulic flow model to simulate flows in the drainage channel. The 1D flow model was integrated with a two-dimensional (2D) inundation model to simulate flooding in the floodplain. The 1D2D SOBEK model is a physically-based computational model developed by Deltares (<https://www.deltares.nl/en/>). SOBEK has wide applications in studies for flood forecasting, irrigation control system, drainage system optimization (Suman & Akther, 2014; Doong et al., 2016; Haile& Rientjes, 2005; DHONDIA & STELLING, 2004).

In SOBEK, the St. Venant equations are solved for the a succession of cross-sections of the main channel and the overbank, which is perpendicular to the river channel using a finite difference approximation, which allows the use of rectangular grids (SOBEK-User Manual, 2019). Firstly, the water level is interpolated in the 1D computational grid points and later is imported into to the 2D flood model. In SOBEK, 2D flood flows are simulated by solving the continuity equation and the momentum equation in x-and y-directions. A detailed description of SOBEK can be found in different versions of SOBEK-user manuals such as (SOBEK-User Manual, 2019).

For the current study, the 1D2D SOBEK model for Nyabugogo Commercial Hub in Kigali downtown was used. This model was first built by (Manyifika, 2015) for flash floods assessment in Kigali using satellite rainfall products. The model was adopted and improved by (Ali, 2016) in his MSc research, where he has

focused on the detailed digital urban terrain characterization for flood modeling in Kigali. The summary of the model is given below, and details about the model setup can be found in (H. T. Ali, 2016).

Firstly, the channel characteristics such as cross-sections obtained from the topographical survey together with water level, river bed, and friction factor were used to build a 1D schematization in the SOBEK NETTER. SOBEK-Rural 1D Flow has coupled with SOBEK Overland Flow(2D) module. The three upstream inflows were defined for the model; the first is the contributing upstream area called upstream. The second was from the outlet of the Yanze sub-catchment, and the last is from the outlet of the Mpazi sub-catchment. They used the a 2D boundary nodes for upstream inflows to the model.

They defined the surface roughness, which normally indicates the resistance to the flow of water in the flood model domain; the roughness was defined using Manning's equation. The orthophoto 0.25m resolution for the study area was used for six of the land-use classes in order to define roughness shown in table 4-5:

Table 4-5:Manning's Roughness Coefficient adopted from (Ali, 2016)

Class	Landcover	Manning's Roughness Coefficient, n (s/m-3)
1	River	0.03
2	Roads	0.025
3	Residential area	0.035
4	Commercial area	0.032
5	Green area	0.04
6	Buildings	1.Solid 1 2. Partially 0.7 3. Hallow 0.3

As shown in the table, the model was used to evaluate the effects of buildings on flooding by considering three cases. Firstly, buildings are considered as solid objects, and in this case, the building completely blocks the flow of flooding water. Secondly, the building was considered a partial object. Thirdly, buildings were considered as hallow objects with a relatively small roughness value. For the buildings considered as solid objects; they require DEM to include heights of buildings.

The effects of DTM resolution were also evaluated using 5m, 10m,15m, and 20m DEM resolutions. This was done because the representation of the physical process of the real world depends on the grid resolution. The small sizes enable accurate representation of urban topography, but they are computationally expensive. On the other side, large sizes lose important system details as a result of the averaging. However, they are less computation expensive. In their results, the large resolution, such as 20m, failed to represent some features such as hill ridges and valleys, whereas the small resolution 5m represented well urban features.

The sensitivity analysis was conducted on upstream and downstream conditions, and they found that the conditions were not very sensitive to the model. The model was calibrated only with the roughness coefficient, which was available. The other parameters, such as the recorded flood depths in the study area in the past, were not available.

Under the current study, the same model was adopted to simulated the floods from extreme rainfall under changing climate and land use. 10m DEM resolution was selected to run the model under the current study. This resolution was selected in order to enable urban topographical representation but also to reduce the computation time required for a small DEM resolution of 5m as there were 18cases to simulate. Each case was built separately, and the simulation time interval was 15min. The 10m DEM resolution case obtained

from (Ali, 2016) model was imported in the SOBEK schematization, and the boundary inflows were changed regarding the determined inflows boundaries from extreme rainfall under changing climate and land-use changes. The model was run, and the results were exported in ASCII file format and were visualized in ArcGIS environments. And then, floods maps from different cases were compared to evaluate the effects of climate and land-use changes on flooding.

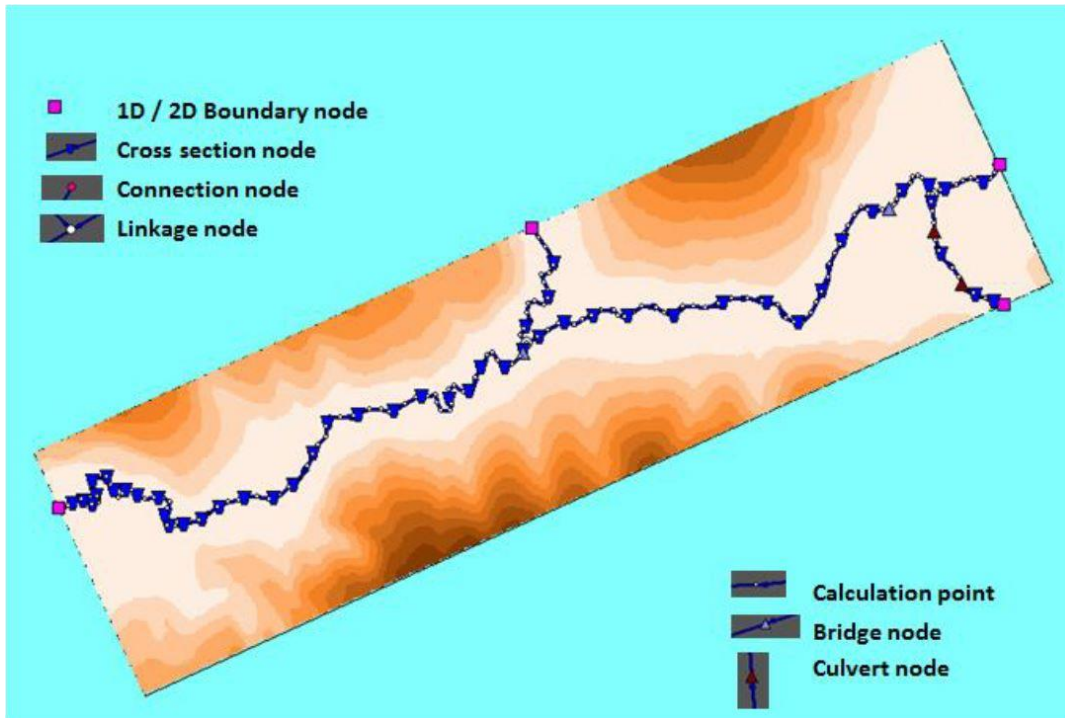


Figure 4-4: 1D2D SOBEK schematization of Nyabugogo commercial hub flood model by (Manyifika, 2015; Ali, 2016)

5. RESULTS

This chapter represents the findings and outcomes of the adopted methods with regard to the main objective and the specific objectives of this study. Therefore, explanations and interpretations are given to results found with how climate change and land-use interventions will affect discharge hydrographs and flooding in the Nyabugogo catchment. The results are presented based on the specific objectives adopted in this study from the first to the last objective.

5.1. Objective One: To acquire climate change data (precipitation) from RCMs, compare and analyze the projections among the set of RCMs

5.1.1. Regional circulation models

Regional Circulation Models used in this study were from CORDEX-Africa, as mentioned earlier. From the screening of RCMs based on the approach mentioned in the chapter 4, only three RCMs (RCA4, REMO2009, and CanCM4) remained and were used in this research. The preprocessing of RCMs outputs using Python algorithm enabled the data to work with them in other software such as Excel. After preprocessing, the comparison between observed historical rainfall and raw baseline and future rainfall projections was performed to evaluate the performance of RCMs in reproducing observed rainfall before further use.

5.1.2. Monthly rainfall distribution in Nyabugogo catchment

Figure.[5-1] shows the distribution of monthly rainfall for different stations in the Nyabugogo catchment from raw simulated rainfall and observed data in the baseline period (1981-2005). All models failed to reproduce the monthly rainfall patterns except in June and July that marks the dry season with very low rainfall. In the remaining months, CanCM4 showed an overestimation while REMO and RCA4 showed an underestimation of monthly rainfall. The ensemble mean of RCMs was computed by using the arithmetic mean method, and it shows an improvement in capturing the monthly rainfall with the highest amount in the short rain season (October, November, and December).

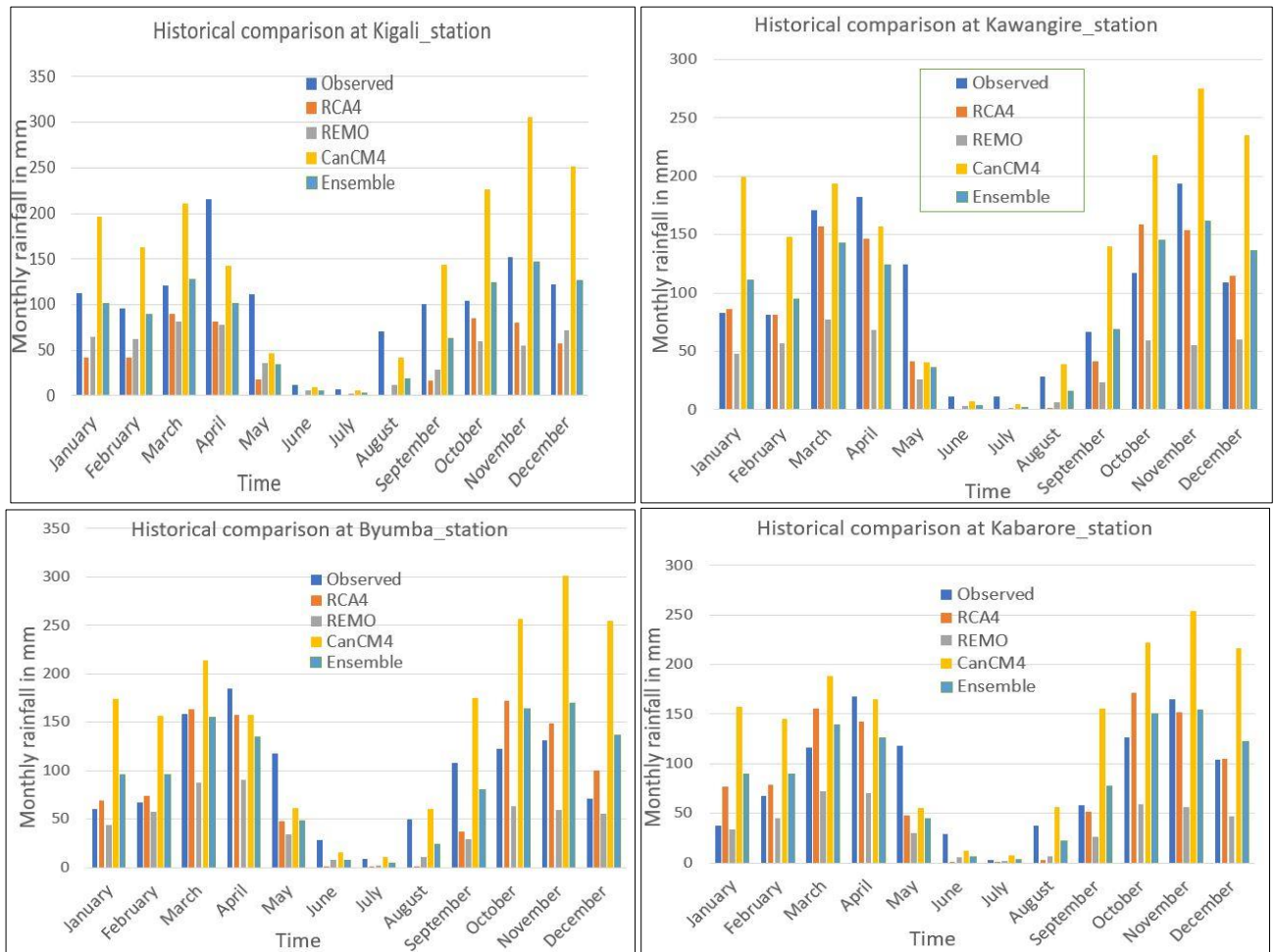
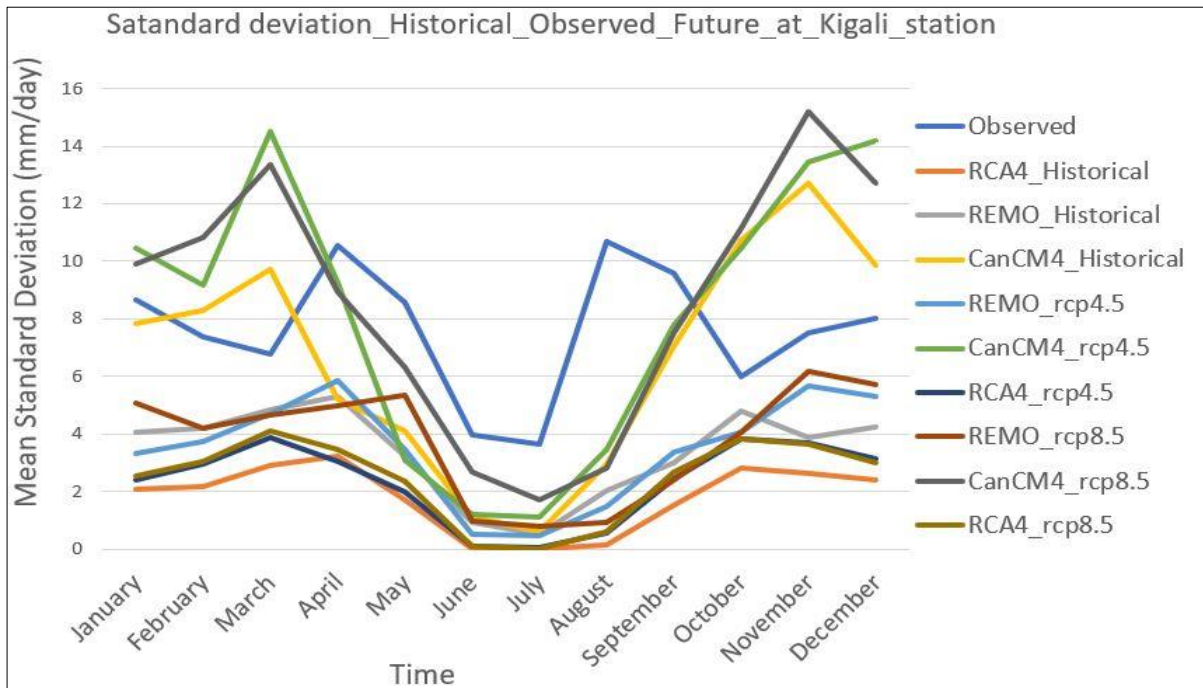


Figure 5-1: Observed and simulated RCMs monthly rainfall for the historical period(1981-2005)

5.1.3. Standard deviation of observed and raw simulated RCMs rainfall

Further analysis for the performance of RCMs in reproducing observed rainfall was done by comparing the standard deviation for observed data and simulated rainfall for both baseline (1981-2005) and future (2021-2050) periods. The results of the standard deviation of daily mean monthly rainfall in figure. [5-2] indicated differences between observed and simulated rainfall. Each model reacted differently, where a high standard deviation was found for CanCM4 for both historical and future periods. This high standard deviation indicates the high variability in monthly and intra-monthly rainfall simulated by this model. The observed rainfall showed a high standard deviation compared to RCA4 and REMO; this may be attributed to irregular values in the observed datasets, which could not be reproduced by these models. The standard deviation for raw future projections for each model hardly showed any difference between RCP 4.5 and RCP 8.5 and also between baseline and future, which shows less variability in raw simulated and raw projected rainfall.

Fig.[5-2], show the example of standard deviation for observed and RCMs simulated and projected rainfall at Kigali station.



5.1.4. Results from Empirical Quantile Mapping for RCMs outputs

Figure 5-2: The daily mean monthly rainfall standard deviation at Kigali station

Fig.[5-3] shows the CDF of raw RCMs simulations in baseline and future projections with observed data, respectively, before applying the quantile mapping method. For the uncorrected simulated rainfall at all stations, REMO and RCA4 showed higher cumulative distribution functions compared to the observed rainfall. This means the underestimation of rainfall by these RCMs except CanCM4, which over-estimate the rainfall. However, the CDFs of raw RCMs simulations hardly showed any difference between baseline and future rainfall compared to the CDFs of observed rainfall. Moreover, the CDFs of the ensemble mean of RCMs showed some improvement in CDF by averaging the over-estimating and under-estimating RCMs, especially for the raw amount of rainfall.

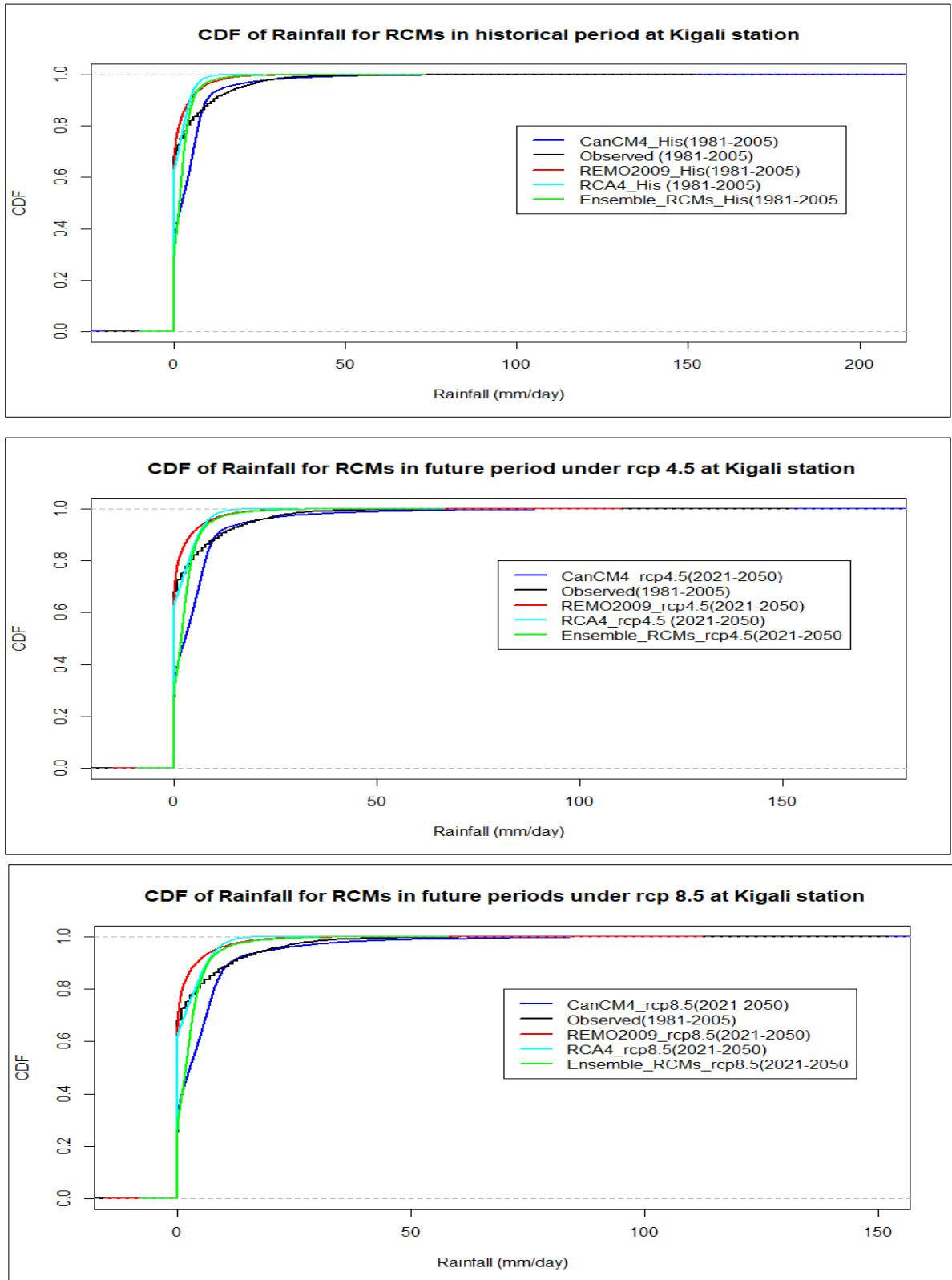


Figure 5-3: CDFs of uncorrected RCM simulations in the baseline(top) and future projections under RCP4.5 and 8.5 scenarios (bottom) compared to CDF of observed rainfall at Kigali station.

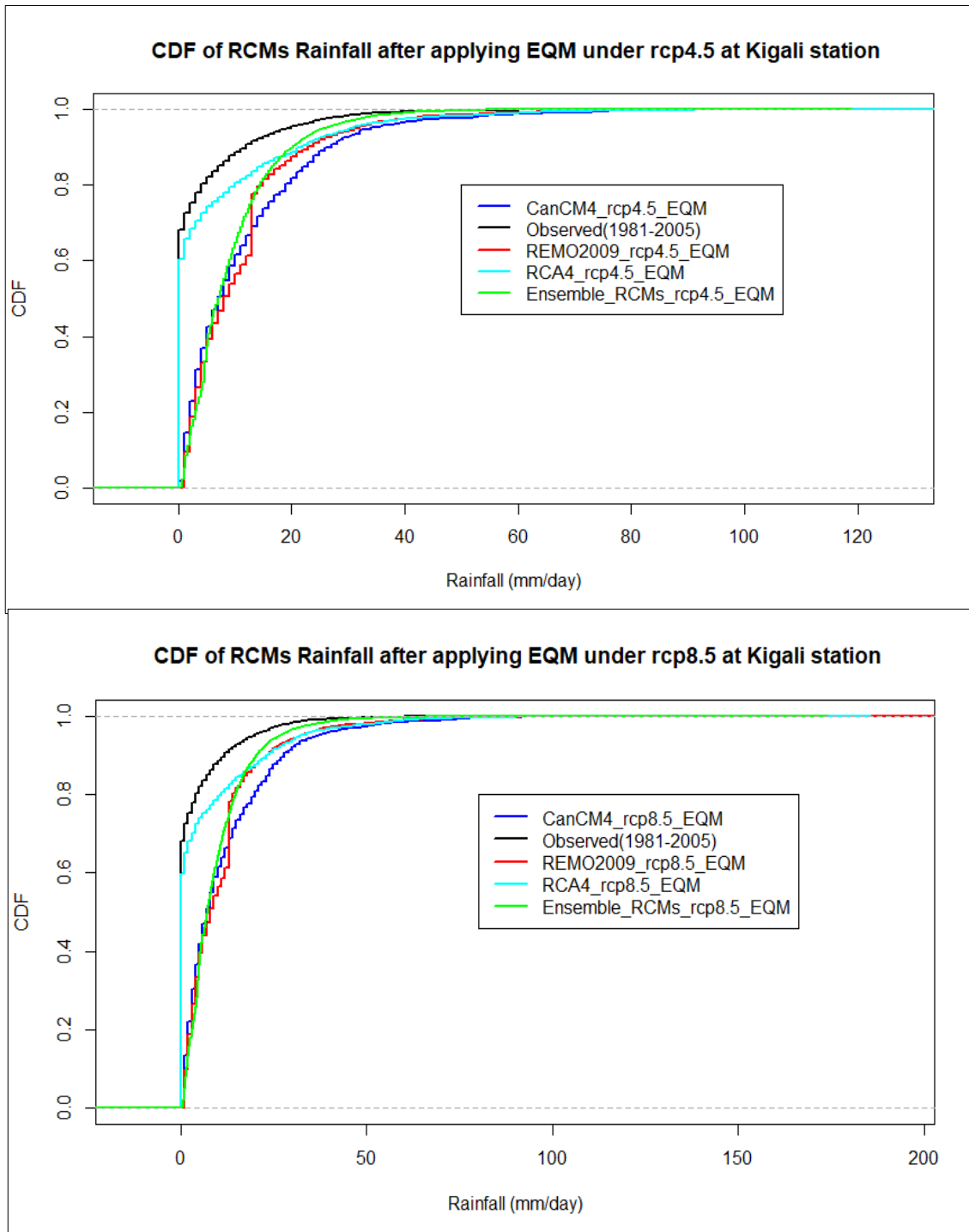


Figure 5-4: CDFs of the results from empirical quantile mapping of RCMs for RCP4.5 and 8.5 with comparison to the observed rainfall respectively

With quantile mapping works with finding difference between daily uncorrected baseline and future variables which were added to the observed rainfall, therefore the future rainfall projections were obtained. This The results of quantile are presented in CDFs in fig.[5-4]. The CDFs from quantile mapping showed significant differences in rainfall projections for both scenarios RCP4.5&8.5 compared to the observed rainfall in the baseline period. The CDFs of RCMs show an increase in rainfall amount for future periods. With the CanCM4 showing the largest increase while RCA4 showed the smallest increase. The ensemble

mean represents the average between the three models. RCP8.5 emission scenario showed more increase in rainfall amount for the future compared to the RCP4.5 emission scenario.

5.1.5. Relative changes in Rainfall

The results are represented in fig.[5-5] for Kigali and Kawangire gauging stations show the relative differences in average monthly rainfall for the future period (2021-2050) compared to observed rainfall in the baseline period (1981-2005). For the rainfall projections, the three RCMs differ for each month. Basically, extreme rainfall and floods occur in the Nyabugogo catchment during the long rainy season from March to May and in the short rainy season from September to December. RCA4 and the ensemble mean of RCMs for RCP4.5 indicated a likely decrement in the future rainfall amount for the months of February, May, June, July, and August

From the fig.[5-5], RCMs and the ensemble mean show that the wettest month will be November while the driest is August. Moreover, relative changes computed using the ensemble showed that the rainfall would increase in November by 14% and 24% for RCP4.5 and RCP8.5, respectively, at Kigali station. The expected highest increase at Kawangire station is also in November by 21% and 31% for RCP4.5 and RCP8.5, respectively. Annual rainfall changes were computed, and the increase is 5.6 % for RCP4.5 and 14.74% for RCP8.5 at Kigali station. At Kawangire station it will be 3.5 % for RCP4.5 and 21% for RCP8.5; at Kabarore station, the annual change expected increase is 3.2% for RCP4.5 and 10% for RCP8.5. Last but not least, the annual changes at Byumba station will be 6% for RCP4.5 and 16% for RCP8.5.

The rainfall pattern in the Nyabugogo catchment will be affected by climate change, and extreme rainfall is likely to happen in the rainy season. The overall results from the delta change method showed a declining trend of rainfall for the RCP4.5 emission scenario and an increasing trend for the highest emission scenario, RCP8.5. For the future period, a significant increase in rainfall was found mainly for the last years of the study period (2046, 2047, 2048, and 2049).

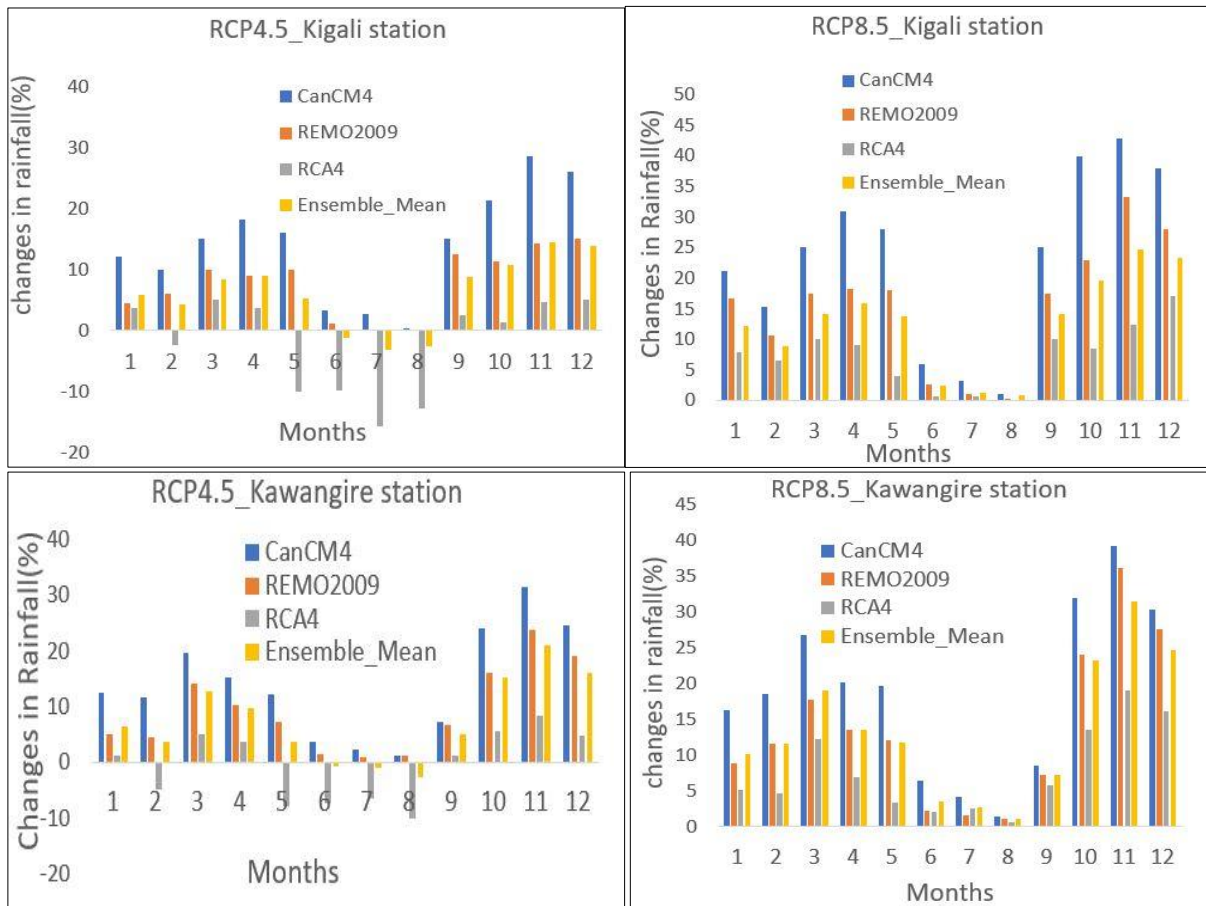


Figure 5-5: Relative changes in average monthly rainfall between baseline(1981-2005) and future periods (2021-2050) for RCP4.5 and 8.5 at Kigali and Kawangire station.

5.2. Objective Two: To derive extreme rainfall and analyze their change between baseline and future periods

5.2.1. Extreme rainfall frequency analysis

Fig.[5-6] shows extreme rainfall based on the 99th percentile of the datasets for all stations obtained for baseline and future periods for RCP4.5 and 8.5. The results indicated that for the climate change with RCP8.5, the extreme rainfall events will become more frequent in the study area. However, the results for RCP4.5 showed decreasing trends in extreme rainfall frequency and magnitude. The difference in extreme rainfall was observed for four stations. This indicates the spatial variability of extreme rainfall in the coming future.

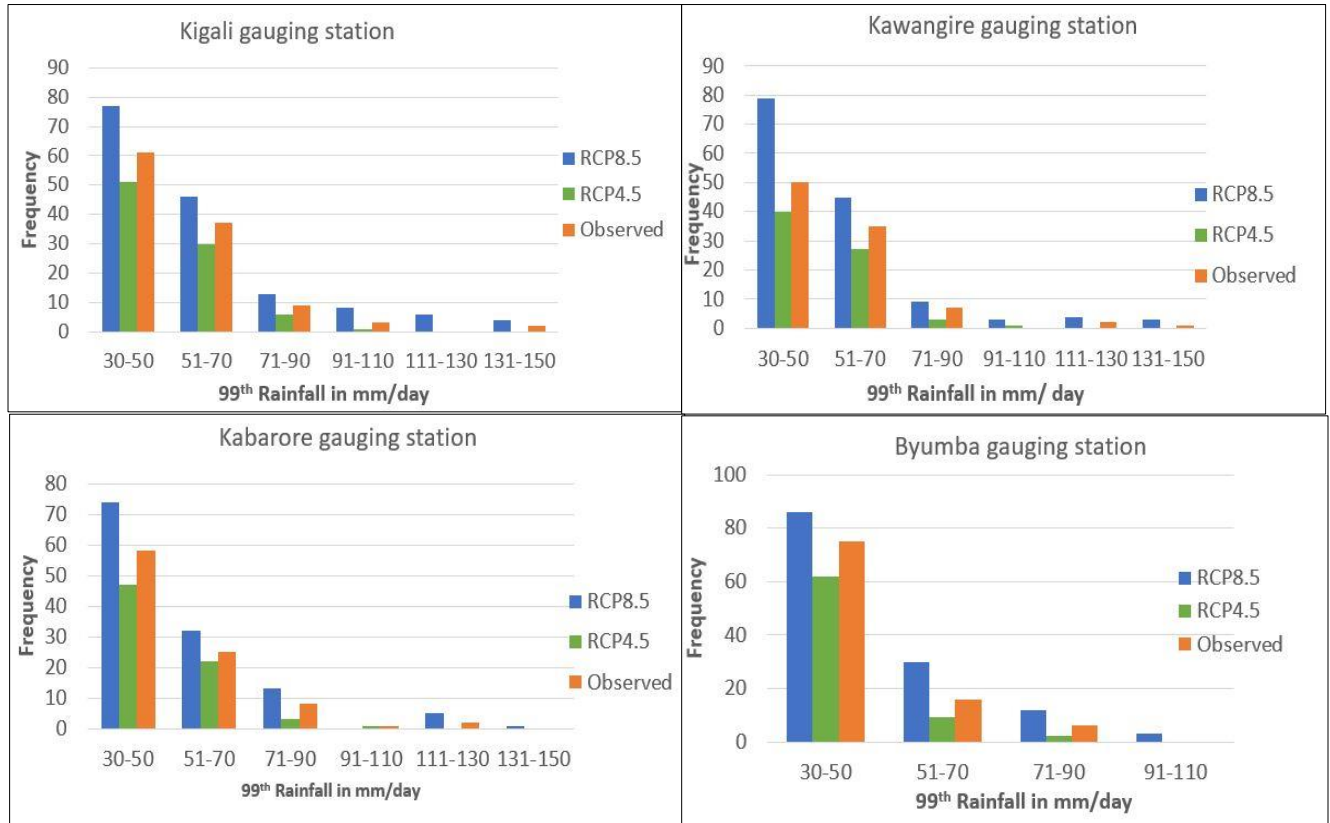


Figure 5-6: Frequency distribution of extreme rainfall (99th percentile)

5.2.2. Design extreme rainfall using Gumbel Distribution

By applying the procedure of probability distribution by means of the Gumbel distribution function, the parameters were estimated, and they were used to determine daily extreme rainfall for different return periods. Gumbel Distribution parameters (standard deviation, average, coefficient of variation, location, and scale parameters) were used to develop the CDF plot for the series of annual maximum rainfall. The rainfall data used for Gumbel distribution were the ensemble mean of RCMs EQM for both emission scenarios (RCP4.5&RCP8.5) and observed data in the baseline period. Fig.[5-7] represents the generated CDF for daily extreme rainfall for different return periods at Kigali and Kawangire stations. The derived rainfall show changes in extreme rainfall due to climate change. Relative to the observed rainfall in the baseline period (1981-2005), there will be a decreasing pattern in magnitude for mentioned return periods under RCP4.5 emission scenario. A significant increase in daily extreme rainfall was obtained for the RCP8.5 scenario for all stations, where the highest magnitude is 188 mm at Kigali station for return period of 100 years which is a 24.5% increase compared to daily extreme rainfall derived from observed data. Table 5-1, shows changes in extreme rainfall magnitude for different return periods. Fig.[5-7] shows changes in magnitude and return periods of extreme rainfall for projected rain for both emission scenarios RCP4.5 and RCP8.5 relative to observed rainfall in the baseline period (1981-2005).

Table 5-1: : Deriving daily extreme rainfall for 10,50 and 100- year return periods for different stations

Kigali				Kawangire			
Return Period (Years)	Baseline(Obs)	RCPs4.5	RCP8.5	Return Period (years)	Baseline(Obs)	RCPs4.5	RCP8.5
10	102.04	79.5	123.6	10	96	83	111.12
50	136.78	101.06	169.45	50	127.4	105.6	146.09
100	151.5	110.2	188.8	100	140.67	115.15	160.85

Byumba				Kabarore			
Return Period (years)	Baseline(Obs)	RCPs4.5	RCP8.5	Return Period (years)	Baseline(Obs)	RCPs4.5	RCP8.5
10	69.8	72.56	83.2	10	90.5	75.76	97.95
50	87.74	92.73	106.8	50	118.85	93.84	127.9
100	95.3	102.05	116.78	100	130.87	101.5	140.6

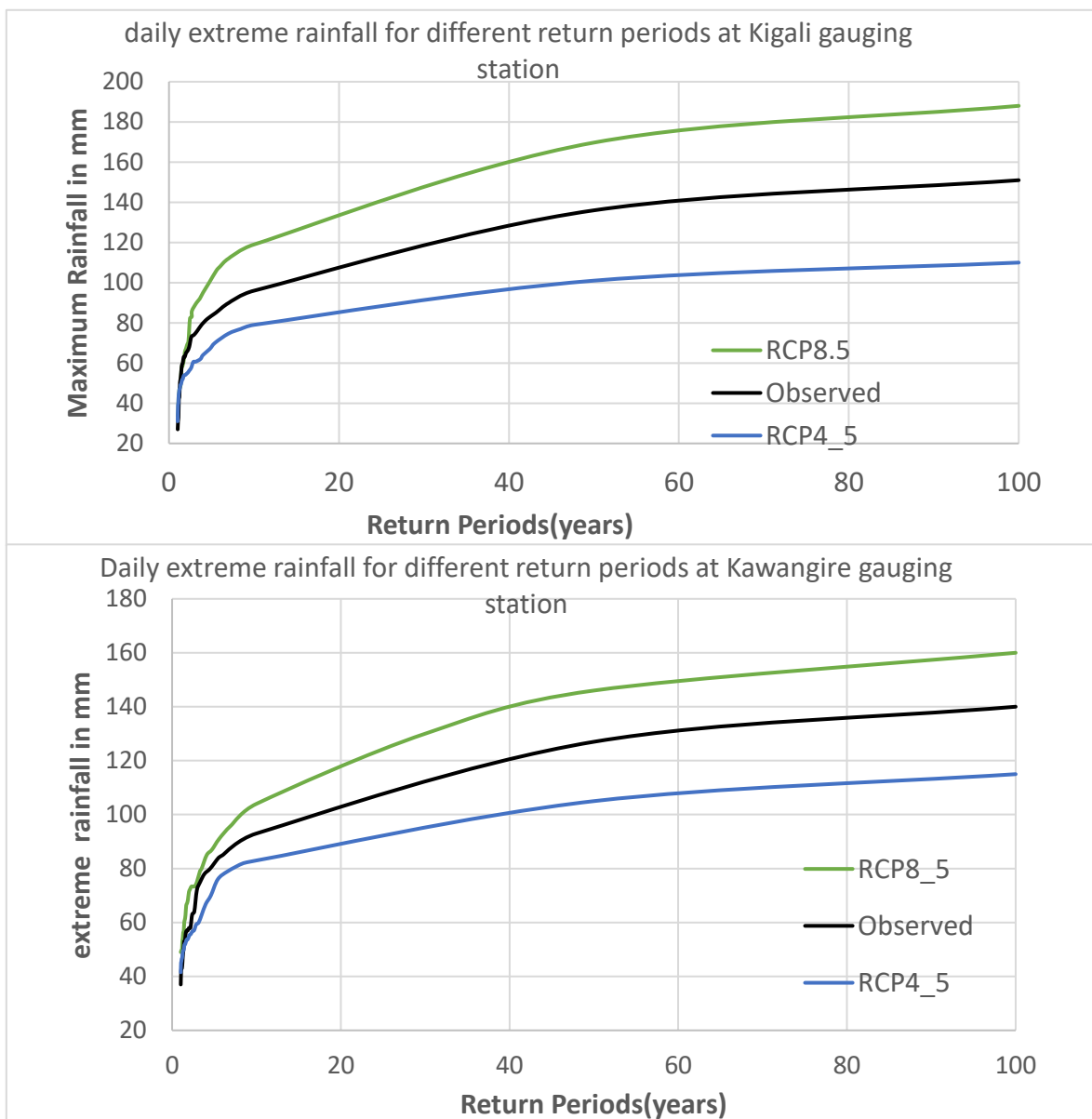


Figure 5-7: CDF of Gumbel distribution of daily extreme rainfall for different return periods at Kigali and Kawangire stations, respectively.

The rainfall (mm/day) for 10,50, and 100 years return periods were selected for flood modeling, and rainfall for each of the mentioned return periods was used for daily rainfall distribution to design the storm hyetograph that was required in HEC-HMS hydrological model.

5.2.3. 24-Hour rainfall distribution

Table 5-2: Short duration peak intensities for the storm in mm recorded at Gitega-(Kigali)station

Day	Daily total rainfall	10-min Max	20-Min Max	30-min Max	40-min Max	50-Min Max	1Hour Max	2-Hours Max	3-Hours Max	6-Hours Max
16/03/2019	40	4.8	9	13.6	16.2	19.6	22.2	29.4	31.4	34
02/04/2019	48.6	3.8	5.8	8.4	11	13.2	15.8	26.2	30.8	44.2
10/04/2019	39.1	8	14	19	22.5	25.7	27.5	35.5	36.5	37.7
23/05/2019	57	8	13.2	15.4	18	20.4	22.6	38.6	43.8	49.4
11/10/2019	53.3	6	9.6	12.2	16.5	19.5	22.3	35.7	41.7	51.9
13/11/2019	26.8	6.2	8.6	10.8	11.8	13.2	14	20	24.6	26.6
12/12/2019	15.6	5.4	7	8	12.2	13.8	14	15.2	15.4	15.6
15/01/2020	24.2	5.8	7.2	8.6	9.2	10.4	11.8	13.4	19.6	23
19/01/2020	32.4	6	11	15.2	18.4	21.6	24.6	30.2	31.8	32.2
16/02/2020	36	10.6	18.4	22.8	25.8	28	32.4	35.8	36	36
03/03/2020	18	5.4	6.8	8	8.6	9.2	9.4	13.2	16.2	17.8

As mentioned earlier, rainfall at Gitega meteorological station was observed at 10-minute rainfall for the period March 2019 to March 2020 were available. Therefore, Hourly rainfall distributions from Gitega station were compared with theoretical storm distributions from other studies in the region (Fiddes 1974 “The prediction of storm rainfall in East Africa,” Schmidt and Schulze 1987 “Design stormflow and peak discharge rates for small catchments in South Africa”).

The Gitega CDF of hourly rainfall was developed, and it falls between Synthetic Storm Type 2 and Type 3 of the region. As Gitega CDF was developed based on only 11 events because of the short record and missing data, Synthetic Storm Type 3 is used for the sub-daily disaggregation of rainfall at Kigali and other stations in the Nyabugogo catchment. This is due to the missing values and very short time records rainfall for other stations.

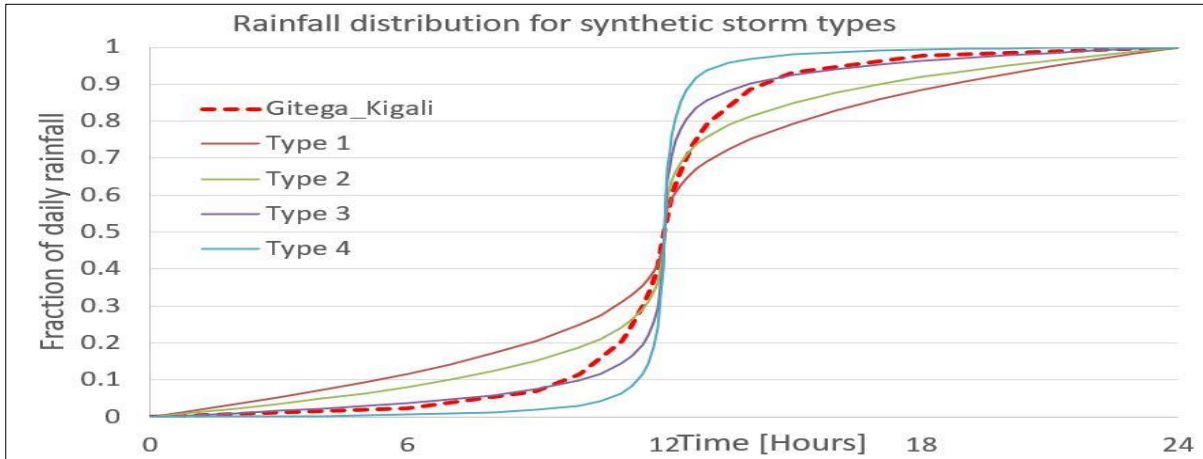


Figure 5-8: Comparison of hourly rainfall distribution of Gitega_Kigali to synthetic storm types in the region (Fiddes 1974, Schmidt and Schulze 1987)

5.3. Objective three: To develop a rainfall-runoff model for simulating impacts of climate and land-use changes on streamflow in the Nyabugogo catchment

5.3.1. Geomorphological parameters

5.3.1.1. Hydrological soil groups and curve numbers

The SCS CN classification of soil groups discussed in the chapter4 produced hydrological soil groups (HSG) as in fig.[5-9]. The classification showed that the eastern part of the catchment (Muhazi sub catchment) is dominated by HSG D while the remaining of the catchment is dominated by HSG A and C. Overall, hydrological soil groups A and D are dominant in the catchment.

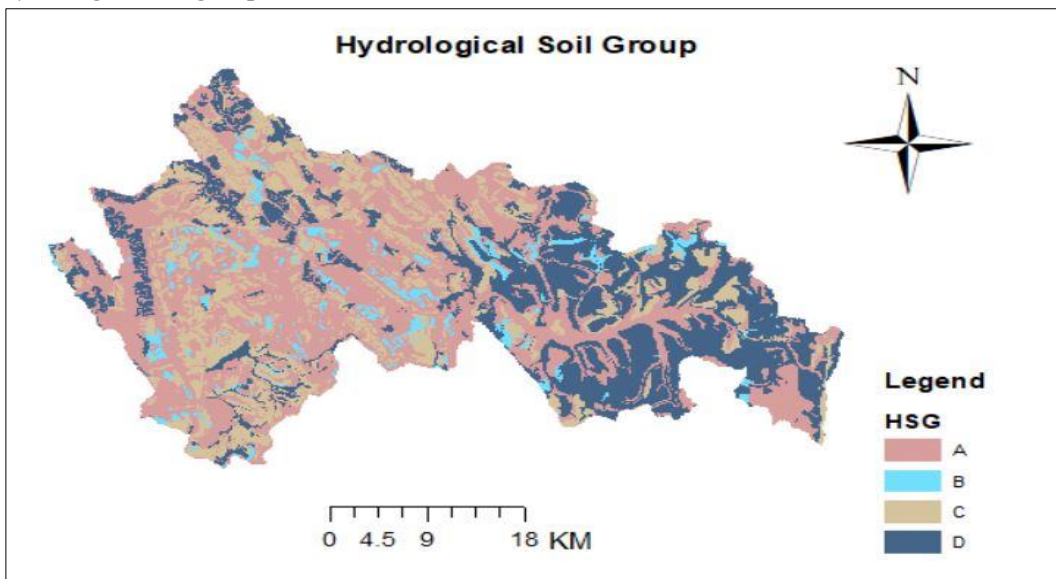


Figure 5-8: Hydrological Soil Groups in Nyabugogo Catchment

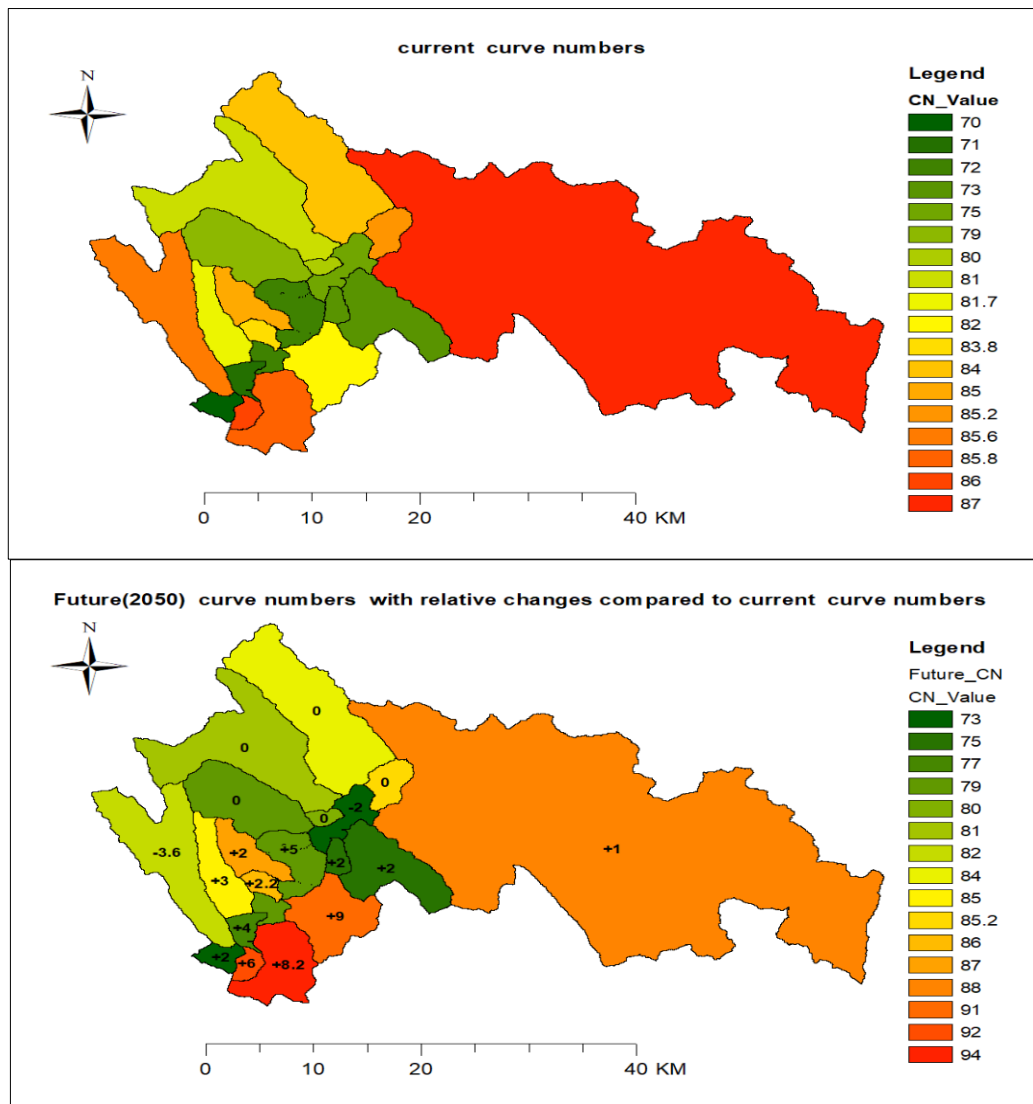


Figure 5-9: Curve number for current (up) and future period (down) respectively

The hydrological soil groups together with land-use were used to produce curve number (CN) for each sub catchment based on the (SCS, 1972) classification. The CN was produced twice based on the existing(current case) and land-use planning of 2050. The soil was assumed to remain unchanged in the future; hence hydrological soil groups remained the same. The developed curve numbers for existing land use are in the range of 71 to 87, with the flood plains of Nyabugogo having a lower CN. These CN values are in the range of values found by (Manyifika, 2015) with a slight difference which might be due to the different land-use classification. As mentioned earlier, the future land-use planning was available only for the city of Kigali and its greater region. Therefore, the changes were found in CN for the sub catchments found in the city of Kigali. The flood-plain showed both positive and negative changes in which reach1 showed negative changes in the future. Yanze sub catchment showed a decrease in CN value for the future. CN for the future periods is between 73-94. The subbasins outside of Kigali were considered to remain the same as no planned land-use data were available, and no many changes would be expected to take place in rural land-use during the study period(2021-2050).

5.3.1.2. Other physical characteristics of the basins

As it was described in chapter 4, the main physical characteristics were estimated for each subbasin. Refer to table 5-5, the primary physical characteristics such as area, channel length, watershed, and channel slopes were determined first, and they were used to estimate the other parameters such as time of concentration and lag time needed for the SCS UH transform method and Lag time needed for channel routing in HEC-HMS respectively.

Table 5-3: The main physical characteristics of basins

Basin	Area (km ²)	Basin slope(%)	SCS Lag Time (min)	Channel Length (km)	Slope channel(%)	Channel Lag time (min)
Byabagabo	8.5	0.255	46.34	3.42	1.75	42.34
Gatare	5.3	0.253	52.2	2.26	0.66	32.96
Gikondo	52.7	0.15	191.84	9.93	0.96	124.64
Kajevuba	61.42	0.283	362.2	13.8	0.63	150.4
Karuruma	35.55	0.344	152.85	13	2.4	143.32
Misare	8.14	0.236	76.21	4	0.95	53.3
Mpazi	8.25	0.21	56.56	4	2.8	41
Murama	18.17	0.3	82.73	6.8	3.82	74.36
Mwange	126.3	0.34	529.18	25.8	1.26	252
Nyacyonga	25.9	0.31	93.33	8	2.87	91.45
Rufigiza	54.13	0.19	301.54	13.6	0.94	162.48
Rusine	67	0.34	386.62	18.4	1.58	191.97
Rusumo	128.9	0.333	296.15	23.7	1.7	232.78
Yanze	96.7	0.354	161.32	16.2	1.5	342.9
Muhazi	876	0.18	NA	NA	NA	NA
Floodplain						
Reach1	16	0.252	242.3	11.7	0.13	149.95
Reach2	42	0.217	515.67	15.7	0.32	139.09
Reach3	7	0.225	222.58	5	0.22	164.04

Reach4	12	0.265	265	5.5	0.18	180
--------	----	-------	-----	-----	------	-----

5.3.2. Rainfall-runoff model outputs from calibration and validation of gauged sub catchments

5.3.2.1. Results for Yanze and Rusumo basins

The HEC-HMS model was calibrated first for two subbasins (Yanze and Rusumo) based on the available river discharge for these basins. The results of calibration and validation for selected storms events in 2011-2012 are shown in table 5-4 for the Yanze basin. Fig.[5-11] illustrates the comparison between observed and simulated hydrographs for Yanze basin.

Table 5-4: Selected events, calibrated and validated parameters for Yanze basin

Basin	Period	Date	Initial Abstraction (mm)	Recession Coefficient (per day)	Initial discharge (m ³ /s/km ²)	Discharge Threshold (m ³ /s)	NS E	RVE
Yanze	Calibration	11 to 23/02/2011	3.3341	0.60989	0.0023	3.6136	0.75	0.25
		22/09 to 01/10/2011	8.95	0.6823	0.0038979	2.5	0.72	-2.36
		28/03 to 02/04/2012	8.5	0.72334	0.0039129	3	0.67	-4.6
	Validation	22 to 30/10/2012	6.93	0.672	0.00337	3.0267	0.66	2.4
		15 to 23/11/2012					0.53	9

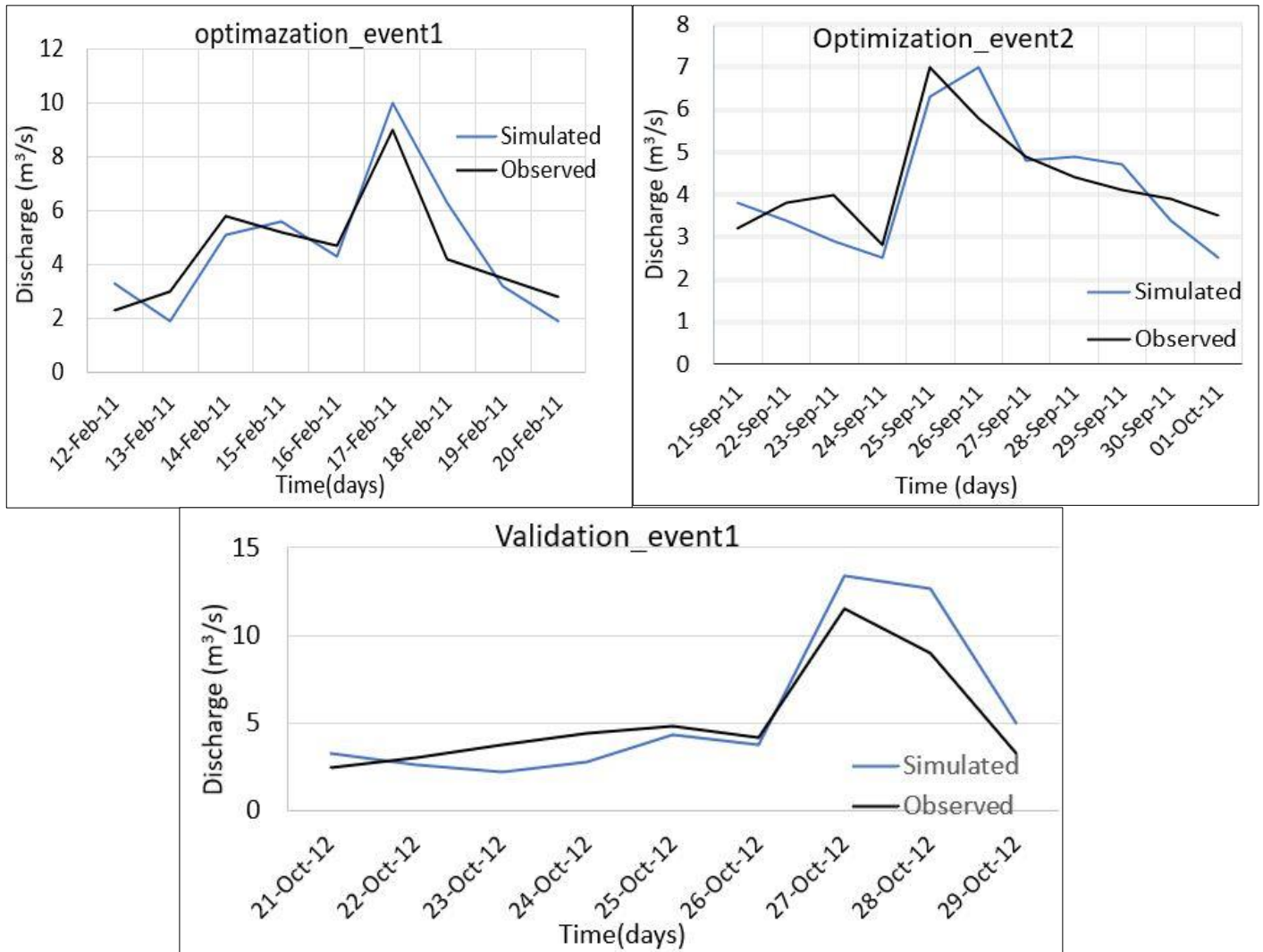


Figure 5-10: Comparison of simulated and observed hydrograph for Yanze subcatchment (2011-2012)

Due to the short records of discharges data, three events from 2011 were used for calibration. These events were between 5-to 14 days because events methods applied are suitable for a maximum of 14days (Feldman, 2000). Need improvements Manual calibration was used. The calibration process was performed by adjusting the initial abstraction, initial baseflow, threshold discharge, and recession coefficient. Therefore, the total number of adjusted parameters was 4. Moreover, a sensitivity analysis was performed and revealed that the initial baseflow was the most sensitive parameter. The calibrated model was further validated by using three events from 2012. To evaluate the performance of the model, the objective functions NS and RVE were applied. As shown in the results, NS for Yanze basin were in an acceptable range. Moriasi et al. (2007) indicated the NS that is greater than 0.5 indicates adequate performance. RVE was also in the acceptable range except for one validation event where the RVE value is 9%.

The results from several trials of the calibration of the Rusumo basin model failed to reproduce the observed discharge. it showed problems such as the average of the calibrated initial abstraction was 150mm. This number was very high, based on the fact that the total rainfall volume for a particular event could not reach this value. The reasons for these improper results may be attributed to the poor quality of the observed discharge data in this basin. These results are similar to results by (Manyifika, 2015) who found a high value

of RVE (32.5) for this basin after multiple calibrations and he claimed this weakness to be caused by the poor quality of discharge data. Therefore, in this study, the model parameters from the Rusumo model were not considered for further use.

5.3.2.2. Calibration and validation results for Muhazi Lake Subbasin

Muhazi Lake subbasin was considered a separate entity because it covers a big area and it contains a lake which makes its hydrological processes differ from other subbasins. The model for the Muhazi Lake subbasin was calibrated to match the simulated with the observed discharge outflow from this lake.

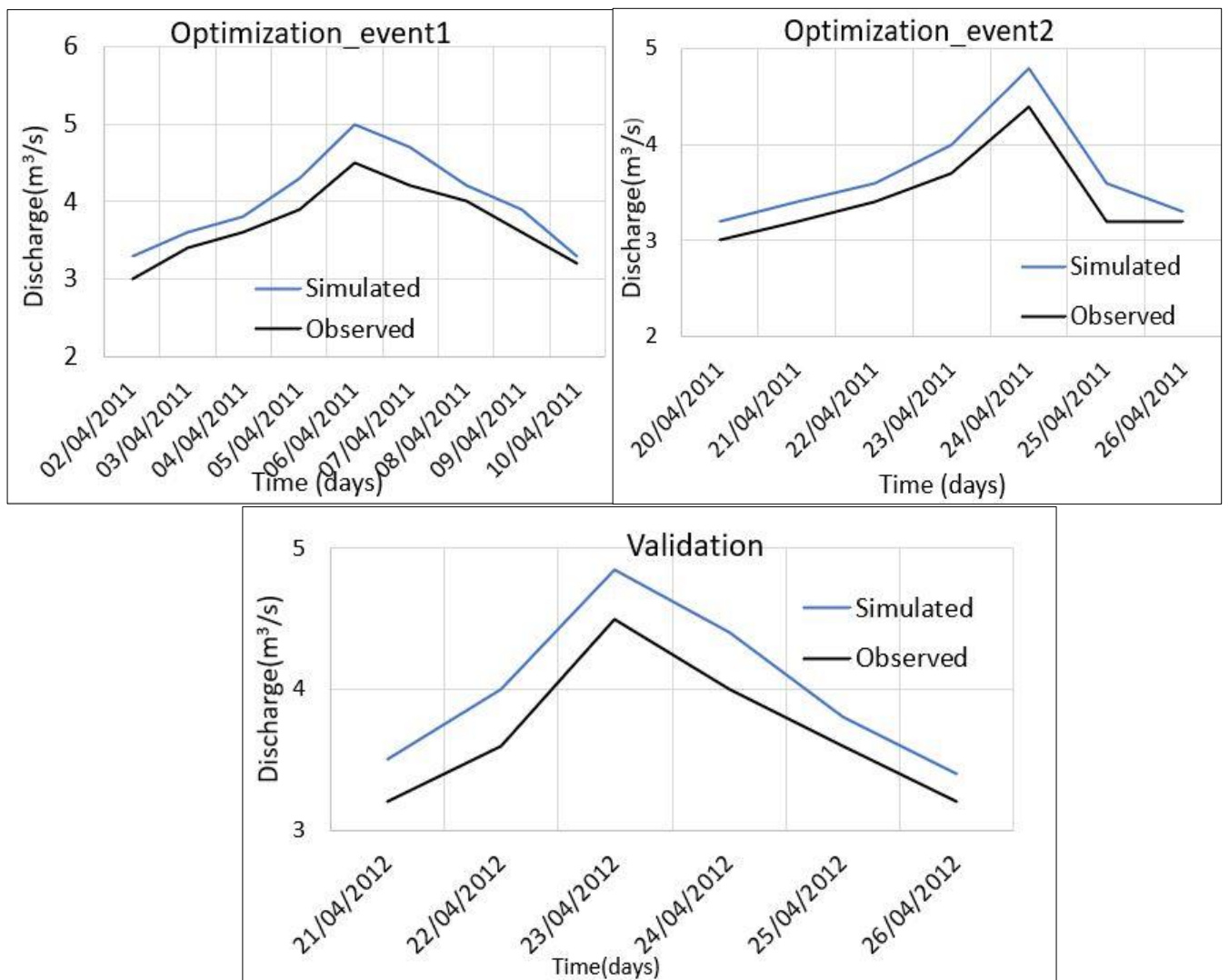


Figure 5-11: Comparison of simulated and observed discharge for calibration (top graph) and validation (bottom graph) for Muhazi lake basin

The overall performance of the model for this basin was relatively good as the objective functions were in an acceptable range. NSE was between 0.6-0.72 for both calibration and validation. RVE was in an acceptable range for calibration, but it was a bit high for validation -12%. Moreover, the observed discharge for this basin showed that the lake keeps almost all the rainfall from this basin due to the small difference observed in its daily outflow discharges between rainy periods and dry periods.

Table 5-5: : Muhazi lake basin selected events , calibrated and validated parameters

Period	Date	SCS Lag time(min)	Routing Lag time(min)	Initial abstraction (mm)	Recession Coefficient (per day)	Threshold Discharge (m ³ /s)	NSE	RVE
Calibration	02 to 10/04/2011	380	406.8	14	0.87625	3.5	0.72	-0.54
	20to 26/04/2011	650	230	15.4	0.967	2.7	0.63	-0.32
	02to10/04/2012	700	329	8	0.963	3.3	0.68	-1.69
Validation	20to26/04/2012	510	321.667	13	0.9354		0.62	-12

5.3.3. Parameter regionalization

So far, two subbasins (Yanze and Muhazi lake) were calibrated and validated. The remaining subbasins are ungauged. In order to build the rainfall-runoff model for the entire Nyabugogo catchment, there was a need to transfer parameters from gauged to ungauged subbasins. The process of transferring parameters from gauged to ungauged basins involves the analysis of factors such as the physical characteristics of the basin that influence a certain parameter. Normally, methods such as multiple regression analysis give the possibility to observe the influences of a single factor in the presence of others. The factors with a strong positive influence on the parameter can be used to transfer that parameter from a gauged to the ungauged basin. However, those methods require enough samples from multiple subbasins to give significant results (Pereira & Keller, 1982). Therefore, for this study, those methods could not be used because only one basin (Yanze) parameters was available to be transferred as the Muhazi Lake subbasin was considered a separate entity. Therefore, in this study, a simplified approach was used, and model parameters from Yanze were assigned to all ungauged basins, including the Rusumo subbasin.

5.3.4. Rainfall-runoff model outputs for the entire Nyabugogo catchment

The entire Nyabugogo catchment model in HEC-HMS was set up by importing the basin file of all subbasins. Two rainfall-runoff events in 2013 were selected to run the model for the Nyabugogo catchment. As many basins were ungauged, the calibrated and validated parameters from Yanze subbasin were assigned to ungauged basins, including Rusumo, and were used to run the model. Fig5-13 shows the comparison between simulated and observed discharges at the outlet of the Nyabugogo catchment

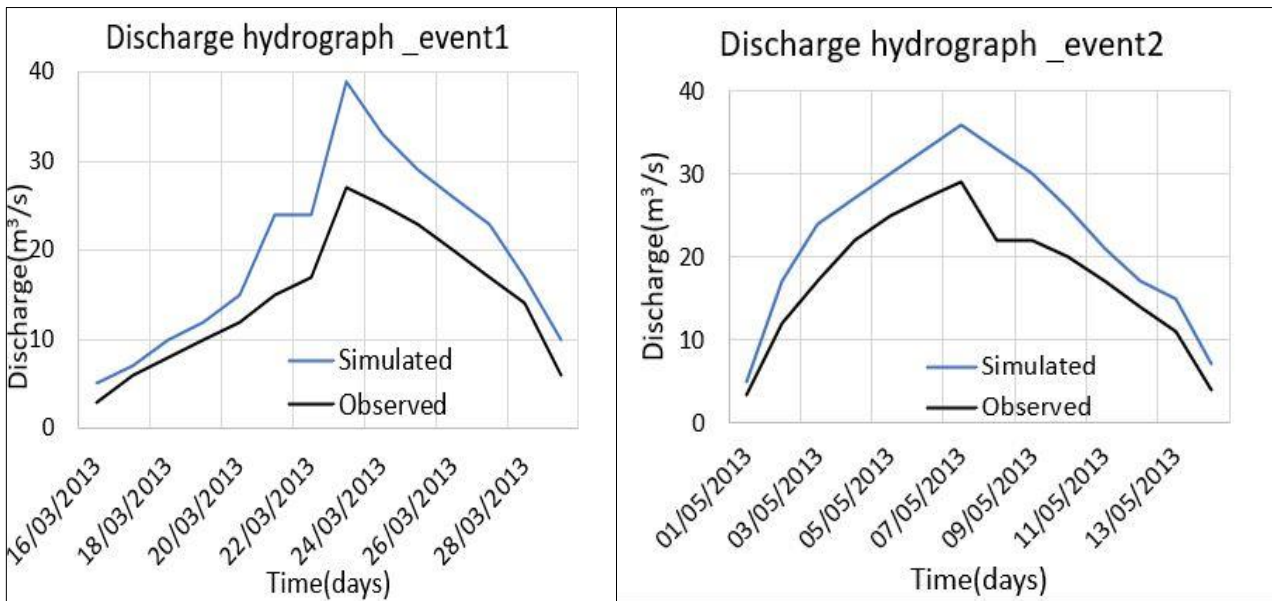


Figure 5-12: Comparison of simulated and observed streamflow hydrographs for Nyabugogo for two events in 2013

The efficiency of the Nyabugogo model was evaluated through the objective functions. NSE values were satisfactory, 0.6 and 0.55 for the two events, respectively. However, the values of the Relative Volumetric Error (RVE) were high for both events (21 and 18.78), and they indicate the difference between simulated and observed discharge. The author understands that the transfer of optimum parameters from Yanze to all ungauged basins together with the poor quality found in observed discharges may lead to this difference. However, the model was taken for the simulation of boundary conditions for the flood model with consideration of its limitations.

5.4. Impacts of climate change and land-use changes on streamflow

The model for the entire Nyabugogo catchment was used to simulate runoff from extreme rainfall for different return periods. To assess the impacts of land use and climate changes on the hydrology of the Nyabugogo catchment, the simulated peak hydrographs in HEC-HMS for different cases were compared. Table [5-6] shows the expected changes in peak discharges between baseline and future periods for the considered cases. As shown in the results, RCP4.5 reduced the peak discharges from observed rainfall in the baseline while RCP8.5 increased the observed peak discharges for all return periods with the highest peak discharges obviously found for 100 years return periods. Land-use changes showed a larger increase of streamflow and peak discharges for all return periods compared to climate change. The effect of land-use interventions combined with climate change for RCP8.5 significantly increased the peak discharges compared to the current case.

Table 5-6: Summary of the results for peak flows for current and expected land use and climate change scenarios with expected changes as percentage in brackets for Nyabugogo catchment

Return Periods (Years)	Current Case(m ³ /s)	Impact of land use change only (m ³ /s)	Impacts of climate change only		Combined impacts of land use and climate change	
			RCP4.5(m ³ /s)	RCP8.5(m ³ /s)	RCP4.5(m ³ /s)	RCP8.5(m ³ /s)
10	49.2	62.8(29.09%)	36.8(-25.2%)	53.5(22.04%)	47.7 (-3.05%)	79.6 (51%)

50	73.3	109.8(37.9%)	48.6(-33.7%)	101.1(26.87%)	62.1(-15.27%)	121.4(63.3%)
100	85.3	124.1(45.85)	54.3(-36.34%)	109.3(29.64%)	68.9(-19.22%)	141(69.62)

5.4.1. Inflow boundaries to the flood model

The main purpose of rainfall-runoff modeling was to find the boundary inflows for the flood model. The presented discharge hydrographs in fig.5-14 and fig.5-15 show the aggregated inflows from all subbasins in Nyabugogo catchments. For the flood model, three different inflows boundaries were required with regards to the schematization of the flood model domain developed by (Manyifika, 2015). The upstream area, Yanze, and Mpazi subbasins, constitute the inflow boundaries for the flood model. Fig.[5-14] and fig.[5-15] show the contribution from each of the inflow boundaries and total streamflow hydrograph estimated from extreme rainfall for the 100 years return period for respective cases.

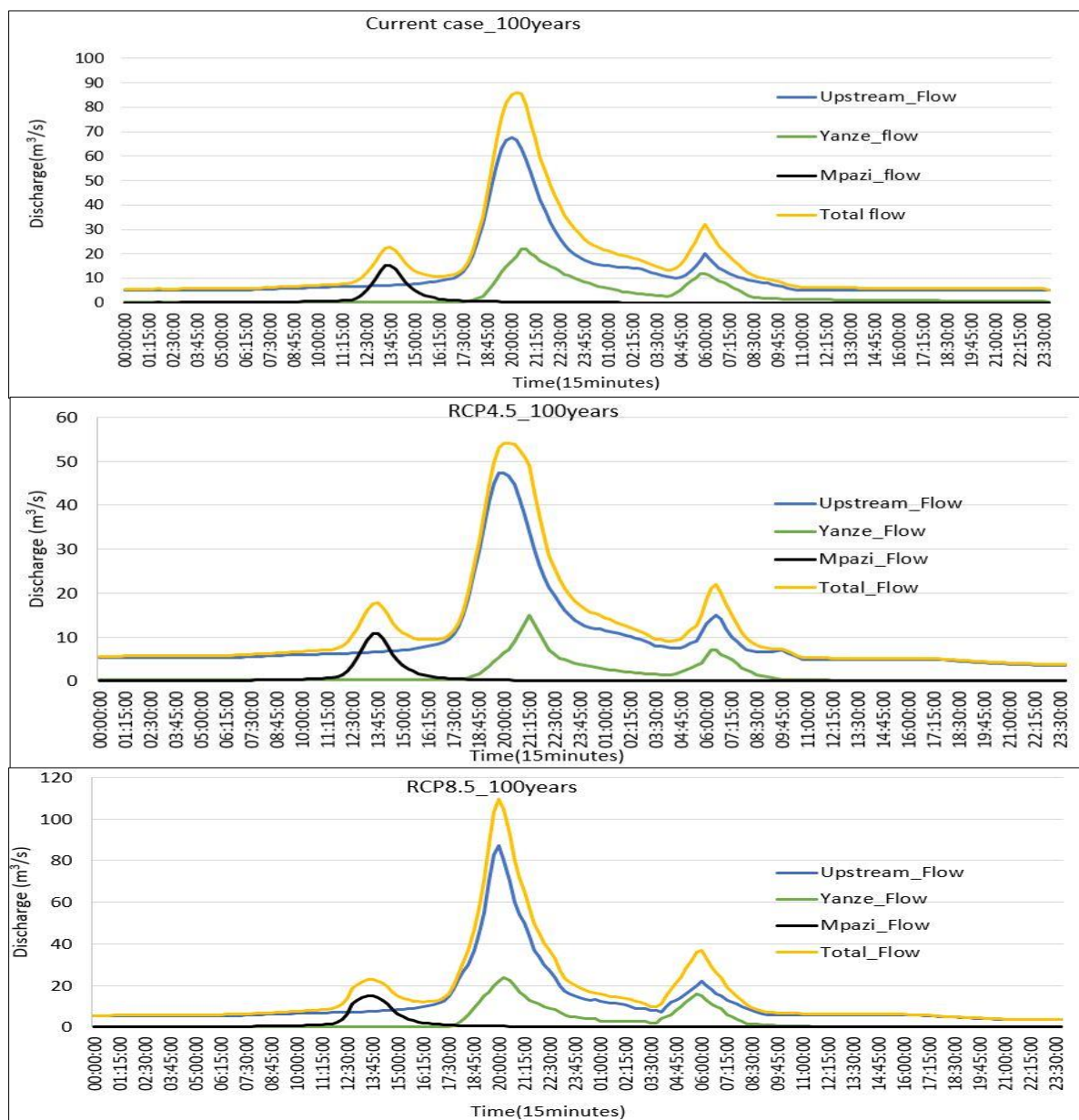


Figure 5-13: Streamflow hydrograph for 100-year return period extreme rainfall of the current case, RCP4.5 and RCP8.5 scenarios respectively

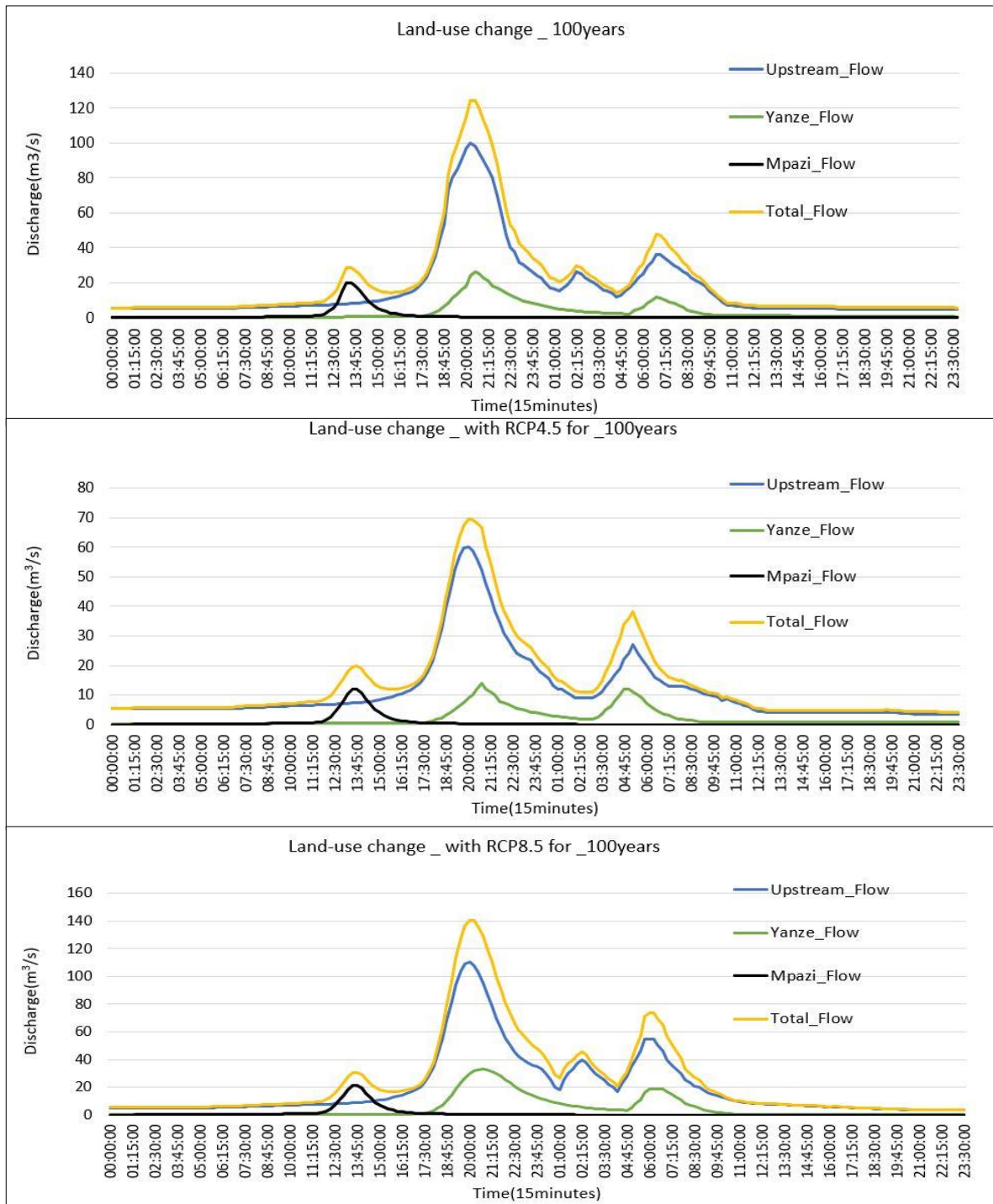


Figure 5-14: Streamflow hydrography for 100year return period extreme rainfall due to land use change only (top) and land use combined with RCP4.5 and RCP8.5 scenarios respectively

5.5. Objective Four: To simulate Flooding for Nyabugogo commercial hub under changing climate and land use.

The main objective of the flood modeling under the current study was to explore the flooding in the Nyabugogo commercial hub in Kigali in the window of climate and land-use changes using the SOBEK 1D2D flood model. Three flood characteristics (i.e., water depth, velocity, and flood extent or area of inundation) were determined and analyzed for different scenarios studied.

The boundary inflows were computed in HEC-HMS with 15 minutes intervals. Therefore, the simulation time interval in the flood model was 15minutes. The model was run for the boundary inflows from different six scenarios, i.e., current case, impacts of land-use change only, impacts of climate change for both RCP4.5 and RCP8.5, and combined effects of land-use change with climate change for both RCP4.5 and RCP8.5. For each case, the flooding for return periods of 10, 50, and 100-years was modelled. Therefore, the total number of simulations made was 18. The longest simulation took two and half days, while the shortest simulation period was 12hours. The simulation time was increasing by an increase in return periods. The settings and the simulation periods were kept the same for all cases to enable the comparison.

The simulation outputs are presented in three graphs showing the changes and comparison for mean water depth, mean velocity, and inundation areas a respectively between all cases modelled. Secondly, results are presented in in maps to show the possible flooding conditions for the different scenarios with for a return period of 100-year period. Finally the table showing the derived statistics for each case is also provided.

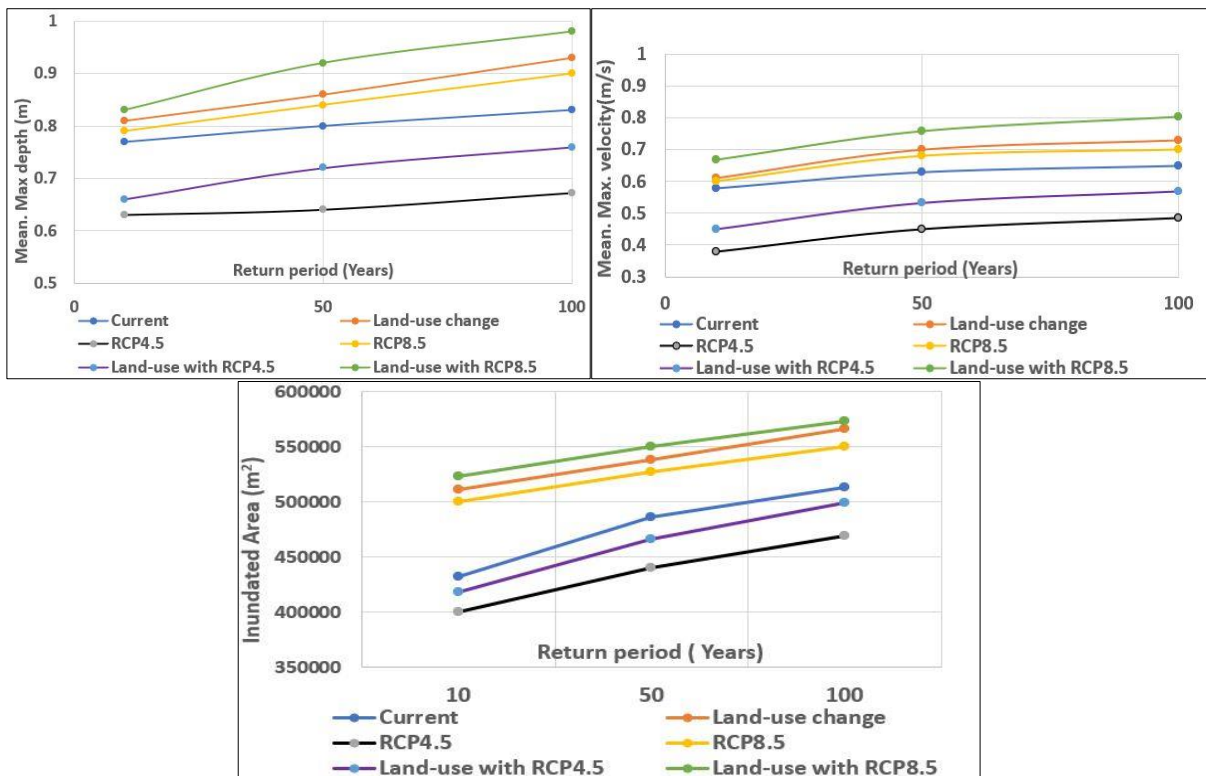


Figure 5-15: Mean maximum depth(left), mean maximum velocity(right) and area of inundation(bottom) of different for scenarios

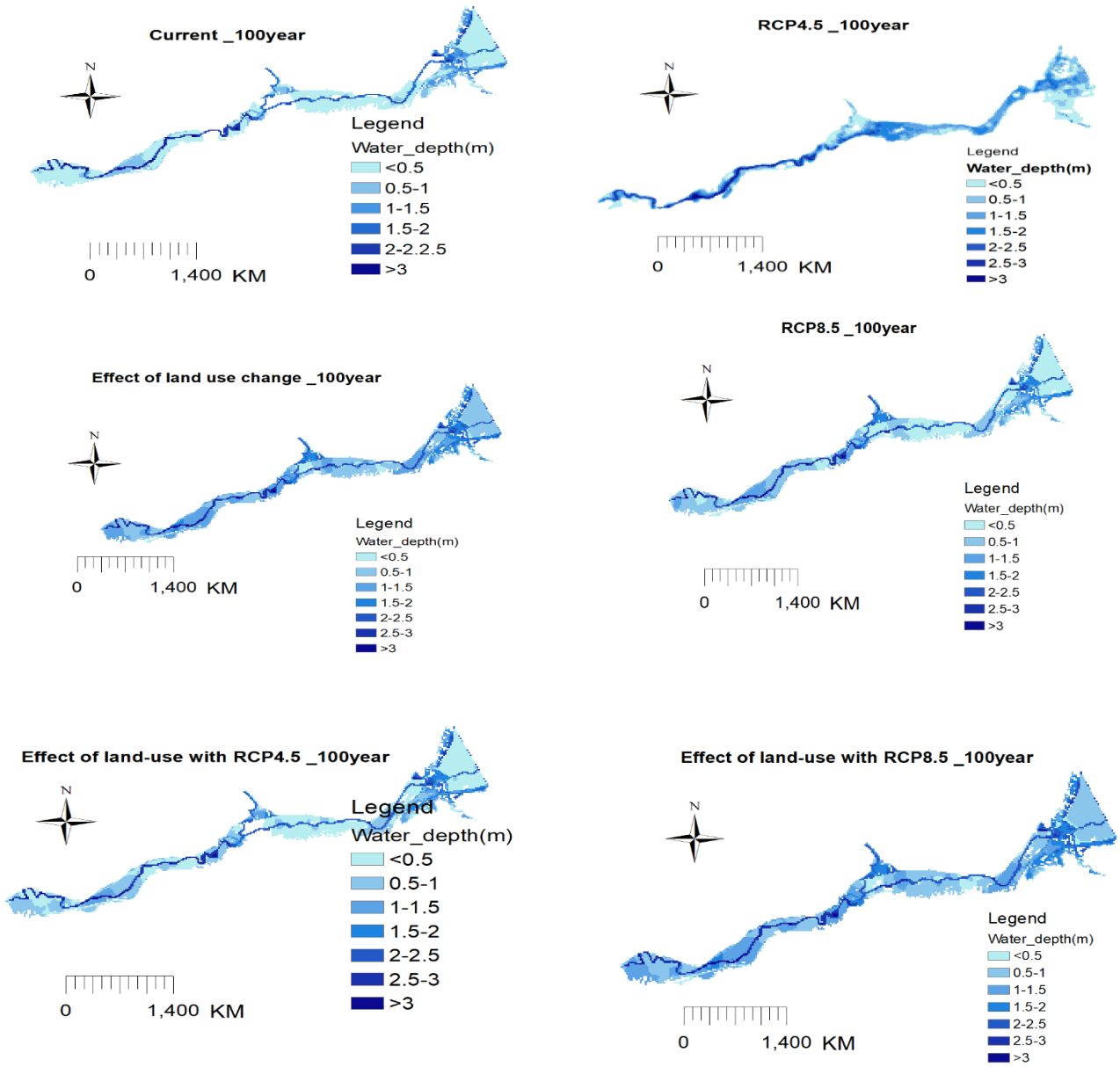


Figure 5-16: Maximum flood depth for different scenarios for the 100-year return period

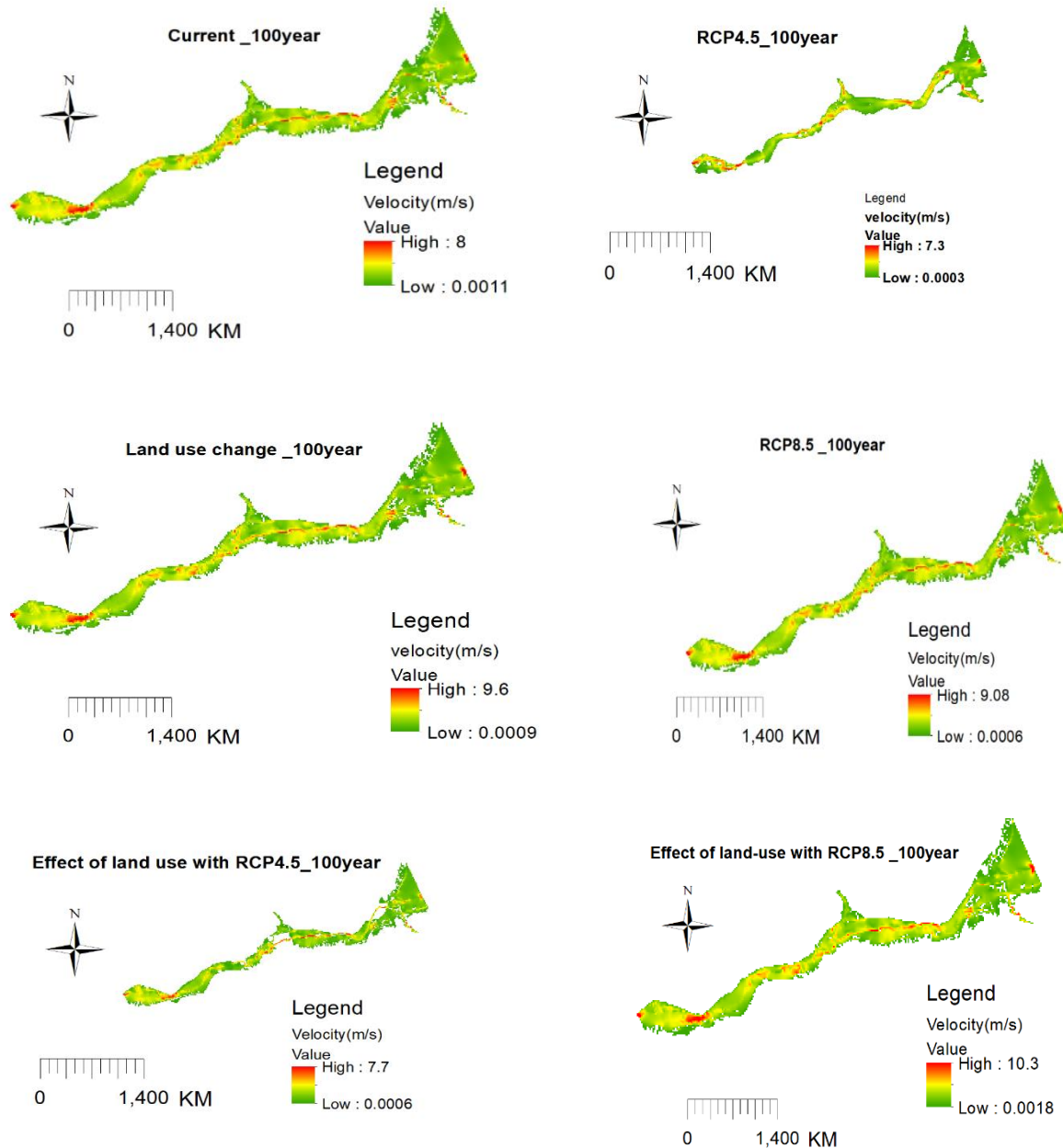


Figure 5-17: Maximum velocity for different scenarios for 100-year return period

5.5.1. Effects of land use change

As stated previously, to evaluate the impacts of land-use change on flooding, the inflow boundary estimated from using the rainfall for the current period or baseline was used while changing the parameters related to land use in hydrological models. Therefore, the flood model was forced by these inflow boundaries. The flood simulation results have shown an increase in all floods characteristics in the future compared to the current case. The increase in maximum water depth, maximum velocity, and flood extent for 10, 50, and 100-year return periods are presented in table 5-7. The increase in flood characteristics for the future period is attributed to the changes observed in land-use /cover between 2012(current case) and 2050 for the

future. The increase of 8.51% for built-up areas in Nyabugogo catchment was observed for the land use of 2050 compared to land use of 2012. Basically, the increase in built-up areas introduces hard surface such as paved and sealed areas thus, reduce the infiltration capacity of the area and accelerate and increase floods.

5.5.2. Effects of climate change

The results from this study show that the flooding due to extreme rainfall under medium emission scenario RCP4.5 are expected to reduce in water depth, velocity, and areas of inundation compared to the current period. This reduction is associated with the decrease observed in extreme rainfall and boundary inflows under RCP4.5. Climate change under the higher emission scenario RCP8.5 showed the increase in flood characteristics for all return periods compared to the current case.

5.5.3. Combined effects of climate and land use change

The last attempts have been taken to check how much land-use changes such as an increase in impervious areas could influence the flooding with changing climate for the time horizon 2050. Land use changes together with RCP4.5 showed a slight increase in flooding compared to RCP4.5 alone. This is due the to the increase that was observed due to land-use changes. RCP8.5 combined with land use changes showed an increase in flooding for all return periods. This increase is combined the increases observed for both land use and rcp8.5. Therefore, more increase in built-up areas together with climate change under the higher emission scenario (RCP8.5) will exacerbate flooding in the areas.

Table 5-7: Maximum flood depth statistics derived from different scenarios

Scenario	Return Period	Maximum Flood Depth (m)				Velocity(m/s)				Area of inundation(m2)
		Min	Mean	Max	STD	Min	Mean	Max	STD	
Current	10	0.0002	0.77	3.65	0.76	0.0023	0.58	7	0.36	432300
	50	0.0003	0.8	4.2	0.79	0.0012	0.63	7.5	0.38	486000
	100	0.0003	0.83	4.76	0.8	0.0011	0.65	8	0.43	512700
Land-use effect	10	0.0001	0.8	4.7	0.79	0.0009	0.61	8	0.4	511100
	50	0.0001	0.86	5	0.8	0.0013	0.67	9.2	0.44	537900
	100	0.0001	0.93	5.6	0.81	0.0009	0.71	9.6	0.46	566500
RCP4.5	10	0.0001	0.63	3	0.75	0.0023	0.38	5.7	0.33	342500
	50	0.0003	0.64	3.5	0.76	0.0022	0.45	6.33	0.34	440300
	100	0.0002	0.67	4.2	0.77	0.0006	0.48	7.3	0.35	441400

RCP8.5	10	0.0006	0.79	4.34	0.77	0.0011	0.53	7.8	0.37	500000
	50	0.0007	0.88	4.7	0.8	0.0006	0.68	8.62	0.43	527100
	100	0.0006	0.9	5.2	0.82	0.0009	0.7	9.08	0.44	560000
Land-use with RCP4.5	10	0.0001	0.66	3.25	0.76	0.0004	0.45	6.5	0.34	418000
	50	0.0003	0.72	4.13	0.77	0.0008	0.53	7.2	0.37	466600
	100	0.0003	0.76	4.7	0.78	0.0013	0.57	7.7	0.38	499500
Land-use with RCP8.5	10	0.0002	0.83	4.5	0.79	0.0009	0.62	8.4	0.41	513600
	50	0.001	0.98	5.5	0.82	0.0018	0.76	9.4	0.48	540200
	100	0.001	1.08	6.4	0.84	0.0016	0.80	10.3	0.50	575000

6. DISCUSSION

6.1. Acquiring climate change data (precipitation) from RCMs, compare and analyze the projections among the set of RCMs

To evaluate the performance of RCMs, their rainfall simulations were compared with monthly observed rainfall data from the nearest ground-based rain gauge stations for the period 1981-2005. It was observed that all RCMs failed to represent the monthly observed rainfall. It is obvious that the RCMs lack ability to reasonably represents temporal variability of the rainfall time series. Similar results were reported by (Stefanidis et al., 2020). This may be attributed to the difference in the spatial resolution between RCM and gauge measurements. For instance, the RCM has a spatial resolution of 44 km, whereas the gauges measured rainfall from a single point. Piani et al. (2010) also claimed that this mismatch of observed and simulated data are mainly due to the used of large grid boxes, simplified physics, or incomplete knowledge of the earth's climate system. Individually, REMO2009 and RCA4 both underestimated whereas, CanCM4 overestimated the observed monthly rainfall. Many factors may contribute to the disparity among the different climate models' performance. These RCM models are, e.g., are driven by different GCMs. However, it was clear that the ensemble of the three models gave a better agreement with the observed rainfall. This complies with other studies such as (Nikulin et al., 2012); in the case of the ensemble, the errors between models cancel each other and reduce the deviations from observed data (Ayugi et., 2020, Endris et al. (2013).

The disparities in the different RCMs compared to the gauge measurement required correction to prevent propagating errors into hydrological and flood modeling. Therefore, this study used the quantile mapping method to adjust the future daily rainfall. The CDFs of baseline (1981-2005), future (2021-2050), uncorrected, and corrected RCM model daily rainfall data were compared to assess the effect of the quantile mapping adjustment. Prior comparison of the baseline and future uncorrected data showed that all climate models, except CanCM4, underestimated the observed daily rainfall by the gauges. However, after applying quantile adjustment, all models showed an increased daily rainfall except RCA4. The CDF of the ensemble mean, however, showed the intermediate behavior. Empirical quantile mapping used to correct the future rain have many merits as it corrects mean, standard deviation, high extreme, keep variabilities in projected variables (Amengual et al., 2012a). This method works with finding the difference in CDFs between the uncorrected and corrected variables between baseline and future time periods based on the observed rainfall. However, the CDFs show the difference in low precipitation intensities but hardly show changes in a high amount of precipitation. Therefore, the other functions should be used to better show changes in corrected and uncorrected variables.

The future climate depends on current and future human behavior, which is unpredictable. Therefore, scenarios are used to characterize the range of plausible future climates and illustrate the consequences of the policy choices (Moss et al., 2008). In that context, two scenarios that characterize the greenhouse gases emission for future periods were used in this study. The medium stabilization pathway RCP4.5 with varying levels of mitigation and the most aggressive RCP8.5 were compared. Based on the results, future monthly rainfall would increase in both rainy seasons, although the wettest (November) month occurs in the short rain season and the driest month found was August. Furthermore, the difference in rainfall intensities was found among the gauging station's locations, which indicated the spatial variability of the rainfall in the future.

Additionally, the future annual rainfall increased for both RCPs, with the high increase found in the RCP 8.5. The reduction of rainfall in some months was observed for RCP4.5. The increase of future rainfall due to RCP8.5 and the decrease due to RCP4.5 was also found in other regions such as Selman Yogyakarta

(Annisa & Nugroho, 2021). The reduction and increase of rainfall between two representative concentration pathways can be attributed to the fact that the International Energy Agency (IEA) “business as usual scenario” focusing on the year 2050 showed that RCP8.5 over-estimates by 234.5 Gt of CO₂ whereas RCP4.5 underestimates by 385.5 Gt CO₂ (Schwalm et al., 2020). As it is recognized, the emission of greenhouse gases affects meteorological processes. Therefore, the scenarios are used to present the decision-makers with the outcomes of the plausible choices to inform their decisions.

The findings in this study about changes in future rainfall are in line with other studies in Rwanda. Nahayo et al. (2018) used MIROC_4h under RCP 4.5 for future projections of precipitation in 4-climatological regions of Rwanda for the 2015-2035 window. The future projections indicated that there would be an increase in rainfall for the majority of the months. This increase in rainfall was also noticed by (Rukundo & Doğan, 2016) after using special reports emission scenarios for rainfall projection for the period 2011-2040. Uhorakeye & Möller (2017) studied the potential impacts of climate change on the future of Rwanda hydropower generation for periods for RCP4.5 and RCP8.5. The results for both scenarios showed considerable reductions in annual precipitations for the period of 2030 to 2060. They also found that the inter-annual variations in total annual rainfalls are expected to dominate the future climate, where changes are expected to reach 50%. Therefore, the future rainfall conditions for Rwanda are uncertain as some studies suggested increases while others find decreases in rainfall. Both scenarios were disclosed in the current study.

6.2. Deriving extreme rainfall and analyze their change between baseline and future periods.

The flooding events are associated with many factors; the most important is the intensity of the rainfall. The floodings are likely to happen during high extreme rainfall events than small intensities. Therefore, the changes in extreme rainfall analysis between current and future periods were done. The most severe events at the 99th percentile were analysed. The results showed that the extreme rainfall events would become more frequent and increase in magnitude under RCP8.5 compared to the current case. Future climate under RCP4.5 showed a reduction in rainfall extremes.

On the other hand, the Gumbel distribution function was fitted by the annual maximum rainfall to derive the extreme rainfall for 10, 50, and 10years return periods. The behavior of both RCPs found in the previous analysis was similar to the Gumbel distribution function analysis. More precisely, the extreme rainfall showed an increase in magnitude for RCP8.5, while the RCP4.5 reduced extreme rainfall magnitude for all return periods compared to the baseline period. The reduction of extremes under RCP4.5 was also reported by (Shrestha 2021) and decrease the number of days receiving more than 20mm. The increase of heavy and extremes rainfall due to climate change for RCP8.5 was reported in other regions like Europe (Rajczak & Schär, 2017) in Dar Salam in Tanzania (Brown, 2020). The increase of extreme rainfall in east Africa was believed to be associated with ENSO- El Niño, especially in a short rain season (Macleod & Caminade, 2019; Wainwright et al., 2020). Climate models did not show yet the clear effects of ENSO on future extreme rainfall. Though the IPCC AR5 reports with high confidence that ENSO will remain the leading mode of interannual variability through the twenty-first century, and rainfall associated with ENSO will become more severe (Christensen, 2019). The reduction of rainfall associated with drought is influenced by ENSO- La Nina (Wainwright et al., 2020).

The expected increase of extreme rainfall in the region of East Africa that will experience severe flooding was found in studies such as (Nicholson 2017). An increase of extreme rainfall events due to climate change was reported in Rwanda in various studies such as Uhorakeye & Möller, 2017; Icyimpaye et al., 2021).

6.3. Developing rainfall-runoff model for simulating impacts of climate and land-use changes on streamflow in Nyabugogo catchment

The simulation results have shown a significant increase in streamflow and peak flows due to the land use of 2050. The increase of 8.5% of impervious areas observed for the future was attributed to this increase as the impervious areas reduced the infiltration capacity of the basin and increased runoff. This study's findings comply with the study by (Wheater & Evans, 2009) who found that the discharges will increase due to land-use changes. The increase of peak discharges due to land use was also obtained in the findings of (Rukundo & Doğan, 2016), who found a significant increase of peak discharges in Kigali with projected land use of 2040. Climate change for RCP4.5 showed streamflow and peak flow reduction, whereas RCP8.5 increased future peak flow and streamflow. The combined effects of land use and climate for RCP8.5 showed more increase in streamflow and peak flows. The increase of and reduction of streamflow and peak flows observed for climate change are associated with the reasons related to climate change that was discussed in the above section. However, the case of land-use change that increased the peak flow and streamflow can be attributed to the urbanization scenario, which will yield the increase in flood volume and flood peaks because soil water storage capacity will be reduced due to built-up areas. Therefore, this decreases soil water content and increase direct runoff.

The rapid expansion of the city of Kigali is the main reason for the increase in the built-up areas and impervious areas in Nyabugogo catchment that, in return, increase streamflow hydrographs and flooding. The main four driving factors associated with this expansion have been identified. The spatial expansion of the city of Kigali has been significantly influenced by its topography that is made by mountains, valleys, and plains. The hills slopes that are surrounding the city vary between 45 to 50 percent and wetlands area with less than 2 percent (Manirakiza et al. 2019). These steep slopes create discontinuity in the city development leading to a scattered pattern of settlement on the hills.

Rural-urban migration has been the major factor in Kigali's urban expansion. Kigali has been receiving rural immigrants since 1982, and the rate of rural-urban immigration increased at the beginning of industrialization as all industries were almost located in Kigali (Nduwayezu et al., 2021). People from all provinces surrounding Kigali, especially college graduates, migrate to Kigali to search for good economic opportunities. For instance, in 2012, the net migration was 434695 people, whereas the population in Kigali was 1,132,686 (NISR, 2012). Most of the migrants live in informal settlements hence contributing to urban sprawl (Manirakiza et al. 2019).

The third factor is concerning the socio-economic attributes; the improvements and construction of economic infrastructures to boost economic development and to attract investors has been the priority in urban planning since 2000 (Manirakiza et al. 2019). The city of Kigali has established a special economic zone (SEZ) which is located in 10Km in the east of the city Centre and is occupying 276 ha (Nduwayezu et al. 2021). The workers for this zone dwell in the surrounding areas that were typical rural areas and now are classified as an urban zone.

The fourth contributing driving factor for Kigali city growth is the urban plans and policies. The plans and policies were designed in different periods to deal with emerging modernization, specifically in the post-genocide era. The Kigali authorities introduced Kigali Conceptual Master Plan in 2007, which was projected to 2040. The plan was revised in 2013 and 2020 for the 2050 projection. (Nduwayezu et al. 2021).

Unprecedented Kigali growth is associated with the government decision to shift from rural and agriculture-based economy to urban and services-based economies. Therefore, it is in that context the rapid urbanization is a key part of the overall economic development, and Kigali city as the capital city plays a central role. However, uncoordinated spatial expansion leads to socio-economic and environmental sustainability challenges due to the high demand for land.

It is obvious that the city of Kigali will continue to expand. The city managers and planners should develop urban growth needs, environmental and socio-economic planning, and policies to coordinate urban expansion and its consequences. For the case of expected flooding and high streamflow hydrographs associated with future land use of 2050 that was revealed in this study, the construction of urban drainage systems and promoting high-rise buildings are required as they can contribute positively toward sustainable urbanization.

6.4. Simulating flooding for Nyabugogo commercial hub under changing climate and land-use.

The flood modeling was conducted for the present time and future time periods. The results showed that the upstream areas contribute more water to the flood model compared to Yanze and Mpazi subbasins. However, these two subbasins contribute more water to the flood model after Muhazi lake compared to the rest of the subbasins. Similar results were reported by (Manyifika 2015) after classifying the basins based on their contribution to the flood model during extreme rainfall.

Three flood characteristics (i.e., water depth, velocity, and flood extent) were evaluated in this study for the present time and future time periods for RCP4.5 and 8.5. The behaviors observed for extreme rainfall that propagated in streamflow for all scenarios were transmitted into floods characteristics. For instance, the high values for water depth, velocity, and areas of inundation were found for land-use cases compared to climate change for both RCP4.5 and 8.5. The climate change for RCP8.5 showed an increase for all flood characteristics. RCP4.5 showed a reduction in all floods characteristics relative to current floods. The combined land use with RCP4.5 showed a slightly increase compared to RCP4.5 alone. Land-use with RCP8.5 showed a higher increase in all flood characteristics compared to all other scenarios. This indicated the effects of combined climate change for RCP8.5 and land-use change will exaggerate floodings in the Nyabugogo catchment.

The current study found that the flood model is sensitive to the number of inflow boundaries. This was revealed from the fact that the flood characteristics increase in value by an increase in return periods with the 100-years return period showed the higher values compared to 10 and 50 years. This was confirmed by the findings by (Manyifika 2015, Ali 2016). In their study, they forced flood model with small inflow boundaries and floods characteristics obtained was small compared to the results of the current study whose inflows boundaries were high.

The current study results revealed that Nyabugogo catchment, specifically its flood-prone area, will experience more intense floods due to land-use changes, and the climate change under RCP8.5 will worsen the flooding conditions. The main reason for this increase is the urbanization that will increase the built-up areas as discussed above. The increase of extreme rainfall due to RCP8.5 results for some phenomena such as El Niño will increase the magnitude of flooding in the Nyabugogo catchment. The study results are in line with other studies in the region as the East Africa region will experience high and heavy flooding due to climate change. The urban expansion in east Africa cities will exacerbate flooding under changing climate (Brown, 2020). Also reported East Africa as the region the will experience more frequent and severe floods as result of climate change (WMO, 2019; Nicholson, 2017; Osima et al., 2018)

As the increase in heavy precipitation results in frequent devastating floods, therefore, the dense drainage structure should be planned in the city of Kigali and surrounding to carry water before inundating the area. The increase in vegetation that can help to increase infiltration of water and reduce overland runoff would be promoted.

7. CONCLUSION AND RECOMMENDATION

7.1. Conclusion

This study integrated various tools such as regional climate models, two RCPs (4.5 and 8.5), GIS, hydrologic and hydrodynamic models to assess impacts of climate change and future land use scenarios on flooding in the Nyabugogo catchment between 1981-2005 and (2021-2050).

The comparison of RCM simulations with observed data in the baseline period indicated that all RCMs simulations failed to reproduce the monthly rainfall in Nyabugogo catchment as they deviated from the observed rainfall except in the dry season (July and August). This indicated the inability of the RCMs to represent the regional climate and the possible uncertainties in the future projections. Therefore, the inherent systematic errors in RCMs due to spatial and temporal resolution and other reasons should not be neglected. Among the three RCMs used, CanCM4 showed an over-estimation of the observed monthly rainfall while two remaining RCMs, RCA4 and REMO2009, showed an under-estimation. These discrepancies between observed and simulated rainfall from RCMs revealed the need for bias adjustment before the further use of these outputs in water resource assessment. However, the ensemble mean of the three RCMs was calculated, and it showed an improvement in simulating monthly rainfall in comparison with observed rainfall.

The empirical quantile mapping method was applied to determine the corrected future rainfall projections. The outputs from quantile mapping revealed the increment of rainfall in short and long rain seasons for all RCMs except RCA4, and the ensemble mean for RCP4.5 that indicated a likely decrement in the future rainfall amount for the months of February, May, June, July, and August. Future rainfall projections showed that November will be the wettest month of the year while August will be the driest. This indicated the shift of rainfall regimes as historically driest month used to be July. The annual rainfall showed a small increase for RCP4.5 while RCP8.5 showed a significant increase for all meteorological gauging stations. This reveals that people in charge have to be prepared for the future high magnitude of rainfall in order to overcome the impacts that might be attached such extreme rainfall such as floods.

The purpose of this study was to use the extremes from RCMs for future flood forecasting. Therefore, extreme rainfall was determined. By using the Gumbel distribution function, 1-day extreme rainfall was derived for 10, 50, and 100 years return period. The results revealed that relative to the observed rainfall in the baseline period (1981-2005), there will be a decreasing pattern in the magnitude of extreme rainfall under the RCP4.5 emission scenario for the period (2021-2050). A significant increase in daily extreme rainfall was obtained for the RCP8.5 scenario for all stations, with the highest magnitude is 188mm at Kigali station for 100 years return periods which is a 24.5% increase compared to observed data in the baseline period (1981-2005). Some studies and IPCC R5 reported that these increases in extreme rainfall will be the results of El Niño

The rainfall-runoff model was developed to simulate streamflow and peak flows, which were later used as inflow boundaries to the flood model. In order to assess the impacts of land-use changes on streamflow and peak flow, the planned future land-use of 2050 was used. The future classification revealed the increase in built-up areas from 2.6% to 8.5%, which will read to increase in impervious areas. The main reason for impervious areas increase in the Nyabugogo catchment is the rapid expansion of the city of Kigali due to the continuation migration of people from other provinces to the city of Kigali. The other reason is the unprecedented Kigali growth is associated with the government decisions to shift from rural and agricultural based economy to urban and services-based economy. Therefore, it is in that context the rapid urbanization is a key part of the overall economic development, and Kigali city as the capital city plays a central role. in

return, read to more built-up areas and impervious areas. This increase in impervious areas was found to be the main reason of increase streamflow and peak flows in the Nyabugogo catchment in the future. Therefore, future land-use management is required in order to be able to reduce the expected increase in streamflow and flood hydrographs which will lead to flooding.

The SOBEK 1D2D flood model was forced by the inflow boundaries from different scenarios under land-use changes and climate change. The results showed an increase for all three flood characteristics (water depth, velocity, and flood extent) analysed for land-use change. The increase was observed as increasing in return periods. The floods characteristics under RCP4.5 showed a decreasing trends. Climate change under RCP8.5 showed the increase of flood characteristics for all return periods. The combined effects of land-use change and climate change under RCP8.5 showed more increase in flood characteristics. The obtained results for flood characteristics contradicted the current study hypothesized that climate change has more impacts on flooding because it was observed that land-use change will have more impacts on flooding in Nyabugogo catchment than climate change. However, the combination of land-use change, such as an increase in impervious areas together with climate change under the high emission scenarios, will exacerbate the flooding in Nyabugogo commercial hub, which complies with the second part of the hypothesis.

The novelty of the current study is that it is the first research using extreme rainfall data from regional climate models for flood prediction in the study area. It is concluded that climate models can be applied for streamflow and flood prediction as the climate models are now the available tools that can be used to study the future climate and the associated impacts.

The findings of this study contributed to the national water resources management and infrastructure work based on the current and future rainfall conditions. Both increase/ decrease of the future precipitation has to be taken into consideration by the decision-makers. The water reservoirs must be planned in case of rainfall reduction and would be an option for long-term measures to adapt to climate change, especially in dry periods. Drainage network systems must be planned in case of rainfall increase especially during the wet period where there is a high significant increase of rainfall that could lead to floodings. The investments in environmental measures and infrastructure for adapting to expected changes would require financial and human resources. Therefore, the early action with consideration of deep investigation in studies using available data and climate projections can help to be prepared and mitigate the devastating impacts of climate change. On the other hand, proper land use management and follow up to planned land use are urgently need as the land use change was found to be the many contributor of flooding in the Nyabugogo catchment.

If flooding is not addressed, it will continue to drain cities' financial resources and threaten lives and livelihoods in the city of Kigali and its greater region.

7.2. Limitations of this study

1. Climate models can be used to study the future climate. But it is noted that simulations and future projections of these models are associated with biases. Though the bias corrections methods can be applied, however not allow biases or errors can be removed. Therefore, their results are associated with certain degree of uncertainties, and this should be considered before their further applications.

2. The main challenge in this study was the observed discharge data scarcity that was required for the calibration and validation of the rainfall-runoff model. The long records of the observed discharge data starting from the same period as the considered baseline period (1981) could have enabled to test of the model performance for different decades. However, due to poor quality and huge gaps in observed discharge data and non-overlapping periods of records for gauged catchments resulted in using only events of 2011-2013 for calibration and validation of the model.

3. Observed discharge data were available only for three sub catchments and the entire Nyabugogo catchment for the mentioned period. Therefore, due to the data shortage and poor data quality, the optimum parameters obtained after validating the rainfall-runoff model for the Yanze sub catchment were donated to other ungauged basins. The use of the optimum parameters from a single subcatchment reduced the model performance, which was observed in the objective functions. More gauged sub catchments would have helped to improve the performance of the model. Secondly, the applied sub-models in HEC-HMS hydrological model were mainly based on the available data. This limited the opportunity to apply different methods for comparison.

4. The available land-use data used for the baseline period was from 2012. The land-use of period between (1981-2005) would be good to use because the extreme rainfall used for the current cases was based on the observed data rainfall for the period of (1981-2005).

7.3. Recommendations

1. The current study suggests an attractive benchmark for RCMs and Rwandan climate change studies and extremes. The intensification of extreme rainfall observed in RCMs projections call for further studies on how to translate climate projections estimates toward implementation of sound adaptation strategies. As the flood continue to become more frequent and show an increase in the future, other tools rather than hydrological models such as machine learning can be used for flood/prediction forecasting in the Nyabugogo catchment. This will help in early flood warning systems with different lead times that promising countermeasures against flood hazards and losses.

2. The current study analysed the future rainfall based on RCMs projections. It is suggested that related studies should be done in other regions of Rwanda. The analysis should include more climate factors that affect the hydrological cycle such as temperature, wind, humidity, and studies related to changes in future atmospheric circulation to better understand the future climate over Rwanda. In addition, simulating the fine time scale such as daily and hourly scale cloud increase the significant conclusions on the effect of climate change on hydrometeorological hazards.

3. It's always necessary in hydrological studies to calibrate and validate the hydrological models in order to have confidence in its performance. However, for the current study area, observed data showed to be of poor quality but also very limited, with very few catchments being gauged. This limits the assessment of the rainfall-runoff model and its application as some methods cannot be applied at all in case of data scarcity. The recommendation for Rwanda Water Board is to increase the number of gauging stations and systematic recording of the water levels and discharge. This will help to reduce the claimed poor quality in observed hydrological data. A similar recommendation was also given by (Manyifika, 2015).

4. The flood model used under the current study is used for the third time to explore flooding in Nyabugogo commercial hub. However, the model was not calibrated because of the absence of recorded floods characteristics. Therefore, I recommend the use of other products such as satellites maps for the calibration of the hydraulic flood model simulations.

LIST OF REFERENCES

- Abimbola, O. P., Wenninger, J., Venneker, R., & Mittelstet, A. R. (2017). The assessment of water resources in ungauged catchments in Rwanda. *Journal of Hydrology: Regional Studies*, 13(August 2017), 274–289. <https://doi.org/10.1016/j.ejrh.2017.09.001>
- Ahbari, A., Stour, L., Agoumi, A., & Serhir, N. (2018). Estimation of initial values of the HMS model parameters: Application to the basin of Bin El Ouidane (Azilal, Morocco). *Journal of Materials and Environmental Science*, 9(1), 305–317. <https://doi.org/10.26872/jmes.2018.9.1.34>
- Akter, T., Quevauviller, P., Eisenreich, S. J., & Vaes, G. (2018). Impacts of climate and land use changes on flood risk management for the Schijn River, Belgium. *Environmental Science and Policy*, 89(November 2017), 163–175. <https://doi.org/10.1016/j.envsci.2018.07.002>
- Ali, H. T. (2016). Digital Urban Terrain Characterization for 1D2D Hydrodynamic Flood Modelling in Kigali, Rwanda. *Thesis*. Retrieved from http://www.itc.nl/library/papers_2016/msc/wrem/ali.pdf
- Ali, M., Khan, S. J., Aslam, I., & Khan, Z. (2011). Simulation of the impacts of land-use change on surface runoff of Lai Nullah Basin in Islamabad, Pakistan. *Landscape and Urban Planning*, 102(4), 271–279. <https://doi.org/10.1016/j.landurbplan.2011.05.006>
- Amengual, A., Homar, V., Romero, R., Alonso, S., & Ramis, C. (2012a). A statistical adjustment of regional climate model outputs to local scales: Application to Platja de Palma, Spain. *Journal of Climate*, 25(3), 939–957. <https://doi.org/10.1175/JCLI-D-10-05024.1>
- Amengual, A., Homar, V., Romero, R., Alonso, S., & Ramis, C. (2012b). Projections of the climate potential for tourism at local scales: Application to Platja de Palma, Spain. *International Journal of Climatology*, 32(14), 2095–2107. <https://doi.org/10.1002/joc.2420>
- Annisa, H. N., & Nugroho, B. D. A. (2021). Analysis and Projections of Rainfall using representative concentration pathways (RCPs) Scenarios in Sleman Yogyakarta. *IOP Conference Series: Earth and Environmental Science*, 653(1). <https://doi.org/10.1088/1755-1315/653/1/012099>
- Ayugi, B., Tan, G., Gnitou, G. T., Ojara, M., & Ongoma, V. (2020). Historical evaluations and simulations of precipitation over East Africa from Rossby centre regional climate model. *Atmospheric Research*, 232(August 2019), 104705. <https://doi.org/10.1016/j.atmosres.2019.104705>
- Baltas, E. A., Dervos, N. A., & Mimikou, M. A. (2007). Technical note: Determination of the SCS initial abstraction ratio in an experimental watershed in Greece. *Hydrology and Earth System Sciences*, 11(6), 1825–1829. <https://doi.org/10.5194/hess-11-1825-2007>
- Birhanu, A., Masih, I., van der Zaag, P., Nyssen, J., & Cai, X. (2019). Impacts of land use and land cover changes on hydrology of the Gumara catchment, Ethiopia. *Physics and Chemistry of the Earth*, 112(July 2018), 165–174. <https://doi.org/10.1016/j.pce.2019.01.006>
- Brassel, K. E., & Reif, D. (1979). A Procedure to Generate Thiessen Polygons. *Geographical Analysis*, 11(3), 289–303. <https://doi.org/10.1111/j.1538-4632.1979.tb00695.x>
- Brown, V. (2020). *Flooding in East Africa*. 1–20. Retrieved from [https://reliefweb.int/sites/reliefweb.int/files/resources/CFF_Report_Design - Dar es Salaam-final 2020 - singles_compressed.pdf](https://reliefweb.int/sites/reliefweb.int/files/resources/CFF_Report_Design_-_Dar_es_Salaam-final_2020_-_singles_compressed.pdf)
- Bucchignani, E., Mercogliano, P., Panitz, H. J., & Montesarchio, M. (2018). Climate change projections for the Middle East–North Africa domain with COSMO-CLM at different spatial resolutions. *Advances in Climate Change Research*, 9(1), 66–80. <https://doi.org/10.1016/j.accre.2018.01.004>
- Byamukama. (2009). National Strategy on Climate Change and Low Carbon Development for Rwanda Baseline Report. *Yoga Journal*, (219), 35–42. <https://doi.org/10.4210/SSEE.PBS.2011.0002>
- Cannon, A. J., Sobie, S. R., & Murdock, T. Q. (2015). Bias correction of GCM precipitation by quantile mapping: How well do methods preserve changes in quantiles and extremes? *Journal of Climate*, 28(17), 6938–6959. <https://doi.org/10.1175/JCLI-D-14-00754.1>
- Casas, M. C., Rodríguez, R., Prohom, M., Gázquez, A., & Redaño, A. (2011). Estimation of the probable maximum precipitation in Barcelona (Spain). *International Journal of Climatology*, 31(9), 1322–1327. <https://doi.org/10.1002/joc.2149>
- City of Kigali. (2013). *City development plan (2013-2018)*. 1–98. Retrieved from https://kigalicity.gov.rw/fileadmin/templates/Documents/policies/Kigali_City_Development_Plan__2013-2018__City_development_Plan_.pdf
- Crookston, B. M., & Tullis, B. P. (2012). Scour prevention in bottomless arch culverts. *International Journal of Sediment Research*, 27(2), 213–225. [https://doi.org/10.1016/S1001-6279\(12\)60029-8](https://doi.org/10.1016/S1001-6279(12)60029-8)
- D. N. Moriasi, J. G. Arnold, M. W. Van Liew, R. L. Bingner, R. D. Harmel, & T. L. Veith. (2007). Model

- Evaluation Guidelines for Systematic Quantification of Accuracy in Watershed Simulations. *Transactions of the ASABE*, 50(3), 885–900. <https://doi.org/10.13031/2013.23153>
- Darji, K., Khokhani, V., Prakash, I., Mehmood, K., & Pham, B. T. (2019). Rainfall-Runoff Modelling Using HEC-HMS Model: An Application of Regression Analysis. *Journal of Emerging Technologies and Innovative Research (JETIR)*, 6(5), 226–234.
- Darji, K., Prakash, I., Mehmood, K., & Pham, B. T. (2019). *Rainfall-Runoff Modelling Using HEC-HMS Model: An Application of Regression Analysis*. (May).
- Deltares. (2013). *Sobek 1D/2D*. Retrieved from https://content.oss.deltares.nl/delft3d/manuals/SOBEK_User_Manual.pdf
- DHI. (2007). MIKE SHE User Manual: User Guide 1. *MIKE by DHI*, 1.
- DHONDIA, J. F., & STELLING, G. S. (2004). Sobek One Dimensional – Two Dimensional Integrated Hydraulic Model for Flood Simulation – Its Capabilities and Features Explained. *Hydroinformatics*, (June), 1867–1874. https://doi.org/10.1142/9789812702838_0230
- Doong, D. J., Lo, W., Vojinovic, Z., Lee, W. L., & Lee, S. P. (2016). Development of a new generation of flood inundation maps—a case study of the coastal city of Tainan, Taiwan. *Water (Switzerland)*, 8(11). <https://doi.org/10.3390/w8110521>
- Dosio, A., Panitz, H. J., Schubert-Frisius, M., & Lüthi, D. (2015). Dynamical downscaling of CMIP5 global circulation models over CORDEX-Africa with COSMO-CLM: evaluation over the present climate and analysis of the added value. *Climate Dynamics*, 44(9–10), 2637–2661. <https://doi.org/10.1007/s00382-014-2262-x>
- Dottori, F., & Todini, E. (2013). *Testing a simple 2D hydraulic model in an urban flood experiment*. 1320(June 2012), 1301–1320. <https://doi.org/10.1002/hyp.9370>
- Emam, A. R., Mishra, B. K., Kumar, P., Masago, Y., & Fukushi, K. (2016). Impact assessment of climate and land-use changes on flooding behavior in the upper ciliwung river, jakarta, Indonesia. *Water (Switzerland)*, 8(12). <https://doi.org/10.3390/w8120559>
- Enayati, M., Bozorg-Haddad, O., Bazrafshan, J., Hejabi, S., & Chu, X. (2020). Bias correction capabilities of quantile mapping methods for rainfall and temperature variables. *Journal of Water and Climate Change*, 1–19. <https://doi.org/10.2166/wcc.2020.261>
- Endris, H. S., Omondi, P., Jain, S., Lennard, C., Hewitson, B., Chang'a, L., ... Tazalika, L. (2013). Assessment of the performance of CORDEX regional climate models in simulating East African rainfall. *Journal of Climate*, 26(21), 8453–8475. <https://doi.org/10.1175/JCLI-D-12-00708.1>
- Fan, Y., Ao, T., Yu, H., Huang, G., & Li, X. (2017). A coupled 1D-2D hydrodynamic model for urban flood inundation. *Advances in Meteorology*, 2017. <https://doi.org/10.1155/2017/2819308>
- Feldman, A. (2000). Hydrologic Modeling System Technical Reference Manual. *Hydrologic Modeling System HEC-HMS Technical Reference Manual*, (March), 148.
- FONERWA. (2019). *Detailed Design of Flood Control Measures in the Volcano Region, Rwanda*.
- Gumindoga, W., Rientjes, T., Shekede, M. D., Rwasoka, D. T., Nhapi, I., & Haile, A. T. (2014). Hydrological impacts of urbanization of two catchments in Harare, Zimbabwe. *Remote Sensing*, 6(12), 12544–12574. <https://doi.org/10.3390/rs61212544>
- Haile, A. T., Akawka, A. L., Berhanu, B., & Rientjes, T. (2017). Changes in water availability in the Upper Blue Nile basin under the representative concentration pathways scenario. *Hydrological Sciences Journal*, 62(13), 2139–2149. <https://doi.org/10.1080/02626667.2017.1365149>
- Han, D., & Bray, M. (2006). Automated Thiessen polygon generation. *Water Resources Research*, 42(11), 2–6. <https://doi.org/10.1029/2005WR004365>
- Huber, D. G., Gullede, J., & Ph, D. (2011). SCIENCE EXTREME WEATHER & CLIMATE CHANGE : UNDERSTANDING THE LINK AND by. *Solutions*, December(1), 1–13.
- Icyimpaye, G., Abdelbaki, C., & Mourad, K. A. (2021). Hydrological and hydraulic model for flood forecasting in Rwanda. *Modeling Earth Systems and Environment*, (May 2016). <https://doi.org/10.1007/s40808-021-01146-z>
- Jakada, H., Chen, Z., Luo, M., Zhou, H., Wang, Z., & Habib, M. (2019). Watershed characterization and hydrograph recession analysis: A comparative look at a karst vs. non-karst watershed and implications for groundwater resources in Gaolan River basin, Southern China. *Water (Switzerland)*, 11(4). <https://doi.org/10.3390/w11040743>
- Jakob Themeßl, M., Gobiet, A., & Leuprecht, A. (2011). Empirical-statistical downscaling and error correction of daily precipitation from regional climate models. *International Journal of Climatology*, 31(10), 1530–1544. <https://doi.org/10.1002/joc.2168>
- Jarraud, M., & Steiner, A. (2012). Climate Change 2014 Synthesis Report IPCC. In *Managing the Risks of*

- Extreme Events and Disasters to Advance Climate Change Adaptation: Special Report of the Intergovernmental Panel on Climate Change* (Vol. 9781107025). <https://doi.org/10.1017/CBO9781139177245.003>
- Jothityangkoon, C., Hirunteeaykul, C., Boonrawd, K., & Sivapalan, M. (2013). Assessing the impact of climate and land use changes on extreme floods in a large tropical catchment. *Journal of Hydrology*, 490(February 2018), 88–105. <https://doi.org/10.1016/j.jhydrol.2013.03.036>
- Jubb, I., Canadell, P., & Dix, M. (2013). *Representative Concentration Pathways*. Australian Government, Department of the Environment. 1–19.
- K. Warner, P. van de L. (2018). Climate Change PROFILE Climate Change. *Ministry of Foreign Affairs of the Netherlands*, (July), 14. Retrieved from www.government.nl/foreign-policy-evaluations
- Kent, K. M. (1973). A method for estimating volume and rate of runoff in small watersheds. *Soil Conservation Service*, (April), 64.
- Konrad, C. P. (2003). Effects of Urban Development on Floods. *U.S. Geological Survey*, d(November), 1–4.
- Kuswanto, H., Andari, S., & Permatasari, E. O. (2015). Identification of extreme events in climate data from multiple sites. *Procedia Engineering*, 125, 304–310. <https://doi.org/10.1016/j.proeng.2015.11.067>
- Lutz, A. F., ter Maat, H. W., Biemans, H., Shrestha, A. B., Wester, P., & Immerzeel, W. W. (2016). Selecting representative climate models for climate change impact studies: an advanced envelope-based selection approach. *International Journal of Climatology*, 36(12), 3988–4005. <https://doi.org/10.1002/joc.4608>
- Macleod, D., & Caminade, C. (2019). The moderate impact of the 2015 El Niño over East Africa and its representation in seasonal reforecasts. *Journal of Climate*, 32(22), 7989–8001. <https://doi.org/10.1175/JCLI-D-19-0201.1>
- Manirakiza, V., Mugabe, L., & Nsabimana, A. (2019). *City Profile : Kigali , Rwanda*. <https://doi.org/10.1177/0975425319867485>
- Manyifika, M. (2015). Diagnostic assessment on urban floods using satellite data and hydrologic models in Kigali, Rwanda. *Thesis*, 88. Retrieved from http://www.itc.nl/library/papers_2015/msc/wrem/manyifika.pdf
- Manyifika, M., & Rientjes, T. H. M. (2010). *Diagnostic assesment on urban floods using satellite data and hydrologic models in Kigali , Rwanda .*
- Maraun, D. (2013). Bias correction, quantile mapping, and downscaling: Revisiting the inflation issue. *Journal of Climate*, 26(6), 2137–2143. <https://doi.org/10.1175/JCLI-D-12-00821.1>
- Mascaro, G., White, D. D., Westerhoff, P., & Bliss, N. (2015). Journal of geophysical research. *Nature*, 175(4449), 238. <https://doi.org/10.1038/175238c0>
- Mignot, E., Paquier, A., & Haider, S. (2006). *Modeling floods in a dense urban area using 2D shallow water equations*. 186–199. <https://doi.org/10.1016/j.jhydrol.2005.11.026>
- Ministry of Foreign Affairs of the Netherlands. (2018). Climate Change PROFILE Climate Change. *Ministry of Foreign Affairs of the Netherlands*, 14. Retrieved from www.government.nl/foreign-policy-evaluations
- Mishra & Singh, V. P., S. K. (2013). Soil Conservation Service Curve Number (SCS-CN) Methodology. *Water Science & Technology Library*, 42.
- Mishra, S. K., Jain, M. K., & Singh, V. P. (2004). Evaluation of the SCS-CN-based model incorporating antecedent moisture. *Water Resources Management*, 18(6), 567–589. <https://doi.org/10.1007/s11269-004-8765-1>
- Moss, R., Babiker, M., Brinkman, S., Calvo, E., Carter, T., Edmonds, J., ... Zurek, M. (2008). Towards New Scenarios for Analysis of Emissions, Climate Change, Impacts and Response Strategies. In *IPCC Expert Meeting Report*. Retrieved from http://www.osti.gov/energycitations/product.biblio.jsp?osti_id=940991
- Munyaneza, O., Nzeyimana, Y. K., & Wali, U. G. (2011). *Hydraulic structures design for flood control in the Nyabugogo wetland , Rwanda. 8560783*(December), 1–12.
- Munyaneza Omar, Umaru Garba Wali, N. K. Y. (2013). *Hydraulic Structures Design for Flood Control in the Nyabugogo Wetland, Rwanda. 6*(2), 26–37.
- Nahayo, L., Habiyaremye, G., Kayiranga, A., Kalisa, E., Mupenzi, C., & Nsanzimana, D. F. (2018). Rainfall Variability and Its Impact on Rain-Fed Crop Production in Rwanda. *American Journal of Social Science Research*, 4(1), 9–15. Retrieved from <http://www.aiscience.org/journal/ajssrhttp://creativecommons.org/licenses/by/4.0/>
- Natarajan, S., & Radhakrishnan, N. (2021). Simulation of rainfall–runoff process for an ungauged catchment using an event-based hydrologic model: A case study of koraiyar basin in Tiruchirappalli city, India. *Journal of Earth System Science*, 130(1). <https://doi.org/10.1007/s12040-020-01532-8>

- National Institute of Statistics of Rwanda (NISR). (2012). Rwanda - Rwanda Population and Housing Census 2012. *Rwanda*, 226(4676), 1–51. Retrieved from file:///C:/Users/user/Downloads/RPHC4_Population_Projections.pdf
- Nduwayezu, G., Manirakiza, V., Mugabe, L., & Malonza, J. M. (2021). Urban Growth and Land Use/Land Cover Changes in the Post-Genocide Period, Kigali, Rwanda. *Environment and Urbanization ASIA*, 12(1_suppl), S127–S146. <https://doi.org/10.1177/0975425321997971>
- Nhapi, I. (2011). Assessment of Water Pollution Levels in the Nyabugogo Catchment, Rwanda. *The Open Environmental Engineering Journal*, 4(1), 40–53. <https://doi.org/10.2174/1874829501104010040>
- Nicholson, S. E. (2017). Climate and climatic variability of rainfall over eastern Africa. *Reviews of Geophysics*, 55(3), 590–635. <https://doi.org/10.1002/2016RG000544>
- Nikulin, G., Jones, C., Giorgi, F., Asrar, G., Büchner, M., Cerezo-Mota, R., ... Sushama, L. (2012). Precipitation climatology in an ensemble of CORDEX-Africa regional climate simulations. *Journal of Climate*, 25(18), 6057–6078. <https://doi.org/10.1175/JCLI-D-11-00375.1>
- Noguer, M., Jones, R., & Murphy, J. (1998). Sources of systematic errors in the climatology of a regional climate model over Europe. *Climate Dynamics*, 14(10), 691–712. <https://doi.org/10.1007/s003820050249>
- Ogega, O. M., Koske, J., Kung'u, J. B., Scoccimarro, E., Endris, H. S., & Mistry, M. N. (2020). Heavy precipitation events over East Africa in a changing climate: results from CORDEX RCMs. *Climate Dynamics*, 55(3–4), 993–1009. <https://doi.org/10.1007/s00382-020-05309-z>
- Olawoyin, R. (2017). Objective assessment of the Thiessen polygon method for estimating areal rainfall depths in the River Volta catchment in Ghana. *Ghana Journal of Geography*, 9(2), 151–174.
- Osima, S., Indasi, V. S., Zaroug, M., Endris, H. S., Gudoshava, M., Misiani, H. O., ... Dosio, A. (2018). Projected climate over the Greater Horn of Africa under 1.5 °C and 2 °C global warming. *Environmental Research Letters*, 13(6). <https://doi.org/10.1088/1748-9326/aaba1b>
- Pachauri, R. K. (2014). *Climate Change 2014 Synthesis Report*.
- Pereira, L. S., & Keller, H. M. (1982). Factors affecting recession parameters and flow components in eleven small Pre-Alp basins. *Hydrological Aspects of Alpine and High-Mountain Areas. Proc. Exeter Symposium, July 1982*, (138), 233–242.
- Piani, C., Weedon, G. P., Best, M., Gomes, S. M., Viterbo, P., Hagemann, S., & Haerter, J. O. (2010). Statistical bias correction of global simulated daily precipitation and temperature for the application of hydrological models. *Journal of Hydrology*, 395(3–4), 199–215. <https://doi.org/10.1016/j.jhydrol.2010.10.024>
- Pilgrim, D. H. (1987). Australian rainfall and runoff. *A Guide to Flood Estimation*, (May), 374.
- Ponce, V. M., & Hawkins, R. H. (1996). Runoff Curve Number: Has It Reached Maturity? *Journal of Hydrologic Engineering*, 1(1), 11–19. [https://doi.org/10.1061/\(asce\)1084-0699\(1996\)1:1\(11\)](https://doi.org/10.1061/(asce)1084-0699(1996)1:1(11))
- Rajczak, J., & Schär, C. (2017). Projections of Future Precipitation Extremes Over Europe: A Multimodel Assessment of Climate Simulations. *Journal of Geophysical Research: Atmospheres*, 122(20), 10,773–10,800. <https://doi.org/10.1002/2017JD027176>
- Rätty, O., Räisänen, J., & Ylhäisi, J. S. (2014). Evaluation of delta change and bias correction methods for future daily precipitation: Intermodel cross-validation using ENSEMBLES simulations. *Climate Dynamics*, 42(9–10), 2287–2303. <https://doi.org/10.1007/s00382-014-2130-8>
- REMA. (2019). *Republic of Rwanda Rwanda Environment Management Authority Assessment of Climate Change Vulnerability in*.
- Report(TR-55), S. C. T. (1986). Urban Hydrology for Small. *Soil Conservation*, (Technical Release 55 (TR-55)), 164. Retrieved from <http://scholar.google.com/scholar?hl=en&btnG=Search&q=intitle:Urban+Hydrology+for+Small+watersheds#1>
- Rogger, M., Agnoletti, M., Alaoui, A., Bathurst, J. C., Bodner, G., Borga, M., ... Viglione, A. (2016). *Water Resources Research*. (June 2013), 5209–5219. <https://doi.org/10.1002/2017WR020723>. Received
- Rukundo, E., & Doğan, A. (2016). Assessment of climate and land use change projections and their impacts on flooding. *Polish Journal of Environmental Studies*, 25(6), 2541–2552. <https://doi.org/10.15244/pjoes/63781>
- Saberifar, R., & Noor, P. (2017). *Analyzing the Effects of Urban Development on Flooding in the Cities (Case Study : Birjand City)*. 2(2), 177–186.
- Samuelsson, P., Jones, C. G., Willén, U., Ullerstig, A., Gollvik, S., Hansson, U., ... Wyser, K. (2011). The Rossby Centre Regional Climate model RCA3: Model description and performance. *Tellus, Series A: Dynamic Meteorology and Oceanography*, 63(1), 4–23. <https://doi.org/10.1111/j.1600-0870.2010.00478.x>

- Saxton, K. E., & Willey, P. H. (2009). *the Spaw Model for Agricultural Field and Simulation*. 1–36.
- Schwalm, C. R., Glendon, S., & Duffy, P. B. (2020). RCP8.5 tracks cumulative CO2 emissions. *Proceedings of the National Academy of Sciences of the United States of America*, *117*(33), 19656–19657. <https://doi.org/10.1073/PNAS.2007117117>
- SCS. (1972). 4.4 The Curve Number Method. *Soil Conservation*, 121–144.
- Shongwe, M. E., van Oldenborgh, G. J., van den Hurk, B., & van Aalst, M. (2011). Projected changes in mean and extreme precipitation in Africa under global warming. Part II: East Africa. *Journal of Climate*, *24*(14), 3718–3733. <https://doi.org/10.1175/2010JCLI2883.1>
- Shrestha, S., & Roachanakanan, R. (2021). Extreme climate projections under representative concentration pathways in the Lower Songkhram River Basin, Thailand. *Heliyon*, *7*(2), e06146. <https://doi.org/10.1016/j.heliyon.2021.e06146>
- Siebert, A., Dinku, T., Vuguziga, F., Twahirwa, A., Kagabo, D. M., delCorral, J., & Robertson, A. W. (2019). Evaluation of ENACTS-Rwanda: A new multi-decade, high-resolution rainfall and temperature data set—Climatology. *International Journal of Climatology*, *39*(6), 3104–3120. <https://doi.org/10.1002/joc.6010>
- Smithers, J. C., & Schulze, R. E. (2004). The estimation of design rainfalls for South Africa using a regional scale invariant approach. *Water SA*, *30*(4), 435–444. <https://doi.org/10.4314/wsa.v30i4.5095>
- Stefanidis, S., Dafis, S., & Stathis, D. (2020). Evaluation of regional climate models (Rcms) performance in simulating seasonal precipitation over mountainous central pindus (greece). *Water (Switzerland)*, *12*(10). <https://doi.org/10.3390/w12102750>
- Stevens, A. J., Clarke, D., & Nicholls, R. J. (2016). Trends in reported flooding in the UK: 1884–2013. *Hydrological Sciences Journal*, *61*(1), 50–63. <https://doi.org/10.1080/02626667.2014.950581>
- Suman, A., & Akther, F. (2014). River Flood Modelling Using SOBEK: A Case Study from Ciliwung Catchment, Indonesia. *International Journal of Engineering Research*, *3*(11), 662–668. <https://doi.org/10.17950/ijer/v3s11/1108>
- Survsy, A. L. (n.d.). *Double-Mass Curves Double-Mass Curves*.
- Syvitski, J. P. M., & Robert Brakenridge, G. (2013). Causation and avoidance of catastrophic flooding along the Indus River, Pakistan. *GSA Today*, *23*(1), 4–10. <https://doi.org/10.1130/GSATG165A.1>
- Tamiru, A., & Rientjes, T. H. M. (2005). *Effects of Lidar Dem Resolution in Flood Modelling : a Model Sentitivity Study for the City of Tegucigalpa , Honduras*. 168–173.
- Teutschbein, C., & Seibert, J. (2010). Regional climate models for hydrological impact studies at the catchment scale: A review of recent modeling strategies. *Geography Compass*, *4*(7), 834–860. <https://doi.org/10.1111/j.1749-8198.2010.00357.x>
- Teutschbein, C., & Seibert, J. (2012). Bias correction of regional climate model simulations for hydrological climate-change impact studies: Review and evaluation of different methods. *Journal of Hydrology*, *456–457*, 12–29. <https://doi.org/10.1016/j.jhydrol.2012.05.052>
- Thiemebl, M. J., Gobiet, A., & Heinrich, G. (2012). Empirical-statistical downscaling and error correction of regional climate models and its impact on the climate change signal. *Climatic Change*, *112*(2), 449–468. <https://doi.org/10.1007/s10584-011-0224-4>
- Tramblay, Y., Bouvier, C., Martin, C., Didon-Lescot, J. F., Todorovik, D., & Domergue, J. M. (2010). Assessment of initial soil moisture conditions for event-based rainfall-runoff modelling. *Journal of Hydrology*, *387*(3–4), 176–187. <https://doi.org/10.1016/j.jhydrol.2010.04.006>
- Uhorakeye, T., & Möller, B. (2017). Impacts of expected climate change on hydropower generation in Rwanda. *African Journal of Engineering Reserach*, *5*(October), 83.
- United States Department of Agriculture. (1986). Urban Hydrology for Small. *Soil Conservation*, (Technical Release 55 (TR-55)), 164. Retrieved from <http://scholar.google.com/scholar?hl=en&btnG=Search&q=intitle:Urban+Hydrology+for+Small+watersheds#1>
- USDA-SCS. (2004). Part 630 Hydrology National Engineering Handbook Chapter 10 Estimation of Direct Runoff from Storm Rainfall. *National Engineering Handbook*.
- Vivekanandan, N. (2017). IJRISS | Volume I, Issue VI. *International Journal of Research and Innovation in Social Science*, *1*(Vi), 2454–6186. Retrieved from www.ijriss.org
- Vuuren, D. P. Van, Edmonds, J., Kainuma, M., Riahi, K., Nakicenovic, N., Smith, S. J., & Rose, S. K. (2011). *The representative concentration pathways : an overview*. 5–31. <https://doi.org/10.1007/s10584-011-0148-z>
- Wainwright, C. M., Finney, D. L., Kilavi, M., Black, E., & Marsham, J. H. (2020). Extreme rainfall in East

- Africa, October 2019–January 2020 and context under future climate change. *Weather*, 2(January).
<https://doi.org/10.1002/wea.3824>
- Wheater, H., & Evans, E. (2009). Land use, water management and future flood risk. *Land Use Policy*, 26(SUPPL. 1), 251–264. <https://doi.org/10.1016/j.landusepol.2009.08.019>
- Williams, G. B. (1922). Flood discharges and the dimensions of spillways in India. *The Engineer*, pp. 321–322.
- World Meteorological Organization. (2019). The Global Climate in 2015 - 2019. *Centre for Research on the Epidemiology of Disasters National Institute for Space Research*, (1179), 32.
- Wu, M., Nikulin, G., Kjellström, E., Belušić, D., Jones, C., & Lindstedt, D. (2020). The impact of regional climate model formulation and resolution on simulated precipitation in Africa. *Earth System Dynamics*, 11(2), 377–394. <https://doi.org/10.5194/esd-11-377-2020>
- Yang, C., Christensen, H. M., Corti, S., von Hardenberg, J., & Davini, P. (2019). The impact of stochastic physics on the El Niño Southern Oscillation in the EC-Earth coupled model. *Climate Dynamics*, 53(5–6), 2843–2859. <https://doi.org/10.1007/s00382-019-04660-0>
- Zhou, Q., Leng, G., Su, J., & Ren, Y. (2019). Comparison of urbanization and climate change impacts on urban flood volumes: Importance of urban planning and drainage adaptation. *Science of the Total Environment*, 658, 24–33. <https://doi.org/10.1016/j.scitotenv.2018.12.184>

